Physics – Uspekhi **60** (6) 559 – 585 (2017)

REVIEWS OF TOPICAL PROBLEMS

PACS numbers: **41.20. – q**, 42.50.Wk, **44.40. + a**

Fluctuation-electromagnetic interaction under dynamic and thermal nonequilibrium conditions

G V Dedkov, A A Kyasov

DOI: https://doi.org/10.3367/UFNe.2016.12.038006

Contents

Abstract. We systematically summarize theoretical developments related to the relativistic and nonrelativistic fluctuation-electromagnetic interaction of bodies of different temperatures moving translationally and (or) rotationally relative to one another. The small-particle–plate and small-particle–vacuum background configurations are considered as the basic ones. A method is presented for calculating the basic characteristics of this interaction: the conservative–dissipative forces and torques, the heating (cooling) rates, and the intensities of thermal and nonthermal radiation fluxes that arise under 'Cherenkov friction' conditions. Experimental results and possible applications are discussed.

G V Dedkov, A A Kyasov
Berbekov Kabardino-Balkarian State University,
ul. Chernyshevskogo 173, 360004 Nalchik,
Kabardino-Balkarian Republic, Russian Federation
E-mail: gv_dedkov@mail.ru, aa_kyasov@mail.ru

Received 1 August 2016, revised 28 November 2016
Uspekhi Fizicheskikh Nauk **187** (6) 599 – 627 (2017)
DOI: https://doi.org/10.3367/UFNr.2016.12.038006
Translated by K A Postnov; edited by A M Semikhatov

Keywords: fluctuation-electromagnetic interaction of moving bodies, Casimir friction, quantum friction, thermal and nonthermal radiation under translational–rotational motion of particles in a vacuum

1. Introduction

The role of fluctuation-electromagnetic interaction between individual molecules and larger bodies was apparently clearly realized for the first time by P N Lebedev in the last decade of the 19th century. For example, in a paper on the study of the ponderomotive action of electromagnetic waves on resonators [1], Lebedev wrote: 'From the point of view of the electromagnetic theory of light we should state that between two molecules, as between two vibrators in which electromagnetic oscillations are excited, ponderomotive forces should be present due to electrodynamic interactions of alternating electric currents in molecules (according to Ampere's law) or of variable electric charges (according to Coulomb's laws). Therefore, we should assert that in this case molecular forces should operate between molecules inherently related to radiation processes. The most interesting and

the most complicated case is that of a physical body in which many molecules simultaneously interact with each other, and oscillations of these molecules, owing to their mutual proximity, are not independent of each other....''

The first theoretical calculation of the dissipative force acting on a moving atom in an equilibrium electromagnetic radiation background was performed by Einstein and Hopf [2]. The next extremely important step was taken in the pioneering papers by Casimir [3], Casimir and Polder [4], and Lifshitz [5], devoted to the attraction force between two thick plates separated by a narrow vacuum gap [3, 5] and to the interaction of two small polarizing particles with surfaces or with each other [4].

On celebrating the recent 150th anniversary of Lebedev's birth, it can be stated that the interaction of electromagnetic radiation with matter and its appearance in the fluctuation-electromagnetic interaction (FEI) between condensed bodies and with a fluctuating electromagnetic field remain topical in physics research. Only during the last two decades have many review papers and monographs been published [6–20]. One of the most important avenues of modern FEI research is the study of dynamically and thermally nonequilibrium systems [6, 8–20].

FEI is due to spatial correlations of quantum and thermal fluctuations of polarization and magnetization of condensed bodies and a vacuum. For atomic particles located beyond the reach of chemical forces, the interaction is mediated by the fields formed by fluctuating electric and magnetic moments (of the dipole or higher order). FEI appears not only as van der Waals–Casimir–Lifshitz and Casimir–Polder conservative forces but also as dissipative forces (quantum friction forces) arising in the relative motion of bodies and as a radiation heat exchange between them. The classical blackbody radiation of heated bodies also has a fluctuational nature.

Unlike static interaction described in detail in classical textbooks [21–28] (see also [7, 8, 12, 18]), FEI between moving bodies demonstrates many new interesting features [6, 10, 11, 13, 14, 19–34]. FEI has wide applications ranging from biology and atomic physics [28] to particle physics, astrophysics, and cosmology [6–8, 12, 20, 35–37]. Measurements of the Casimir forces, in particular, probe the structure of the quantum vacuum and impose restrictions on the amplitude of hypothetical long-range forces deviating from the Newton gravity force [7, 38]. FEI research is also stimulated by nanotechnology because it plays a major role on micro- and nano scales in the interaction between individual pieces of micro and nano-machines [39–44].

From the very beginning, the development of research related to dissipative FEI with or without taking thermal nonequilibrium into account has had no consensus as to the dependence of the dissipative force on distance, velocity, and temperature [45–49]. Later on, this led to a dramatic increase in interest in this problem from numerous research groups [50–104] (this list is by no means exhaustive). Taking the relative motion of bodies, retardation effects, and the difference (in general) between the local temperatures of contacting bodies into account makes the problems technically very complicated. This is probably why, although the relevant technique was developed quite long ago in the form of the Levin–Rytov [21, 22] and Dzyaloshinskii–Lifshitz–Pitaevskii [23] formalism, the solution of nonequilibirium FEI problems came much later [45–49], and other methods were used in calculations of dissipative forces. These methods include nonrelativistic statistical mechanical treatment of the system of moving oscillators using the Kubo formula [50–57] and the Kubo formula in combination with other approaches [47, 59, 71], a dynamic generalization of the Lifshitz formula [66, 67], the Keldysh formalism [78], the quantum perturbation theory [92–96, 102], and quantum scattering theory [103, 104].

Presently, it can be stated that there is complete agreement among the results of most authors concerning the dissipative force acting on a small particle or an atom moving parallel to a smooth homogeneous plate (configuration 2 below), and the dissipative force acting on a small particle moving in an equilibrium electromagnetic background (configuration 3). These results played an important role in comparing different theories and reaching consensus among different authors [11, 15, 52, 58, 63, 73, 74, 88, 99, 102].

Unlike these cases, no generally accepted result has been obtained so far for two parallel plates — the classical Casimir–Lifshitz configuration (configuration 1 below) — that move relativistically and in the absence of the general thermal equilibrium. In particular, the results in [64, 65] imply a zero dissipative quantum friction force at zero temperature for configuration 1 and, as a consequence, for configuration 2 (in contradiction to the results in [63, 73, 74, 80–91] and most other papers).

For these reasons and because of our scientific interests, in considering nonequilibrium FEI effects, we here rely on the results obtained for configurations 2 and 3 and related ones (a particle rotating near the surface and in a vacuum), for which we have developed a systematic relativistic method using the standard fluctuation electrodynamics formalism [80–86, 88–91]. The treatment of configuration 1 is restricted to the nonrelativistic case. We also discuss recent results related to the generation of thermal and nonthermal radiation in the translational and rotational motion of particles in a vacuum and near a transparent dielectric plate [31–34, 100, 105–112]. In Section 8, experiments are considered in which nonequilibrium FEI effects have been or can be observed.

All formulas are written in the Gaussian units, k_B, $\hbar$, and c are the Boltzmann constant, the Planck constant, and the speed of light, and T is the absolute temperature. Indices 1 and 2 (for example, T_1 or T_2) respectively relate to a moving body and a body at rest. One and two primes respectively denote the real and imaginary parts of the dielectric and magnetic polarizability of a particle, $\alpha_{e,m}(\omega)$, and of the dielectric response reaction of the medium $\Delta_{e,m}(\omega)$ (Fresnel amplitudes). In other cases, one or two primes denote the values related to reference frames Σ' and Σ'', and dots over symbols denote time derivatives. Dielectric (magnetic) properties of small particles are taken into account in the isotropic polarizability model. Anisotropy effects in the presence of dynamic and thermal nonequilibrium further complicate the problem, and their consideration goes far beyond the scope of this review.

2. General characteristics of fluctuation-electromagnetic interaction between moving bodies

2.1 Problem setup and geometric configurations

Our calculations of FEI characteristics are based on the direct quantum statistical averaging of the Lorentz force operators and of other physical quantities related to a moving particle in

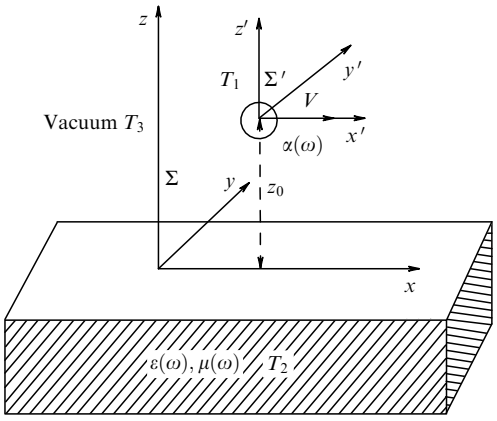

Figure 1. Particle–plate configuration and the reference frames of the plate Σ and the particle Σ'.

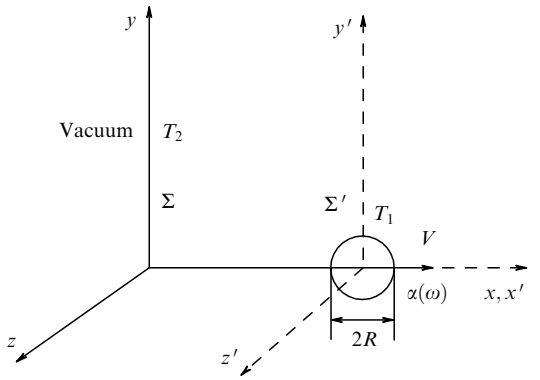

Figure 2. Particle–vacuum background configuration and the reference frames of the vacuum background Σ and the particle Σ'.

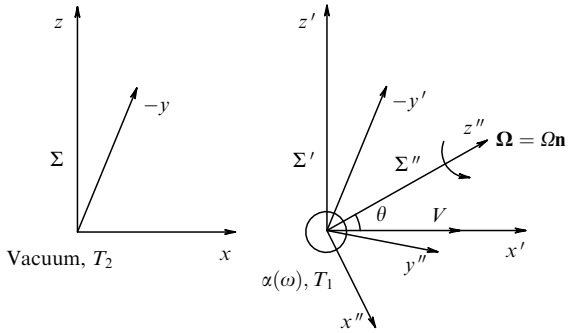

Figure 3. Translational–rotational motion of a particle in a vacuum and the relevant reference frames Σ, Σ', and Σ''.

the presence of several statistically independent sources of spontaneous fluctuations of the electromagnetic field for given temperatures of bodies and the ambient vacuum background (photon gas). In the static case, such an approach was used in [25, 26].

In configurations of type 2 (Fig. 1) and type 3 (Fig. 2), the respective bodies at rest are the plate and the photon gas. They are related to the inertial reference frame Σ. The moving particle (body) has a velocity $0 < V < c$ relative to Σ and is associated with the comoving inertial reference frame Σ'. If the particle rotates relative to Σ' with an angular velocity Ω, an additional reference frame Σ'' rigidly related to the particle is introduced (Fig. 3). The linear rotation velocity is assumed to be nonrelativistic ($\Omega R/c \ll 1$, where R is the radius of the particle). A system of two particles in which one particle is at rest is a modification of configuration 2. We also assume the local thermal equilibrium for the particle with a temperature T_1, for the plate (particle) at rest with a temperature T_2, and for the vacuum background with a temperature T_3. The temperature T_3 can be different from T_1 and (or) T_2. The use of the inertial frames Σ and Σ' provides a unique relation between the components of the electrodynamic and mechanical quantities given in these frames via Lorentz transformations. Clearly, this allows a covariant formulation of the main relations [99].

2.2 Ponderomotive forces and torques; heating rate and emission power of a moving particle

Without loss of generality, we consider one neutral particle (body) moving with the velocity $\mathbf{V}$ relative to a body at rest (see Figs 1 and 2). The Lorentz force acting on the particle from the fluctuating electromagnetic field with vectors $\mathbf{E}$ and $\mathbf{B}$ is

$$\mathbf{F} = \int \langle \rho \mathbf{E} \rangle \, \mathrm{d}^3 r + \frac{1}{c} \int \langle \mathbf{j} \times \mathbf{B} \rangle \, \mathrm{d}^3 r , \tag{1}$$

where ρ and $\mathbf{j}$ are fluctuating charge and current densities, the angular brackets denote complete quantum statistical averaging, and the integrals formally extend to the entire space, although ρ and $\mathbf{j}$ are nonzero only inside the particle volume. By expressing the current $\mathbf{j}$ and charge ρ density as

$$\mathbf{j} = \frac{\partial \mathbf{P}}{\partial t} + c \operatorname{rot} \mathbf{M} , \qquad \rho = -\operatorname{div} \mathbf{P} , \tag{2}$$

where $\mathbf{P}$ and $\mathbf{M}$ are the polarization and magnetization vectors, and using the standard Lorentz transformations for ρ, $\mathbf{j}$, $\mathbf{E}$, $\mathbf{B}$, $\mathbf{P}$, and $\mathbf{M}$, we can represent the energy dissipation integral for the electromagnetic field as [14, 15, 111]

$$\int \langle \mathbf{j} \mathbf{E} \rangle \, \mathrm{d}^3 r = \mathbf{F}\mathbf{V} + \gamma^{-2} \int \langle \mathbf{j}' \mathbf{E}' \rangle \, \mathrm{d}^3 r' , \tag{3}$$

where $\gamma = (1 - V^2/c^2)^{-1/2}$ and primed quantities are related to the comoving frame Σ'. Clearly, the integral in the right-hand side of (3) gives the heat release rate $\mathrm{d}Q'/\mathrm{d}t'$ in the body (i.e., $\mathrm{d}Q' = C_\mathrm{s} \, \mathrm{d}T_1$, where C_s is the body thermal capacity). This integral can be reduced to the form

$$\begin{aligned} \frac{\mathrm{d}Q'}{\mathrm{d}t'} &= \int \langle \mathbf{j}' \mathbf{E}' \rangle \, \mathrm{d}^3 r' = \int \left\langle \left(\frac{\partial \mathbf{P}'}{\partial t'} + c \operatorname{rot} \mathbf{M}' \right) \mathbf{E}' \right\rangle \mathrm{d}^3 r' \\ &= c \oint (\mathbf{M}' \times \mathbf{E}') \, \mathrm{d}\mathbf{s} + \int \left\langle \frac{\partial \mathbf{P}'}{\partial t'} \mathbf{E}' + \frac{\partial \mathbf{M}'}{\partial t'} \mathbf{B}' \right\rangle \mathrm{d}^3 r' \\ &\quad - \int \left\langle \frac{\partial}{\partial t'} (\mathbf{M}' \mathbf{B}') \right\rangle \mathrm{d}^3 r' = \int \left\langle \frac{\partial \mathbf{P}'}{\partial t'} \mathbf{E}' + \frac{\partial \mathbf{M}'}{\partial t'} \mathbf{B}' \right\rangle \mathrm{d}^3 r' . \end{aligned} \tag{4}$$

The surface integral of $\mathbf{M}' \times \mathbf{E}'$ in (4) vanishes because it is taken over an infinitely remote surface, and the integral of $\partial(\mathbf{M}'\mathbf{B}')/\partial t'$ vanishes by the stationarity condition of electromagnetic fluctuations, which we assume everywhere below. Next, by using Lorentz transformations for the quantities in the right-hand side of (4) and the time and volume transformations $\mathrm{d}t' = \gamma^{-1} \, \mathrm{d}t$, $\mathrm{d}^3 r = \gamma^{-1} \, \mathrm{d}^3 r'$, we obtain

$$\int \left\langle \frac{\partial \mathbf{P}'}{\partial t'} \mathbf{E}' + \frac{\partial \mathbf{M}'}{\partial t'} \mathbf{B}' \right\rangle \mathrm{d}^3 r' = \gamma^2 \int \left\langle \frac{\partial \mathbf{P}}{\partial t} \mathbf{E} + \frac{\partial \mathbf{M}}{\partial t} \mathbf{B} \right\rangle \mathrm{d}^3 r . \tag{5}$$

Letting $\mathrm{d}Q/\mathrm{d}t$ denote the integral in the right-hand side of (5), we arrive at the general relation

$$\frac{\mathrm{d}Q'}{\mathrm{d}t'} = \gamma^2 \frac{\mathrm{d}Q}{\mathrm{d}t}\,, \tag{6}$$

which holds irrespective of the size of the moving body. With account for (6), formula (3) takes the form

$$\int \langle \mathbf{j}\,\mathbf{E}\rangle\,\mathrm{d}^3 r = \mathbf{F}\mathbf{V} + \frac{\mathrm{d}Q}{\mathrm{d}t}\,. \tag{7}$$

Physically, this result means that the work done by the fluctuating electromagnetic field is spent to changing the kinetic energy and heat release of the body, although, as we see below, the quantity $\mathrm{d}Q/\mathrm{d}t$ has an independent meaning (see also [102]) and coincides with the heating rate of the body only for nonrelativistic motion. Because the particle temperature T_1 is defined only in the comoving frame Σ', the time evolution of T_1 is described by Eqn (6) with a given $\mathrm{d}Q/\mathrm{d}t$ and a given heat capacity in Σ'.

For a small particle with fluctuation dipole moments $\mathbf{d}(t)$ and $\mathbf{m}(t)$, the polarization and magnetization vectors are

$$\mathbf{P}(\mathbf{r},t) = \mathbf{d}(t)\,\delta(\mathbf{r}-\mathbf{V}t)\,, \qquad \mathbf{M}(\mathbf{r},t) = \mathbf{m}(t)\,\delta(\mathbf{r}-\mathbf{V}t)\,. \tag{8}$$

Using (2) and (8), we can simplify expressions for $\mathbf{F}$ and $\mathrm{d}Q/\mathrm{d}t$ after the integrals over the particle volume are easily calculated using the Maxwell equations

$$\mathrm{rot}\,\mathbf{E} = -\frac{1}{c}\frac{\partial \mathbf{B}}{\partial t}\,, \qquad \mathrm{div}\,\mathbf{B} = 0$$

and the quasi-stationarity condition for fluctuations

$$\mathbf{F} = \left\langle \nabla(\mathbf{d}\mathbf{E} + \mathbf{m}\mathbf{B})\right\rangle, \tag{9}$$

$$\frac{\mathrm{d}Q}{\mathrm{d}t} = \langle \dot{\mathbf{d}}\mathbf{E} + \dot{\mathbf{m}}\mathbf{B}\rangle\,. \tag{10}$$

The dots over $\mathbf{d}$ and $\mathbf{m}$ in (10) denote time derivatives.

The obtained equations can be easily related to the emission power of a particle moving in a vacuum or near the surface of a transparent nonmagnetic medium. Following [105–107], we surround the particle by a sufficiently remote surface σ such that the electromagnetic field on this surface has the wave character (Fig. 4). We write the energy conservation law for the fluctuating field inside the volume Ω (not to be confused with the angular velocity Ω) bounded by the surface σ,

$$-\frac{\mathrm{d}W}{\mathrm{d}t} = \oint_\sigma \mathbf{S}\,\mathrm{d}\boldsymbol{\sigma} + \int_\Omega \langle \mathbf{j}\,\mathbf{E}\rangle\,\mathrm{d}^3 r\,, \tag{11}$$

where $W = [1/(8\pi)]\int_\Omega(\langle \mathbf{E}^2\rangle + \langle \mathbf{H}^2\rangle)\,\mathrm{d}^3 r$ is the field energy in Ω and $\mathbf{S} = [c/(4\pi)]\langle \mathbf{E}\times\mathbf{H}\rangle$ is the Poynting flux vector. In the quasistationary regime ($\mathrm{d}W/\mathrm{d}t = 0$), Eqn (11) implies

$$I = \oint_\sigma \mathbf{S}\,\mathrm{d}\boldsymbol{\sigma} = -\int_\Omega \langle \mathbf{j}\,\mathbf{E}\rangle\,\mathrm{d}^3 r \equiv I_1 - I_2\,, \tag{12}$$

where I is the difference between the emission and absorption powers I_1 and I_2. It follows from (7) and (12) that

$$I = -\left(\frac{\mathrm{d}Q}{\mathrm{d}t} + \mathbf{F}\mathbf{V}\right). \tag{13}$$

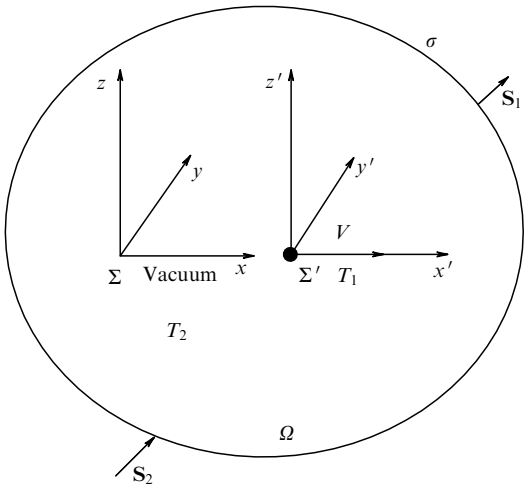

Figure 4. Wave surface σ of an emitting particle in a vacuum background. $\mathbf{S}_1$ and $\mathbf{S}_2$ are the respective Poynting vectors of the emitted and absorbed electromagnetic radiation.

We now consider a more complicated case where the particle is in translational motion with a velocity $\mathbf{V}$ relative to Σ and in rotational motion with the velocity $\Omega\mathbf{n}$ relative to Σ' (see Fig. 3). The comoving rest frame Σ'' has the same angular velocity. The work $\mathrm{d}Q'/\mathrm{d}t' = \int_{\Omega'}\langle \mathbf{j}'\,\mathbf{E}'\rangle\,\mathrm{d}^3 r'$ of the fluctuation field in the frame Σ' is now spent not only to heat the particle but also to slow down its rotation. The corresponding expression for the dipole particle can be easily found after transforming a dipole moment and electromagnetic field vector rotations by passing from the frame Σ' to the rest-frame Σ''. As a result, we obtain

$$\int_{V'} \langle \mathbf{j}'\,\mathbf{E}'\rangle\,\mathrm{d}^3 r' = \langle \dot{\mathbf{d}}'\,\mathbf{E}' + \dot{\mathbf{m}}'\,\mathbf{B}'\rangle = \frac{\mathrm{d}Q''}{\mathrm{d}t'} + M_n'\Omega\,, \tag{14}$$

where $M_n' = \langle \mathbf{d}'\times\mathbf{E}' + \mathbf{m}'\times\mathbf{B}'\rangle_n$ is the projection of the torque on the particle spin axis in the frame Σ'. In (14), it is taken into account that $\mathrm{d}t'' = \mathrm{d}t'$ because the particle rotation is nonrelativistic. We choose the Cartesian rest frame Σ'' associated with the particle such that (see Fig. 3) its z'' axis coincides with the angular velocity unit vector $\mathbf{n} = (\cos\theta, 0, \sin\theta)$ lying in the plane (x', z') of the frame Σ' (here, θ is the angle between the vector $\mathbf{n}$ and the x' axis). Taking the relativistic transformation for the torque vector projections $M_x' = \gamma M_x$, $M_z' = M_z$, $M_y' = M_y$ into account, it is convenient to represent Eqn (14) in the form

$$\int_{V'} \langle \mathbf{j}'\,\mathbf{E}'\rangle\,\mathrm{d}^3 r' \equiv \frac{\mathrm{d}Q'}{\mathrm{d}t'} \equiv \frac{\mathrm{d}Q''}{\mathrm{d}t'} + M_x\gamma\Omega\cos\theta + M_z\Omega\sin\theta\,, \tag{15}$$

where M_x and M_z are the projections of the torque vector in Σ. We note that the torque component M_y does no work on the particle and can induce only its precession. Using (5) and (15), we obtain an equation for the heating rate of the particle in Σ:

$$\frac{\mathrm{d}Q''}{\mathrm{d}t} = \gamma\,\frac{\mathrm{d}Q}{\mathrm{d}t} - \Omega(M_x\cos\theta + M_z\gamma^{-1}\sin\theta)\,. \tag{16}$$

Given the particle heat capacity, Eqn (16) enables calculating the time dependence of its temperature.

Thus, all physically relevant quantities related to a moving particle are expressed through correlators of the electromag-

netic field and fluctuation moments of the particle in the laboratory frame Σ.

2.3 Particle dynamics

In the dynamics of a particle, the change in its mass and the relation of this change to other quantities characterizing FEI are important. This point was first noted by Polevoi [49] in the problem of calculating the dissipative force in the type-1 configuration (see also [10, 11, 100, 107, 108]). By assuming that the translation velocity is directed along the x axis of the frame Σ (see Figs 2 and 3), the dynamic equation can be written as

$$\frac{\mathrm{d}}{\mathrm{d}t}\,\frac{mV}{\sqrt{1-V^2/c^2}} = F_x\,. \tag{17}$$

Equation (17) implies that

$$\gamma^3 m\,\frac{\mathrm{d}V}{\mathrm{d}t} + \gamma V\,\frac{\mathrm{d}m}{\mathrm{d}t} = F_x\,. \tag{18}$$

On the other hand, using energy conservation law (11) in the form

$$-\frac{\mathrm{d}}{\mathrm{d}t}\left(W + \frac{mc^2}{\sqrt{1-\beta^2}}\right) = I \tag{19}$$

and the quasistationarity condition $\mathrm{d}W/\mathrm{d}t = 0$, we obtain

$$-\gamma^3 mV\,\frac{\mathrm{d}V}{\mathrm{d}t} - \gamma\,\frac{\mathrm{d}m}{\mathrm{d}t}\,c^2 = I\,. \tag{20}$$

From (13), (18), and (20), important general relations can be derived:

$$\gamma^3 m\,\frac{\mathrm{d}V}{\mathrm{d}t} = F_x - \beta\gamma^2\,\frac{1}{c}\,\frac{\mathrm{d}Q}{\mathrm{d}t}\,, \tag{21}$$

$$\frac{\mathrm{d}m}{\mathrm{d}t} = \frac{\gamma}{c^2}\,\frac{\mathrm{d}Q}{\mathrm{d}t}\,. \tag{22}$$

Taking (22) into account, it is easy to see that the right-hand side of (21) represents the tangential force F_x' acting on the particle in the reference frame Σ':

$$F_x - \frac{\beta\gamma^2}{c}\,\frac{\mathrm{d}Q}{\mathrm{d}t} = F_x - V\,\frac{\mathrm{d}m}{\mathrm{d}t'} \equiv F_x'\,. \tag{23}$$

Therefore, dynamic equation (21) takes the form

$$\gamma^3 m\,\frac{\mathrm{d}V}{\mathrm{d}t} = F_x'\,. \tag{24}$$

In this derivation, we used the identity $F_x - V\,\mathrm{d}m/\mathrm{d}t' \equiv F_x'$ that follows from time differentiation of the Lorentz transformation for the particle momentum, $p_x = \gamma(p_x' + Vm/c^2)$. Thus, the acceleration of the particle in the laboratory frame Σ is determined by the dissipative force specified in the frame Σ' [107, 108].

The dynamic equations of the rotational motion of the particle can be conveniently written in the frame Σ' (see Fig. 3):

$$I_{ik}\,\frac{\mathrm{d}\Omega_k}{\mathrm{d}t'} = M_i'\,, \tag{25}$$

where I_{ik} are components of the tensor moment of inertia of the particle in Σ', and the projections M_k' of the torque in Σ' must be expressed through the projections M_k in Σ [see text before Eqn (15)]. For a spherical particle, $I_{ik} = I_0\delta_{ik}$. Equations (16), (24), and (25) describe the interrelation and time evolution of the thermal state of the particle and its kinematic and dynamic characteristics.

3. Fluctuation–dissipation relations in dynamically and thermally nonequilibrium systems

The presence of independent sources of spontaneous fluctuations in interacting subsystems ($\mathbf{d}^{\mathrm{sp}}$ and $\mathbf{m}^{\mathrm{sp}}$ for the particle and $\mathbf{E}^{\mathrm{sp}}$ and $\mathbf{B}^{\mathrm{sp}}$ for the medium filling a half-space in configuration 2, or for equilibrium electromagnetic radiation in a vacuum in configuration 3) gives rise to induced fluctuations of $\mathbf{d}^{\mathrm{ind}}$, $\mathbf{m}^{\mathrm{ind}}$, $\mathbf{E}^{\mathrm{ind}}$, and $\mathbf{B}^{\mathrm{ind}}$. The initial expressions for fluctuation force (9), heat exchange rate (10), and the torque $\langle \mathbf{d}\times\mathbf{E} + \mathbf{m}\times\mathbf{B}\rangle$ then become

$$\mathbf{F} = \left\langle \nabla(\mathbf{d}^{\mathrm{sp}}\,\mathbf{E}^{\mathrm{ind}} + \mathbf{m}^{\mathrm{sp}}\,\mathbf{B}^{\mathrm{ind}})\right\rangle + \left\langle \nabla(\mathbf{d}^{\mathrm{ind}}\,\mathbf{E}^{\mathrm{sp}} + \mathbf{m}^{\mathrm{ind}}\,\mathbf{B}^{\mathrm{sp}})\right\rangle, \tag{26}$$

$$\frac{\mathrm{d}Q}{\mathrm{d}t} = \left\langle \dot{\mathbf{d}}^{\mathrm{sp}}\,\mathbf{E}^{\mathrm{ind}} + \dot{\mathbf{m}}^{\mathrm{sp}}\,\mathbf{B}^{\mathrm{ind}}\right\rangle + \left\langle \dot{\mathbf{d}}^{\mathrm{ind}}\,\mathbf{E}^{\mathrm{sp}} + \dot{\mathbf{m}}^{\mathrm{ind}}\,\mathbf{B}^{\mathrm{sp}}\right\rangle, \tag{27}$$

$$\mathbf{M} = \left\langle \mathbf{d}^{\mathrm{sp}}\times\mathbf{E}^{\mathrm{ind}} + \mathbf{m}^{\mathrm{sp}}\times\mathbf{B}^{\mathrm{ind}}\right\rangle + \left\langle \mathbf{d}^{\mathrm{ind}}\times\mathbf{E}^{\mathrm{sp}} + \mathbf{m}^{\mathrm{ind}}\times\mathbf{B}^{\mathrm{sp}}\right\rangle. \tag{28}$$

Clearly, expression (28) vanishes for a nonrotating particle. All quantities in (26)–(28) are calculated within a single formalism in the laboratory frame Σ. As follows from formulas (26)–(28), irrespective of the specific configuration, the calculation of all quantities is reduced to the statistical averaging of the right-hand sides. In configuration 2, in particular, conservative and dissipative components of FEI are determined by the projections F_z and F_x of force (26), and in configuration 3, only the component F_x of the dissipative (tangential) force is nonzero.

The first terms in (26)–(28) describe the contribution from spontaneous fluctuations of the dipole and magnetic moments of the particle to its interaction with the external electromagnetic field. These terms can be calculated in two stages. First, the system of Maxwell equations with point-like spontaneously fluctuating sources (8) for configuration 2 or 3 is solved, with the boundary conditions on the surface $z = 0$ in the first case. As a result, the vectors $\mathbf{E}^{\mathrm{ind}}$ and $\mathbf{B}^{\mathrm{ind}}$ are expressed in terms of $\mathbf{d}^{\mathrm{sp}\,\prime}$ and $\mathbf{m}^{\mathrm{sp}\,\prime}$, and the vectors $\mathbf{d}^{\mathrm{sp}}$ and $\mathbf{m}^{\mathrm{sp}}$ in (26)–(28) are expressed in terms of $\mathbf{d}^{\mathrm{sp}\,\prime}$ and $\mathbf{m}^{\mathrm{sp}\,\prime}$ by relativistic transformations of dipole moments in passing from the frame Σ to the frame Σ'. The subsequent quantum statistical averaging is convenient to perform using fluctuation–dissipation relations (FDRs) specified in the frame Σ'. If the particle rotates, then, clearly, the form of the corresponding FDRs differs from their standard form in the rest frame.

The second terms in the right-hand sides of (26)–(28) describe the interaction of the induced moments with spontaneous fluctuations of the external electromagnetic field. To calculate them, the induced dipole moments of the particles are expressed via fluctuating external fields using linear integral relations containing the dielectric and magnetic polarizability of the particle. Next, after substituting the obtained quantities in (26)–(28), correlators arise that include Fourier components of random electromagnetic fields of the medium. These correlators are expanded using

FDRs containing imaginary parts of the components of the retarded Green's function for a photon in the medium.

3.1 Fluctuation–dissipation relations for dipole moments

For more generality, it is useful to consider configuration 2, in which a particle rotates with an angular velocity Ω relative to the reference frame Σ', which can move with a relativistic velocity V relative to the laboratory frame Σ (see Fig. 3).

To obtain FDRs for dipole moments, we first make a rotational transformation of spontaneous dipole moments of the particle by passing from the frame Σ' to the rotating frame Σ'' in which the particle is at rest,

$$d_i^{\mathrm{sp}\,\prime}(\tau) = A_{ik}(\tau) d_k^{\mathrm{sp}\,\prime\prime}(\tau)\,, \tag{29}$$

$$m_i^{\mathrm{sp}\,\prime}(\tau) = A_{ik}(\tau) m_k^{\mathrm{sp}\,\prime\prime}(\tau)\,. \tag{30}$$

The rotation matrix defined by a unit vector $\mathbf{n}$ is [113]

$$A_{ik}(\tau) = n_i n_k + (\delta_{ik} - n_i n_k)\cos(\Omega\tau) - e_{ikl} n_l \sin(\Omega\tau)\,. \tag{31}$$

Next, we make a partial Fourier transformation of the left- and right-hand sides of Eqns (29) and (30), after which we multiply their corresponding Fourier images. Here, we use the standard FDR defined in the particle rest frame [114]:

$$\left\langle d_i^{\mathrm{sp}\,\prime\prime}(\omega)\, d_k^{\mathrm{sp}\,\prime\prime}(\omega')\right\rangle = 2\pi\hbar\delta_{ik}\delta(\omega+\omega')\alpha_{\mathrm{e}}''(\omega)\coth\frac{\hbar\omega}{2k_{\mathrm{B}}T_1}\,, \tag{32}$$

$$\left\langle m_i^{\mathrm{sp}\,\prime\prime}(\omega)\, m_k^{\mathrm{sp}\,\prime\prime}(\omega')\right\rangle = 2\pi\hbar\delta_{ik}\delta(\omega+\omega')\alpha_{\mathrm{m}}''(\omega)\coth\frac{\hbar\omega}{2k_{\mathrm{B}}T_1}\,, \tag{33}$$

where $\alpha_{\mathrm{e}}''(\omega)$ and $\alpha_{\mathrm{m}}''(\omega)$ are imaginary parts of the electric and magnetic polarizability, and T_1 is the particle temperature. After multiplying Fourier images of (29) and (30) and some transformations, the FDRs of interest take the form

$$\left\langle d_x^{\mathrm{sp}\,\prime}(\omega)\, d_x^{\mathrm{sp}\,\prime}(\omega')\right\rangle = \frac{1}{2}\,2\pi\hbar\delta(\omega+\omega') \times\left[2\cos^2\theta\,\alpha_{\mathrm{e}}''(\omega)\coth\frac{\hbar\omega}{2k_{\mathrm{B}}T_1} + \sin^2\theta\left(\alpha_{\mathrm{e}}''(\omega^+)\coth\frac{\hbar\omega^+}{2k_{\mathrm{B}}T_1} + \alpha_{\mathrm{e}}''(\omega^-)\coth\frac{\hbar\omega^-}{2k_{\mathrm{B}}T_1}\right)\right], \tag{34}$$

$$\left\langle d_z^{\mathrm{sp}\,\prime}(\omega)\, d_z^{\mathrm{sp}\,\prime}(\omega')\right\rangle = \frac{1}{2}\,2\pi\hbar\delta(\omega+\omega') \times\left[2\sin^2\theta\,\alpha_{\mathrm{e}}''(\omega)\coth\frac{\hbar\omega}{2k_{\mathrm{B}}T_1} + \cos^2\theta\left(\alpha_{\mathrm{e}}''(\omega^+)\coth\frac{\hbar\omega^+}{2k_{\mathrm{B}}T_1} + \alpha_{\mathrm{e}}''(\omega^-)\coth\frac{\hbar\omega^-}{2k_{\mathrm{B}}T_1}\right)\right], \tag{35}$$

$$\left\langle d_y^{\mathrm{sp}\,\prime}(\omega)\, d_y^{\mathrm{sp}\,\prime}(\omega')\right\rangle = \frac{1}{2}\,2\pi\hbar\delta(\omega+\omega') \times\left(\alpha_{\mathrm{e}}''(\omega^+)\coth\frac{\hbar\omega^+}{2k_{\mathrm{B}}T_1} + \alpha_{\mathrm{e}}''(\omega^-)\coth\frac{\hbar\omega^-}{2k_{\mathrm{B}}T_1}\right), \tag{36}$$

$$\left\langle d_x^{\mathrm{sp}\,\prime}(\omega)\, d_y^{\mathrm{sp}\,\prime}(\omega')\right\rangle = -\left\langle d_y^{\mathrm{sp}\,\prime}(\omega)\, d_x^{\mathrm{sp}\,\prime}(\omega')\right\rangle = \frac{\mathrm{i}}{2}\sin\theta\,2\pi\hbar\delta(\omega+\omega') \times\left(\alpha_{\mathrm{e}}''(\omega^+)\coth\frac{\hbar\omega^+}{2k_{\mathrm{B}}T_1} - \alpha_{\mathrm{e}}''(\omega^-)\coth\frac{\hbar\omega^-}{2k_{\mathrm{B}}T_1}\right), \tag{37}$$

$$\left\langle d_y^{\mathrm{sp}\,\prime}(\omega)\, d_z^{\mathrm{sp}\,\prime}(\omega')\right\rangle = -\left\langle d_z^{\mathrm{sp}\,\prime}(\omega)\, d_y^{\mathrm{sp}\,\prime}(\omega')\right\rangle = \frac{\mathrm{i}}{2}\cos\theta\,2\pi\hbar\delta(\omega+\omega') \times\left(\alpha_{\mathrm{e}}''(\omega^+)\coth\frac{\hbar\omega^+}{2k_{\mathrm{B}}T_1} - \alpha_{\mathrm{e}}''(\omega^-)\coth\frac{\hbar\omega^-}{2k_{\mathrm{B}}T_1}\right), \tag{38}$$

$$\left\langle d_x^{\mathrm{sp}\,\prime}(\omega)\, d_z^{\mathrm{sp}\,\prime}(\omega')\right\rangle = \left\langle d_z^{\mathrm{sp}\,\prime}(\omega)\, d_x^{\mathrm{sp}\,\prime}(\omega')\right\rangle = \sin\theta\,2\pi\hbar\delta(\omega+\omega')\left[\alpha_{\mathrm{e}}''(\omega)\coth\frac{\hbar\omega}{2k_{\mathrm{B}}T_1} - \frac{1}{2}\left(\alpha_{\mathrm{e}}''(\omega^+)\coth\frac{\hbar\omega^+}{2k_{\mathrm{B}}T_1} + \alpha_{\mathrm{e}}''(\omega^-)\coth\frac{\hbar\omega^-}{2k_{\mathrm{B}}T_1}\right)\right], \tag{39}$$

where $\omega^{\pm} = \omega \pm \Omega$. The FDR for magnetic moments has the form similar to (34)–(39) with the substitutions $\mathbf{d}^{\mathrm{sp}\,\prime} \to \mathbf{m}^{\mathrm{sp}\,\prime}$ and $\alpha_{\mathrm{e}}''(\omega) \to \alpha_{\mathrm{m}}''(\omega)$.

The FDRs (34)–(39) and their magnetic analogs written in the frame Σ' clearly show that rotation of the particle makes the different projections of the dipole and magnetic moment vectors statistically dependent (they acquire correlations). These correlations, in turn, give rise to torque (28), which tends to slow down the particle rotation or change its spin axis, and which affects its heating dynamics [see (16)].

3.2 Fluctuation–dissipation relations for electromagnetic field components

FDRs for a fluctuation electromagnetic field external to the particle are most naturally written in the laboratory frame Σ related to this field. Therefore, the form of these FDRs is preserved, irrespective of the motion of the particle relative to Σ.

The stationarity condition for fluctuations [114] implies that for configuration 2, all possible correlators of the vector components of the equilibrium electromagnetic field are expressed in terms of spectral densities as

$$\left\langle U_i^{\mathrm{sp}}(\omega,\mathbf{k};z) U_j^{\mathrm{sp}}(\omega',\mathbf{k}';z')\right\rangle = (2\pi)^3\delta(\omega+\omega')\delta(\mathbf{k}+\mathbf{k}')\left(U_i^{\mathrm{sp}}(z)U_j^{\mathrm{sp}}(z')\right)_{\omega\mathbf{k}}, \quad i,j=1,2,3, \tag{40}$$

and for configuration 3 they are given by the relations

$$\left\langle U_i^{\mathrm{sp}}(\omega,\mathbf{k}) U_j^{\mathrm{sp}}(\omega',\mathbf{k}')\right\rangle = (2\pi)^4\delta(\omega+\omega')\delta(\mathbf{k}+\mathbf{k}')(U_i^{\mathrm{sp}}U_j^{\mathrm{sp}})_{\omega\mathbf{k}}\,. \tag{41}$$

Here, $\mathbf{k} = (k_x, k_y)$ is a two-dimensional wave vector in (40), and $\mathbf{k} = (k_x, k_y, k_z)$ is a three-dimensional wave vector in (41). In turn, spectral densities of the electromagnetic field correlators are generally expressed in terms of the anti-Hermitian part of the retarded Green's function of a photon in a medium [115]. As a result, for configuration 2, the FDRs take the form

$$\left(E_i^{\mathrm{sp}}(z)E_j^{\mathrm{sp}}(z')\right)_{\omega\mathbf{k}} = \frac{\mathrm{i}}{2}\coth\frac{\hbar\omega}{2k_{\mathrm{B}}T_2}\frac{\omega^2}{c^2}\left(D_{ij}(\omega,\mathbf{k};z,z') - D_{ji}^*(\omega,\mathbf{k};z',z)\right), \tag{42}$$

$$\left(B_i^{\mathrm{sp}}(z)B_j^{\mathrm{sp}}(z')\right)_{\omega\mathbf{k}} = \frac{\mathrm{i}}{2}\coth\frac{\hbar\omega}{2k_{\mathrm{B}}T_2} \times \mathrm{rot}_{il}\,\mathrm{rot}'_{jm}\left(D_{lm}(\omega,\mathbf{k};z,z') - D_{ml}^*(\omega,\mathbf{k};z',z)\right), \tag{43}$$

$$\left(E_i^{\rm sp}(z)B_j^{\rm sp}(z')\right)_{\omega\mathbf{k}} = \frac{\rm i}{2}\coth\frac{\hbar\omega}{2k_{\rm B}T_2}\,\frac{{\rm i}\omega}{c}\,{\rm rot}'_{jm}\left(D_{im}(\omega,\mathbf{k};z,z')-D^*_{mi}(\omega,\mathbf{k};z',z)\right), \quad (44)$$

where ${\rm rot}_{il}=e_{inl}\,\partial/\partial x_n$ and ${\rm rot}'_{jm}=e_{jnm}\,\partial/\partial x'_n$.

The spectral representations of the retarded Green's function for configuration 2, corresponding to FDRs (42)–(44), have the form [81, 82]

$$D_{xx}(\omega,\mathbf{k};z,z') = -\frac{\hbar c^2}{\omega^2}\,\frac{2\pi}{q_0}\exp\left[-q_0(z+z')\right] \times\left[k_x^2\left(1-\frac{\omega^2}{k^2c^2}\right)\Delta_{\rm e}(\omega)+k_y^2\,\frac{\omega^2}{k^2c^2}\,\Delta_{\rm m}(\omega)\right], \quad (45)$$

$$D_{yy}(\omega,\mathbf{k};z,z') = -\frac{\hbar c^2}{\omega^2}\,\frac{2\pi}{q_0}\exp\left[-q_0(z+z')\right] \times\left[k_y^2\left(1-\frac{\omega^2}{k^2c^2}\right)\Delta_{\rm e}(\omega)+k_x^2\,\frac{\omega^2}{k^2c^2}\,\Delta_{\rm m}(\omega)\right], \quad (46)$$

$$D_{zz}(\omega,\mathbf{k};z,z') = -\frac{\hbar c^2}{\omega^2}\,\frac{2\pi}{q_0}\exp\left[-q_0(z+z')\right]k^2\Delta_{\rm e}(\omega), \quad (47)$$

$$D_{xy}(\omega,\mathbf{k};z,z') = D_{yx}(\omega,\mathbf{k};z,z') = -\frac{\hbar c^2}{\omega^2}\,\frac{2\pi}{q_0}\exp\left[-q_0(z+z')\right] \times k_xk_y\left[\left(1-\frac{\omega^2}{k^2c^2}\right)\Delta_{\rm e}(\omega)+\frac{\omega^2}{c^2}\,\Delta_{\rm m}(\omega)\right], \quad (48)$$

$$D_{xz}(\omega,\mathbf{k};z,z') = -D_{zx}(\omega,\mathbf{k};z,z') = -\frac{\hbar c^2}{\omega^2}\,\frac{2\pi}{q_0}\exp\left[-q_0(z+z')\right](-{\rm i}k_x)q_0\Delta_{\rm e}(\omega), \quad (49)$$

$$D_{yz}(\omega,\mathbf{k};z,z') = -D_{zy}(\omega,\mathbf{k};z,z') = -\frac{\hbar c^2}{\omega^2}\,\frac{2\pi}{q_0}\exp\left[-q_0(z+z')\right](-{\rm i}k_y)q_0\Delta_{\rm e}(\omega), \quad (50)$$

where

$$\Delta_{\rm e}(\omega)=\frac{q_0\varepsilon(\omega)-q}{q_0\varepsilon(\omega)+q}\,,\quad \Delta_{\rm m}(\omega)=\frac{q_0\mu(\omega)-q}{q_0\mu(\omega)+q}\,, \quad q=\left(k^2-\frac{\omega^2}{c^2}\,\varepsilon(\omega)\,\mu(\omega)\right)^{1/2},\quad q_0=\left(k^2-\frac{\omega^2}{c^2}\right)^{1/2}, \quad k=(k_x^2+k_y^2)^{1/2}. \quad (51)$$

For the components $D_{ik}(\omega,\mathbf{k};z,z')$ without the imaginary unit i, the anti-Hermitian part of the Green's function reduces to the imaginary part of $D_{ik}(\omega,\mathbf{k};z,z')$. The derivation of formulas (45)–(50) from the initial representation [115] for the retarded Green's function $D_{ik}(\omega,\mathbf{r},\mathbf{r}')$ is given in Appendix A. For configuration 3, the retarded Green's function is given by [115]

$$D_{ik}(\omega,\mathbf{k})=\frac{4\pi\hbar}{\omega^2/c^2-k^2+{\rm i}0\,{\rm sign}\,\omega}\left(\delta_{ik}-\frac{c^2}{\omega^2}\,k_i\,k_k\right), \quad (52)$$

and the FDRs take a simpler form:

$$(E_i^{\rm sp}E_j^{\rm sp})_{\omega\mathbf{k}}=-\frac{\omega^2}{c^2}\coth\frac{\hbar\omega}{2k_{\rm B}T_2}\,{\rm Im}\,D_{ij}(\omega,\mathbf{k}), \quad (53)$$

$$(B_i^{\rm sp}B_j^{\rm sp})_{\omega\mathbf{k}}=-\coth\frac{\hbar\omega}{2k_{\rm B}T_2}\,{\rm rot}_{il}\,{\rm rot}'_{jm}\,{\rm Im}\,D_{lm}(\omega,\mathbf{k}), \quad (54)$$

$$(E_i^{\rm sp}B_j^{\rm sp})_{\omega\mathbf{k}}=-\frac{{\rm i}\omega}{c}\coth\frac{\hbar\omega}{2k_{\rm B}T_2}\,{\rm rot}'_{jm}\,{\rm Im}\,D_{im}(\omega,\mathbf{k}). \quad (55)$$

4. Nonrelativistic motion of a neutral particle near a plain surface

We illustrate the above formalism with the example of a neutral polarized particle performing nonrelativistic uniform translational or rotational motion near a surface. Here and below, we assume that the medium is described by frequency-dependent dielectric and magnetic permeabilities, although in the nonrelativistic limit the results can easily be generalized to the case of a nonlocal dielectric permeability (see [15, 82] for more details).

4.1 Uniform rectilinear motion

In the nonrelativistic limit ($c\to\infty$), with the magnetic moments of the particle ignored, formulas (26), (27) take the form

$$\mathbf{F}=\left\langle\nabla(\mathbf{d}^{\rm sp}\,\mathbf{E}^{\rm ind}+\mathbf{d}^{\rm ind}\,\mathbf{E}^{\rm sp})\right\rangle, \quad (56)$$

$$\frac{{\rm d}Q}{{\rm d}t}=\left\langle\dot{\mathbf{d}}^{\rm sp}\,\mathbf{E}^{\rm ind}+\dot{\mathbf{d}}^{\rm ind}\,\mathbf{E}^{\rm sp}\right\rangle. \quad (57)$$

The induced electric field components can be found from the equations [83]

$$\mathbf{E}^{\rm ind}=-\nabla\Phi^{\rm ind}, \quad (58)$$

$$\Delta\Phi=4\pi\,{\rm div}\,\mathbf{P}, \quad (59)$$

$$\mathbf{P}=\delta(x-Vt)\delta(y)\delta(z-z_0)\mathbf{d}^{\rm sp}(t), \quad (60)$$

where $\Phi^{\rm ind}$ is the induced component of the total electric potential Φ. The solution of Poisson equation (59) must satisfy the boundary conditions on the plate surface $z=0$ with a dielectric permeability $\varepsilon(\omega)$:

$$\Phi(x,y,+0)=\Phi(x,y,-0), \quad \partial_z\Phi(x,y,z)\big|_{z=+0}=\varepsilon\,\partial_z\Phi(x,y,z)\big|_{z=-0}. \quad (61)$$

To solve Eqn (59), we represent the potential Φ and polarization vector $\mathbf{P}$ in the form of Fourier integrals over the two-dimensional wave vector $\mathbf{k}=(k_x,k_y)$ and frequency ω. In particular,

$$\Phi(x,y,z,t)=\frac{1}{(2\pi)^3}\iiint{\rm d}\omega\,{\rm d}^2k\,\Phi(\omega,\mathbf{k};z)\exp\left({\rm i}k_xx+{\rm i}k_yy-{\rm i}\omega t\right). \quad (62)$$

After substituting (62) and a similar decomposition for $\mathbf{P}$ in (59), we obtain

$$\left(\frac{{\rm d}^2}{{\rm d}z^2}-k^2\right)\Phi(\omega,\mathbf{k};z) = 4\pi\delta(z-z_0)\left[{\rm i}k_xd_x^{\rm sp}(\omega-k_xV)+{\rm i}k_yd_y^{\rm sp}(\omega-k_xV)\right] + 4\pi\delta'(z-z_0)d_z^{\rm sp}(\omega-k_xV), \quad (63)$$

where $d_j^{\rm sp}(\omega-k_xV)$ are the Fourier components of the dipole moment projections $\mathbf{d}^{\rm sp}(t)$, $j=x,y,z$. The solution of

Eqn (63) with boundary conditions (61) yields the Fourier image of the induced part of the potential

$$\Phi^{\mathrm{ind}}(\omega,\mathbf{k};z)=\frac{2\pi}{k}\,\Delta(\omega)\exp\left[-k(z+z_0)\right]\times\left[\mathrm{i}k_x d_x^{\mathrm{sp}}(\omega-k_xV)+\mathrm{i}k_y d_y^{\mathrm{sp}}(\omega-k_xV)+k d_z^{\mathrm{sp}}(\omega-k_xV)\right], \tag{64}$$

where $\Delta(\omega)=(\varepsilon(\omega)-1)/(\varepsilon(\omega)+1)$. Taking Eqns (58), (62), and (64) into account, the Fourier components of the induced field can be expressed in terms of the Fourier image of the potential:

$$E_{x,y}^{\mathrm{ind}}(\omega,\mathbf{k};z)=-\mathrm{i}k_{x,y}\Phi^{\mathrm{ind}}(\omega,\mathbf{k};z)\,,\qquad E_z^{\mathrm{ind}}(\omega,\mathbf{k};z)=k\Phi^{\mathrm{ind}}(\omega,\mathbf{k};z)\,. \tag{65}$$

Ultimately, the induced field at the particle location $(x=Vt,0,z_0)$ is

$$\mathbf{E}^{\mathrm{ind}}=\frac{1}{(2\pi)^3}\iiint \mathrm{d}\omega\,\mathrm{d}^2k\,\mathbf{E}^{\mathrm{ind}}(\omega,\mathbf{k};z_0)\exp\left[-\mathrm{i}(\omega-k_xV)t\right]. \tag{66}$$

The first term in the right-hand side of (56) is obtained using (64)–(66) and the Fourier frequency decomposition of $\mathbf{d}^{\mathrm{sp}}(t)$. Here, correlators of the spontaneous dipole moment [formula (32)] appear in the corresponding integral expressions for the force projections $F_{x,z}$. After elementary integration over frequency and wave-vector components taking the analytic properties of $\alpha_{\mathrm{e}}(\omega)$ and $\Delta(\omega)$ (the evenness of real parts and the oddness of imaginary parts) into account, we obtain

$$F_x(T_1)=\frac{\hbar}{\pi^2}\int_0^\infty \mathrm{d}\omega\int_{-\infty}^{+\infty}\mathrm{d}k_x\int_{-\infty}^{+\infty}\mathrm{d}k_y\,kk_x\exp(-2kz)\times\Delta''(\omega)\alpha_{\mathrm{e}}''(\omega^+)\coth\frac{\hbar\omega^+}{2k_{\mathrm{B}}T_1}\,, \tag{67}$$

$$F_z(T_1)=-\frac{\hbar}{\pi^2}\int_0^\infty \mathrm{d}\omega\int_{-\infty}^{+\infty}\mathrm{d}k_x\int_{-\infty}^{+\infty}\mathrm{d}k_y\,k^2\exp(-2kz)\times\Delta'(\omega)\alpha_{\mathrm{e}}''(\omega^+)\coth\frac{\hbar\omega^+}{2k_{\mathrm{B}}T_1}\,, \tag{68}$$

where $\omega^+=\omega+k_xV$ and $k^2=k_x^2+k_y^2$. The corresponding contribution to the heating rate in (57) is expressed by a formula similar to (67) with the substitution $k_x\to-\omega^+$ in the integrand.

To calculate the force components and the heating rate due to spontaneous fluctuations of the plate field, we first find the induced dipole moment of the particle $\mathbf{d}^{\mathrm{ind}}$ using the linear integral relation [116]

$$\mathbf{d}^{\mathrm{ind}}(t)=\int_{-\infty}^{t}\mathrm{d}\tau\,\alpha_{\mathrm{e}}(t-\tau)\,\mathbf{E}^{\mathrm{sp}}(\mathbf{r}_0,\tau)\,, \tag{69}$$

where the spontaneous field of the plate is taken at the particle location point $\mathbf{r}_0=(Vt,0,z_0)$. By substituting the Fourier decomposition of the field $\mathbf{E}^{\mathrm{sp}}(\mathbf{r}_0,\tau)$ in (69), we obtain

$$\mathbf{d}^{\mathrm{ind}}(t)=\frac{1}{(2\pi)^3}\iiint \mathrm{d}\omega\,\mathrm{d}^2k\,\alpha_{\mathrm{e}}(\omega-k_xV)\,\mathbf{E}^{\mathrm{sp}}(\omega,\mathbf{k};z_0)\times\exp\left[-\mathrm{i}(\omega-k_xV)t\right]. \tag{70}$$

Given (70) and $\mathbf{E}^{\mathrm{sp}}(\omega,\mathbf{k};z_0)$, the second terms in formulas (56) and (57) follow. To calculate them, we use the FRD

$$\left\langle\mathbf{E}^{\mathrm{sp}}(\omega,\mathbf{k};z_0)\,\mathbf{E}^{\mathrm{sp}}(\omega',\mathbf{k}';z_0)\right\rangle=2(2\pi)^4k\hbar\exp(-2kz_0)\times\coth\frac{\hbar\omega}{2k_{\mathrm{B}}T_2}\,\Delta''(\omega)\delta(\omega+\omega')\delta(\mathbf{k}+\mathbf{k}')\,. \tag{71}$$

Formula (71) follows from (40), (42), and (45)–(47) in the limit $c\to\infty$. Using (71), the tangential and normal components of the fluctuation force caused by the induced particle dipole moments can be reduced to the form (here and below, we omit the index at z_0)

$$F_x(T_2)=-\frac{\hbar}{\pi^2}\int_0^\infty \mathrm{d}\omega\int_{-\infty}^{+\infty}\mathrm{d}k_x\int_{-\infty}^{+\infty}\mathrm{d}k_y\,kk_x\exp(-2kz)\times\Delta''(\omega)\alpha_{\mathrm{e}}''(\omega^+)\coth\frac{\hbar\omega}{2k_{\mathrm{B}}T_2}\,, \tag{72}$$

$$F_z(T_2)=-\frac{\hbar}{\pi^2}\int_0^\infty \mathrm{d}\omega\int_{-\infty}^{+\infty}\mathrm{d}k_x\int_{-\infty}^{+\infty}\mathrm{d}k_y\,k^2\exp(-2kz)\times\Delta''(\omega)\alpha_{\mathrm{e}}'(\omega^+)\coth\frac{\hbar\omega}{2k_{\mathrm{B}}T_2}\,. \tag{73}$$

The corresponding contribution to the thermal heating rate is also derived from (67) by replacing $k_x\to-\omega^+$. Taking Eqns (67) and (68) into account, the resulting nonrelativistic formulas for $F_{x,z}$ and $\mathrm{d}Q/\mathrm{d}t$ can be reduced to the form [15]

$$F_x=-\frac{\hbar}{\pi^2}\int_0^\infty \mathrm{d}\omega\int_{-\infty}^{+\infty}\mathrm{d}k_x\int_{-\infty}^{+\infty}\mathrm{d}k_y\,kk_x\exp(-2kz)\times\Delta''(\omega)\alpha_{\mathrm{e}}''(\omega^+)\left(\coth\frac{\hbar\omega}{2k_{\mathrm{B}}T_2}-\coth\frac{\hbar\omega^+}{2k_{\mathrm{B}}T_1}\right), \tag{74}$$

$$F_z=-\frac{\hbar}{\pi^2}\int_0^\infty \mathrm{d}\omega\int_{-\infty}^{+\infty}\mathrm{d}k_x\int_{-\infty}^{+\infty}\mathrm{d}k_y\,k^2\exp(-2kz)\times\left(\Delta''(\omega)\alpha_{\mathrm{e}}'(\omega^+)\coth\frac{\hbar\omega}{2k_{\mathrm{B}}T_2}+\Delta'(\omega)\alpha_{\mathrm{e}}''(\omega^+)\coth\frac{\hbar\omega^+}{2k_{\mathrm{B}}T_1}\right), \tag{75}$$

$$\frac{\mathrm{d}Q}{\mathrm{d}t}=\frac{\hbar}{\pi^2}\int_0^\infty \mathrm{d}\omega\int_{-\infty}^{+\infty}\mathrm{d}k_x\int_{-\infty}^{+\infty}\mathrm{d}k_y\,k\exp(-2kz)\times\Delta''(\omega)\alpha_{\mathrm{e}}''(\omega^+)\omega^+\left(\coth\frac{\hbar\omega}{2k_{\mathrm{B}}T_2}-\coth\frac{\hbar\omega^+}{2k_{\mathrm{B}}T_1}\right). \tag{76}$$

Formulas (74)–(76) are more suitable for the following comparison with relativistic results, unlike the formula obtained in [83]. Similar expressions can be obtained for a magnetic particle by replacing the electric polarizability with the magnetic one: $\alpha_{\mathrm{e}}(\omega)\to\alpha_{\mathrm{m}}(\omega)$. The presence of the frequency ω^+ in the hyperbolic cotangent depending on the particle temperature T_1 stresses the actuality of its motion (its dynamic nonequilibrium), while the contributions with the temperature T_2 are due to fluctuations of the immobile plate. In nonrelativistic motion without rotation, the particle heating rate in its rest frame, by virtue of (16), is determined by formula (76) for $\mathrm{d}Q/\mathrm{d}t$, and hence the particle heats even for equal temperatures $T_1=T_2$. In thermal equilibrium $T_1=T_2=T$, in the linear approximation in the particle velocity, Eqn (74) yields a formula for the 'viscous' friction force for the particle in the near field of the plate, which was first derived in [59]:

$$F_x=\frac{3}{2\pi}\frac{\hbar V}{z^5}\int_0^\infty \mathrm{d}\omega\,\alpha''(\omega)\Delta''(\omega)\,\frac{\mathrm{d}}{\mathrm{d}\omega}\left\{\frac{1}{\exp\left[\hbar\omega/(k_{\mathrm{B}}T)\right]-1}\right\}. \tag{77}$$

It is interesting to also consider the case of so-called quantum friction [55–60], where $T_1 = T_2 = 0$. The energy dissipation mechanism for nonrelativistic velocities is thought to be due to the generation of surface excitations [10, 11, 95]. Because the difference between hyperbolic cotangents in formula (74) with $T_1 = T_2 = 0$ is equal to $\operatorname{sign}\omega - \operatorname{sign}(\omega + k_x V)$, from (74) we obtain [83]

$$F_x = \frac{4\hbar}{\pi^2}\int_0^\infty \mathrm{d}k_x\, k_x \int_0^\infty \mathrm{d}k_y\, k \exp(-2kz) \times \int_0^{k_x V} \mathrm{d}\omega\, \alpha''(\omega - k_x V)\Delta''(\omega)\,, \tag{78}$$

with $F_x < 0$ because of the oddness of $\alpha''(\omega)$. For low particle velocities, $\alpha''(\omega) \sim \omega$ and $\Delta''(\omega) \sim \omega$, and Eqn (78) yields the dependence $F_x \propto V^3/z^7$. A formula similar to (78) with a cubic dependence on V was obtained for the quantum friction force between two plates [55, 60]. For an atom with the simplest oscillator form of the polarizability [see Eqn (82) below], formula (78) formally gives a zero force F_x. However, using the effective atomic polarizability of the particle, which takes the field of surface plasmons into account, a finite quantum friction force $F_x \propto \alpha_0^2 V^3/z^{10}$ follows from (78) (here, α_0 is the static polarizability of an atom) [56–58]. With the radiative correction to the polarizability taken into account, the quantum friction force (for an atom) behaves as $F_x \sim \alpha_0^2 V^5/z^9$ with a much smaller numerical value [56, 58]. These results are in full agreement with quantum field calculations [101, 102]. The presence of the quantum friction force at $T_1 = T_2 = 0$ (for atoms and nanoparticles) is due to the different mode distribution of the electromagnetic field near the plate compared to the vacuum modes in the empty space.

From formula (76), in turn, we obtain the heating rate

$$\frac{\mathrm{d}Q}{\mathrm{d}t} = \frac{4\hbar}{\pi^2}\int_0^\infty \mathrm{d}k_x \int_0^\infty \mathrm{d}k_y\, k \exp(-2kz) \times \int_0^{k_x V} \mathrm{d}\omega\, (\omega - k_x V)\alpha''(\omega - k_x V)\Delta''(\omega) \tag{79}$$

and hence $\mathrm{d}Q/\mathrm{d}t > 0$ due to the positive definiteness of the integrand. In addition, as follows from a comparison of (78) and (79), $-F_x V > \mathrm{d}Q/\mathrm{d}t$, i.e., the decrease in the particle kinetic energy due to quantum friction does not entirely transform into heating the particle. Clearly, part of the energy is transmitted to the plate.

In turn, formula (75) generalizes all known results for the nonretarded van der Waals interaction between a particle and a plate. For example, for $V = 0$ and $T_1 = T_2 = T$, using the analytic properties of the integrand and the standard rotation transformation of the frequency integration contour in the complex plane, we can rewrite formula (75) in the form [15]

$$F_z = -\frac{3}{2}\frac{k_\mathrm{B} T}{z^4}\sum_{n=0}^{\infty}{}'\left(1 - \frac{\delta_{n0}}{2}\right)\alpha(\mathrm{i}\xi_n)\Delta(\mathrm{i}\xi_n)\,, \qquad \xi_n = \frac{2\pi k_\mathrm{B} T}{\hbar}\, n\,. \tag{80}$$

Under thermal equilibrium conditions, the force F_z is related to the free energy $\tilde{F}(z, T)$ of the particle–surface system as $F_z = -(\partial\tilde{F}(z,T)/\partial z)_T$, and therefore the expression for $\tilde{F}(z, T)$ is obtained by multiplying (80) by $z/3$. The integration constant depending on temperature should vanish as $T \to 0$ by the Nernst–Planck postulate.

At the zero temperature $T = 0$, dynamic corrections to the force F_z of the (energy) interaction $U(z, V)$ of an atom with a wall were first considered in [117, 118]. Formula (85) includes these results as particular cases. For example, in the limit $T_1, T_2 \to 0$ and with the relation $F_z = -\partial U(z, V)/\partial z$, it follows from (75) that [119]

$$U(z,V) = -\frac{\hbar}{2\pi^2}\int_{-\infty}^{+\infty}\mathrm{d}k_x \int_{-\infty}^{+\infty}\mathrm{d}k_y\, k \exp(-2kz) \times \operatorname{Im}\left[\mathrm{i}\int_0^\infty \mathrm{d}\xi\, \Delta(\mathrm{i}\xi)\alpha(\mathrm{i}\xi + k_x V)\right] + \frac{2\hbar}{\pi^2}\int_0^\infty \mathrm{d}k_x \int_0^\infty \mathrm{d}k_y\, k \exp(-2kz) \times \int_0^{k_x V} \mathrm{d}\omega\, \Delta'(\omega)\alpha''(\omega - k_x V) = U^{(0)}(z,V) + \Delta U(z,V)\,. \tag{81}$$

In particular, for a metallic plate with a plasma-type dielectric function $\varepsilon(\omega) = 1 - \omega_\mathrm{p}^2/\omega^2$, where ω_p is the plasma frequency in a metal, using the resonance approximation for the atomic polarizability

$$\alpha(\omega) = \frac{\alpha(0)\omega_0^2}{\omega_0^2 - \omega^2 - \mathrm{i}0\omega}\,, \qquad \alpha''(\omega) = \frac{\pi\alpha(0)\omega_0}{2}\big(\delta(\omega - \omega_0) - \delta(\omega + \omega_0)\big)\,, \tag{82}$$

where $\alpha(0)$ and ω_0 are the static polarizability of an atom and the atomic transition frequency, the first term in the right-hand side of (81) in the low-velocity limit can be reduced to the form [119]

$$U^{(0)}(z,V) = -\frac{\hbar\alpha(0)\omega_\mathrm{s}\omega_0}{8z^3(\omega_\mathrm{s} + \omega_0)}\left[1 + \frac{3V^2}{2z^2(\omega_\mathrm{s} + \omega_0)^2}\right], \tag{83}$$

where $\omega_\mathrm{s} = \omega_\mathrm{p}/\sqrt{2}$. Formula (83) coincides with the results in [117, 118], where a quantum formula for $\alpha''(\omega)$ was used that takes several resonance lines into account, as well as with quantum perturbation theory calculations [93]. The applicability range of (83) corresponds to the condition $V \ll z(\omega_\mathrm{s} + \omega_0)$. In this case, the term $\Delta U(z, V)$ in (81) is exponentially small [119]. For $z(\omega_\mathrm{s} + \omega_0) \ll V \ll c$, by contrast, the term $\Delta U(z, V)$ dominates, which is absent in [93, 117, 118].

The results obtained can be easily generalized to the case of nonretarded interaction of a particle moving parallel to the walls (made of different materials) of a dielectric gap of width l. In particular, for $T = 0$, the resulting formula for $U(z, l, V)$ takes the form [120]

$$U(z,l,V) = -\frac{\hbar}{2\pi^2}\int_{-\infty}^{+\infty}\mathrm{d}k_x \int_{-\infty}^{+\infty}\mathrm{d}k_y\, k \exp(-2kz) \times \operatorname{Im}\left[\mathrm{i}\int_0^\infty \mathrm{d}\xi\, D(\mathrm{i}\xi, z, l)\alpha(\mathrm{i}\xi + k_x V)\right] + \frac{2\hbar}{\pi^2}\int_0^\infty \mathrm{d}k_x \int_0^\infty \mathrm{d}k_y\, k \exp(-2kz) \times \int_0^{k_x V} \mathrm{d}\omega\, \operatorname{Re}\big[D(\omega, z, l)\big]\alpha''(\omega - k_x V)\,, \tag{84}$$

$$D(\omega, z, l) = \frac{\Delta_1(\omega)\exp(-2kz) + \Delta_2(\omega)\exp\big[-2k(l - z)\big]}{1 - \Delta_1(\omega)\Delta_2(\omega)\exp(-2kl)}\,, \tag{85}$$

where $\Delta_i(\omega) = (\varepsilon_i(\omega) - 1)/(\varepsilon_i(\omega) + 1)$, $i = 1, 2$. Clearly, formula (81) can be derived from (84) in the limit $l \to \infty$.

4.2 Uniform rotation

In the FEI context, the effects of rotational motion of particles in a vacuum were first considered in [31–33] (see Section 5). In [90, 121], braking torques and other quantities were calculated for particles rotating in the near field of a heated plate in particular cases where the rotation axis is perpendicular [90] or parallel [90, 121] to the surface. Using the FEI formalism presented in Section 3, it is easy to obtain more general results for an arbitrary orientation of the particle rotation axis relative to the plate [122]. Here, new features appear that were not considered in [90, 121].

Figure 5 shows the configuration of the systems and reference frames used, Σ, Σ', and Σ''. The frame Σ corresponds to the plate at rest, Σ'' is the rest frame rigidly connected with the particle and rotating with an angular velocity Ω relative to the reference frame Σ'. The unit vector $\mathbf{n}$ of the angular velocity Ω has the components $(\cos\theta, 0, \sin\theta)$, and the angle θ ranges the interval $-\pi/2 \leqslant \theta \leqslant \pi/2$.

The quantities to be calculated, in addition to the attraction force to the surface F_z and the heat exchange rate $\mathrm{d}Q/\mathrm{d}t$ [see (56) and (57)], include the torque components

$$\mathbf{M} = \langle \mathbf{d}^{\,\mathrm{sp}} \times \mathbf{E}^{\,\mathrm{ind}} \rangle + \langle \mathbf{d}^{\,\mathrm{ind}} \times \mathbf{E}^{\,\mathrm{sp}} \rangle \,. \tag{86}$$

Due to the obvious invariance of F_z and $\mathrm{d}Q/\mathrm{d}t$ under rotations about the normal to the plate surface (z and z' axes in Fig. 5), the calculation of these quantities in frames Σ and Σ' gives the same result; however, they are more easily calculated in the frame Σ'. The components of the vector $\mathbf{M}$ are not invariant under rotations about z and z' axes; therefore, at the first stage of calculations, we find them in the frame Σ' and then transform to the frame Σ. To simplify formulas in what follows in this section, we omit primes at the quantities related to the frame Σ'.

The calculation of the first term in (86) and similar terms in (56) and (57) uses FDRs (34)–(39) for dipole moments. Here, the components of the induced field $\mathbf{E}^{\,\mathrm{ind}}$ are given by formulas (64) and (65) at $V = 0$. The calculations are similar to those that led to formulas (67) and (68).

When calculating the second terms in (56), (57), and (86), the induced dipole moment $\mathbf{d}^{\,\mathrm{ind}\,\prime\prime}(t)$ in the rest frame Σ'' of the rotating particle is expressed by a formula equivalent to (69):

$$\mathbf{d}^{\,\mathrm{ind}\,\prime\prime}(t) = \int_0^\infty \mathrm{d}\tau\, \alpha(\tau) \mathbf{E}^{\,\mathrm{sp}\,\prime\prime}(t - \tau) \,, \tag{87}$$

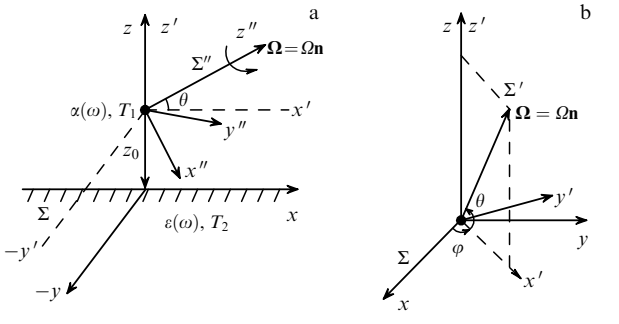

Figure 5. (a) Particle rotating near the plate surface and the reference frames used: (x, y, z), (x', y', z'), and (x'', y'', z''). (b) Reference frames used to describe the rotational and precessional motion.

where the field $\mathbf{E}^{\,\mathrm{sp}\,\prime\prime}(t - \tau)$ is taken at the particle location $(0, 0, z)$; the explicit dependence on the coordinate z is omitted in (87) and below. The vectors $\mathbf{d}^{\,\mathrm{ind}\,\prime\prime}$ and $\mathbf{E}^{\,\mathrm{sp}\,\prime\prime}$ in (87) are related to the vectors $\mathbf{d}^{\,\mathrm{ind}}$ and $\mathbf{E}^{\,\mathrm{sp}}$ in the frame Σ' by the formulas

$$d_i^{\,\mathrm{ind}}(t) = A_{ik}(t) d_k^{\,\mathrm{ind}\,\prime\prime}(t) \,, \tag{88}$$

$$E_i^{\,\mathrm{sp}\,\prime\prime}(t - \tau) = A_{im}^{-1}(t - \tau) E_m^{\,\mathrm{sp}}(t - \tau) \,, \tag{89}$$

where $A_{ik}(t)$ is rotation matrix (31) and $A_{km}^{-1}(t - \tau)$ is the inverse matrix,

$$A_{km}^{-1}(t - \tau) = n_k n_m + (\delta_{km} - n_k n_m) \cos\left[\Omega(t - \tau)\right] + e_{kmp} n_p \sin\left[\Omega(t - \tau)\right] . \tag{90}$$

By multiplying matrices $A_{ik}(t)$ and $A_{km}^{-1}(t - \tau)$, we obtain

$$A_{ik}(t) A_{km}^{-1}(t - \tau) = n_i n_m + (\delta_{im} - n_i n_m) \cos(\Omega\tau) - e_{iml} n_l \sin(\Omega\tau) \,. \tag{91}$$

It is easy to see that the right-hand side of (91) coincides with that of (31) after the corresponding change of indices: $A_{im}(\tau) \equiv A_{ik}(t) A_{km}^{-1}(t - \tau)$; therefore, after substituting (87) in (88) and taking (89) and (91) into account, the components of the induced dipole moment are given by the formula

$$d_i^{\,\mathrm{ind}}(t) = \int_0^\infty \mathrm{d}\tau\, \alpha(\tau) A_{im}(\tau) E_m^{\,\mathrm{sp}}(t - \tau) \,. \tag{92}$$

Next, by representing $E_m^{\,\mathrm{sp}}(t - \tau)$ as a Fourier integral over the frequency and two-dimensional wave vector at the particle location point,

$$E_m^{\,\mathrm{sp}}(t - \tau) = \int \frac{\mathrm{d}\omega\, \mathrm{d}^2 k}{(2\pi)^3} E_m^{\,\mathrm{sp}}(\omega, \mathbf{k}) \exp\left[-\mathrm{i}\omega(t - \tau)\right] , \tag{93}$$

and substituting (93) in (92), we obtain explicit expressions for the projections $d_i^{\,\mathrm{ind}}(t)$ (see Appendix B). Formulas (B4)–(B6) supersede formula (70) in the case of rotational motion of the particle. Further calculations repeat those in Section 4.1 with account for the FDRs presented in Section 3.2. The resulting expressions for F_z, $\mathrm{d}Q/\mathrm{d}t$, and the torque projections $M_{x', y', z'}$ are

$$F_z = -\frac{3\hbar}{32\pi z^4} \int_{-\infty}^{+\infty} \mathrm{d}\omega \Bigg[(2 - \cos^2\theta) \times \left(\Delta'(\omega)\alpha''(\omega) \coth \frac{\hbar\omega}{2k_\mathrm{B}T_1} + \Delta''(\omega)\alpha'(\omega) \coth \frac{\hbar\omega}{2k_\mathrm{B}T_2} \right) + (2 + \cos^2\theta) \left(\Delta'(\omega)\alpha''(\omega_+) \coth \frac{\hbar\omega_+}{2k_\mathrm{B}T_1} + \Delta''(\omega)\alpha'(\omega_+) \coth \frac{\hbar\omega}{2k_\mathrm{B}T_2} \right) \Bigg] , \tag{94}$$

$$\frac{\mathrm{d}Q}{\mathrm{d}t} = \frac{\hbar}{16\pi z^3} \int_{-\infty}^{+\infty} \mathrm{d}\omega\, \omega \Delta''(\omega) \Bigg[(2 - \cos^2\theta)\alpha''(\omega) \times \left(\coth \frac{\hbar\omega}{2k_\mathrm{B}T_2} - \coth \frac{\hbar\omega}{2k_\mathrm{B}T_1} \right) + (2 + \cos^2\theta)\alpha''(\omega_+) \left(\coth \frac{\hbar\omega}{2k_\mathrm{B}T_2} - \coth \frac{\hbar\omega_+}{2k_\mathrm{B}T_1} \right) \Bigg] , \tag{95}$$

$$M_{x'} = -\frac{3\hbar\cos\theta}{16\pi z^3}\int_{-\infty}^{+\infty} \mathrm{d}\omega\, \Delta''(\omega)\alpha''(\omega_+) \times \left(\coth\frac{\hbar\omega}{2k_\mathrm{B}T_2} - \coth\frac{\hbar\omega_+}{2k_\mathrm{B}T_1}\right), \quad (96)$$

$$M_{y'} = -\frac{\hbar\sin\theta\cos\theta}{16\pi z^3}\int_{-\infty}^{+\infty} \mathrm{d}\omega\left[\Delta'(\omega)\left(\alpha''(\omega)\coth\frac{\hbar\omega}{2k_\mathrm{B}T_1} - \alpha''(\omega_+)\coth\frac{\hbar\omega_+}{2k_\mathrm{B}T_1}\right) + \Delta''(\omega)\left(\alpha'(\omega)\coth\frac{\hbar\omega}{2k_\mathrm{B}T_1} - \alpha'(\omega_+)\coth\frac{\hbar\omega_+}{2k_\mathrm{B}T_1}\right)\right], \quad (97)$$

$$M_{z'} = -\frac{2\hbar\sin\theta}{16\pi z^3}\int_{-\infty}^{+\infty} \mathrm{d}\omega\, \Delta''(\omega)\alpha''(\omega_+) \times \left(\coth\frac{\hbar\omega}{2k_\mathrm{B}T_2} - \coth\frac{\hbar\omega_+}{2k_\mathrm{B}T_1}\right), \quad (98)$$

where $\omega_+ = \omega + \Omega$. We note that torque projections (96)–(98) refer to the frame Σ'.

Analysis of the rotational dynamics of a spherically symmetric particle can be conveniently performed in a more general geometry (Fig. 5b), when the orientation of the vector $\Omega\mathbf{n}$ relative to the plate (the reference frame Σ) is defined by angles θ and φ. The system of dynamic equations (25) then reduces to the form [122]

$$I\frac{\mathrm{d}\Omega}{\mathrm{d}t} = M_n\,, \quad (99)$$

$$I\Omega\frac{\mathrm{d}\theta}{\mathrm{d}t} = M_\perp\,, \quad (100)$$

$$I\Omega\cos\theta\frac{\mathrm{d}\varphi}{\mathrm{d}t} = M_y\,, \quad (101)$$

where I is the moment of inertia, M_n is the braking torque along the angular velocity determined by the expression

$$M_n = M_{x'}\cos\theta + M_{z'}\sin\theta = -\frac{\hbar(2+\cos^2\theta)}{16\pi z^3}\int_{-\infty}^{+\infty}\mathrm{d}\omega\,\Delta''(\omega)\alpha''(\omega_+) \times \left(\coth\frac{\hbar\omega}{2k_\mathrm{B}T_2} - \coth\frac{\hbar\omega_+}{2k_\mathrm{B}T_1}\right), \quad (102)$$

and $M_\perp$ is the orientation torque lying in one plane with the vector $\mathbf{n}$ and the z axis,

$$M_\perp = M_{z'}\cos\theta - M_{x'}\sin\theta = \frac{\hbar\sin\theta\cos\theta}{16\pi z^3}\int_{-\infty}^{+\infty}\mathrm{d}\omega\,\Delta''(\omega)\alpha''(\omega_+) \times \left(\coth\frac{\hbar\omega}{2k_\mathrm{B}T_2} - \coth\frac{\hbar\omega_+}{2k_\mathrm{B}T_1}\right). \quad (103)$$

The torque $M_{y'}$ perpendicular to this plane is given by formula (97). In the particular cases $\theta = 0, \pm\pi/2$, formula (102) coincides with results in [90, 121]. Here, as seen from (97) and (103), the direction of the angular velocity does not change with time ($M_{y'} = M_\perp = 0$). Equations (97), (102), and (103) enable a more detailed analysis of the character and stability of the rotational motion.

We first note that the signs of the torques M_n and $M_\perp$, generally speaking, can be different depending on the sign of the frequency integral in the right-hand sides of (102) and (103), which is the same in both cases [122]. If $M_n > 0$, the angular velocity can initially increase. However, the rate of establishing a quasi-equilibrium particle temperature $T_1 \approx T_2$ (which can be calculated by equating the right-hand side of (16) to zero) is much higher than the rate of establishing the dynamic equilibrium [90, 106], and in the quasistationary state we always have $M_n < 0$ [122]. As a result, during most of the time before stopping, the permanent slowing-down regime is realized, in which $M_n < 0$ and the sign of $M_\perp$ depends only on the sign of θ [see (103)] but does not change after the quasi-equilibrium temperature of the particle has been reached.

Next, from (99) and (100) with (102) and (103), we obtain the general relation between the angular velocity Ω and the orientation angle θ at an arbitrary time:

$$\Omega = \frac{\Omega_0\sin\theta_0\tan^2\theta_0}{\sin\theta\tan^2\theta}\,, \quad (104)$$

where Ω_0 and θ_0 are the values of these quantities at $t = 0$. Equation (104) implies that $\theta \to \pm\pi/2$ at the particle braking stage, depending on the sign of θ_0. Thus, for any initial conditions ($\theta_0 \neq 0$), the vector $\Omega\mathbf{n}$ tends to lie perpendicular to the surface, but the states with $\theta = \pm\pi/2$ are reached only at the full stop and are asymptotically stable. The state with the rotation axis parallel to the surface ($\theta = 0$) is unstable, and with any arbitrarily small deviation from this state, the modulus of θ would increase.

The change in the azimuthal angle φ does not affect Ω and θ by causing angular momentum precession relative to the z axis with the rate $\mathrm{d}\varphi/\mathrm{d}t$ according to formulas (97) and (101). In the case of a plate without dielectric losses ($\varepsilon''(\omega) = 0$), the precession rate $\mathrm{d}\varphi/\mathrm{d}t$ is independent of time, $\theta = \theta_0 = \mathrm{const}$ and $\Omega = \Omega_0 = \mathrm{const}$. Such a situation, however, is typical only for a nonretarded interaction with the plate. Accounting for retardation (see Section 6.5 and [112]) shows that the spinning particle is decelerated by its rotation near a transparent plate due to emission.

For $T_1 = T_2 = T$, formulas (102) and (103) in the linear order in the angular velocity take the form

$$M_n = -\frac{\hbar\Omega(2+\cos^2\theta)}{8\pi z^3}\int_0^\infty \mathrm{d}\omega\,\alpha''(\omega)\Delta''(\omega)\left(-\frac{\partial}{\partial\omega}\coth\frac{\hbar\omega}{2k_\mathrm{B}T}\right), \quad (105)$$

$$M_\perp = \frac{\hbar\Omega\sin\theta\cos\theta}{8\pi z^3}\int_0^\infty \mathrm{d}\omega\,\alpha''(\omega)\Delta''(\omega)\left(-\frac{\partial}{\partial\omega}\coth\frac{\hbar\omega}{2k_\mathrm{B}T}\right). \quad (106)$$

Formula (105) is a 'rotational analog' of formula (77) for the friction force acting on a particle moving parallel to the plate surface. For $T_1 = T_2 = 0$, Eqn (102) in turn leads to the formula for the torque of the quantum friction force during rotational motion:

$$M_n = \frac{\hbar(2+\cos^2\theta)}{8\pi z^3}\int_0^\Omega \mathrm{d}\omega\,\Delta''(\omega)\alpha''(\omega-\Omega)\,. \quad (107)$$

To conclude this section, we emphasize the difference between the heating components of a rotating particle from those in translational motion. At equal temperatures $T_1 = T_2$ (including the case $T_1 = T_2 = 0$), a rotating particle heats as in translational motion. But its heating rate in the comoving frame is not given by formula (95): it also includes the rotation energy dissipation rate $-M_n\Omega$ [in accordance with (16)]. Here, $\mathrm{d}Q/\mathrm{d}t < 0$, but $-M_n\Omega + \mathrm{d}Q/\mathrm{d}t > 0$. By adding $-M_n\Omega$ and $\mathrm{d}Q/\mathrm{d}t$ using (102) and (95) with the Ω-independent term

omitted, the frequency dependences in (76) and in the obtained expression turn out to be identical after the change $\omega + k_x V \leftrightarrow \omega + \Omega$.

5. Translational–rotational motion and emission of a neutral particle in a radiative vacuum background

5.1 Tangential force and heating rate in translational motion

In a simplified form, the problem of particle deceleration in an equilibrium electromagnetic radiation background was first discussed by Einstein and Hopf in [2], where they considered the motion of an oscillator relative to black-body radiation. In the more general case of nonrelativistic motion of a neutral particle in thermal equilibrium with the radiation background at a temperature T (see Fig. 2), the tangential braking force was first calculated almost a hundred years later, in [76] (also see [51]). This force is given by

$$F_x = -\frac{\hbar^2 V}{3\pi c^5 k_B T}\int_0^\infty \mathrm{d}\omega\,\omega^5 \alpha''(\omega)\sinh^{-2}\frac{\hbar\omega}{2k_B T}\,. \qquad (108)$$

We note that in the considered (nonrelativistic) limit, formula (108) is valid both in the radiation background frame (the frame Σ of configuration 3) and in the rest frame of a particle moving with velocity V (the frame Σ' of configuration 3). As shown in [123, 124], Eqn (108) can be rewritten in the form coincident with the Einstein and Hopf result under some additional assumptions.

The general relativistic expression for the tangential force within the FEI theory was first derived in [85, 88] and later confirmed by other authors [98, 99, 108]. In the notation used in [85, 88], the corresponding formula has the form

$$\begin{aligned} F_x &= \left\langle \nabla_x(\mathbf{d}^{\,\mathrm{sp}}\,\mathbf{E}^{\,\mathrm{ind}} + \mathbf{m}^{\,\mathrm{sp}}\,\mathbf{H}^{\,\mathrm{ind}}) + \nabla_x(\mathbf{d}^{\,\mathrm{ind}}\,\mathbf{E}^{\,\mathrm{sp}} + \mathbf{m}^{\,\mathrm{ind}}\,\mathbf{H}^{\,\mathrm{sp}})\right\rangle \\ &= -\frac{\gamma\hbar}{\pi c^4}\int_0^\infty \mathrm{d}\omega\,\omega^4\int_{-1}^{1}\mathrm{d}x\,x(1+\beta x)^2 \\ &\times\left\{\alpha_e''\left[\gamma\omega(1+\beta x)\right] + \alpha_m''\left[\gamma\omega(1+\beta x)\right]\right\} \\ &\times\left(\coth\frac{\hbar\omega}{2k_B T_2} - \coth\frac{\gamma\hbar\omega(1+\beta x)}{2k_B T_1}\right). \end{aligned} \qquad (109)$$

The contributions of spontaneous and induced dipole moments in (109) are represented by terms depending on the particle temperature T_1 (in its proper frame Σ') and the radiation background temperature T_2. When $T_1 = T_2 = T$ and $\beta \ll 1$, Eqn (109) reduces to (108). At $T_1 = T_2 = 0$, the tangential force vanishes.

The relativistic calculation of the second important FEI characteristic in this problem, the heating rate $\mathrm{d}Q/\mathrm{d}t$ [see (10) and (27)], leads to the expression [85, 88]

$$\begin{aligned} \dot{Q} &= \left\langle \nabla_x(\dot{\mathbf{d}}^{\,\mathrm{sp}}\,\mathbf{E}^{\,\mathrm{ind}} + \dot{\mathbf{m}}^{\,\mathrm{sp}}\,\mathbf{H}^{\,\mathrm{ind}})\right\rangle + \left\langle \nabla_x(\dot{\mathbf{d}}^{\,\mathrm{ind}}\,\mathbf{E}^{\,\mathrm{sp}} + \dot{\mathbf{m}}^{\,\mathrm{ind}}\,\mathbf{H}^{\,\mathrm{sp}})\right\rangle \\ &= \frac{\gamma\hbar}{\pi c^3}\int_0^\infty \mathrm{d}\omega\,\omega^4\int_{-1}^{1}\mathrm{d}x\,(1+\beta x)^3 \\ &\times\left\{\alpha_e''\left[\gamma\omega(1+\beta x)\right] + \alpha_m''\left[\gamma\omega(1+\beta x)\right]\right\} \\ &\times\left(\coth\frac{\hbar\omega}{2k_B T_2} - \coth\frac{\gamma\hbar\omega(1+\beta x)}{2k_B T_1}\right). \end{aligned} \qquad (110)$$

With Eqn (8), formula (110) allows analyzing the heating and the change in the particle temperature T_1 in its proper frame Σ'.

Next, by substituting (109) and (110) in (23), we immediately obtain the relativistic expression for the force F_x', also in the frame Σ' [107]:

$$\begin{aligned} F_x' &= \frac{\hbar}{\pi c^4}\int_0^\infty \mathrm{d}\omega\,\omega^4\int_{-1}^{1}\mathrm{d}x\,x\left(\alpha_e''(\omega) + \alpha_m''(\omega)\right) \\ &\times\coth\frac{\hbar\omega\gamma(1+\beta x)}{2k_B T_2}\,. \end{aligned} \qquad (111)$$

It is easy to see that for $\beta \ll 1$, formula (111) transforms into (108) if $T_2 = T$ and $\alpha_m''(\omega) = 0$. A significant new point is that formula (111) relates to the case where the particle is not in thermal equilibrium with the background. Formula (111) is important for the subsequent analysis of particle dynamics described by Eqn (24). In specific calculations of dissipative forces acting on atoms, the expression for atomic polarizability can also include contributions from radiative corrections [56, 108, 123].

5.2 Thermal emission of a particle

Formulas (109) and (110) can be used to find another important characteristic of a moving particle, its thermal radiation power [105]. Substituting these formulas in (13) gives

$$\begin{aligned} I &= -\frac{2\hbar\gamma}{\pi c^3}\int_0^\infty \mathrm{d}\omega\,\omega^4\int_{-1}^{1}\mathrm{d}x\,(1+\beta x)^2\alpha''(\omega_\beta) \\ &\times\left\{\frac{1}{\exp\left[\hbar\omega/(k_B T_2)\right]-1} - \frac{1}{\exp\left[\hbar\omega_\beta/(k_B T_1)\right]-1}\right\}, \end{aligned} \qquad (112)$$

where $\omega_\beta = \gamma\omega(1+\beta x)$ and $\alpha''(\omega) = \alpha_e''(\omega) + \alpha_m''(\omega)$. The first term in (112) depending on the temperature T_2 of the radiation background describes the power of absorbed radiation, and the term depending on the particle temperature T_1 describes the radiation power of the particle itself. This formula can be applied, like (109)–(111), under the dipole approximation condition $R \ll \min\left[2\pi\hbar c/(k_B T_1), 2\pi\hbar c/(k_B T_2)\right]$. The opposite case corresponding to the geometric optics limit (short-wave approximation) is considered in Section 6.

As shown in [105], the characteristic time of particle deceleration τ_V is much longer than the time of reaching the quasi-equilibrium temperature τ_Q (as in the case of rotation near a surface [90] or in a vacuum [106]). Then, for $t > \tau_Q$, the particle emission is determined by the corresponding effective (quasi-equilibrium) temperature. In particular, for a spherical conducting particle with the dielectric permeability $\varepsilon(\omega) = \mathrm{i}4\pi\sigma_0/\omega$ (where σ_0 is the static conductivity), the imaginary part of the low-frequency dielectric polarizability is $\alpha_e''(\omega) = 3R^3\omega/(4\pi\sigma_0)$, and the quasi-equilibrium temperature of the particle, which is determined from the condition $\mathrm{d}Q/\mathrm{d}t = 0$ [see (6)], is expressed as [105]

$$T_1 = T_2\left[\frac{1+2\beta^2+\beta^4/5}{(1-\beta^2)^2}\right]^{1/6}. \qquad (113)$$

Correspondingly, using (112) and (113) for the emission and absorption power of the particle, we obtain [105]

$$I_1 = \frac{8\pi^4}{21}\frac{\hbar R^3}{c^3\sigma_0}\left(\frac{k_B T_2}{\hbar}\right)^6\gamma^4\left(1+2\beta^2+\frac{\beta^4}{5}\right), \qquad (114)$$

$$I_2 = \frac{8\pi^4}{21}\frac{\hbar R^3}{c^3\sigma_0}\left(\frac{k_B T_2}{\hbar}\right)^6\gamma^2. \qquad (115)$$

Equations (114) and (115) suggest that in the quasithermal equilibrium with a radiation background, the emission power of a relativistic particle is about $3\gamma^2$ times as high as the absorption power. We also note that the form of the thermal emission spectrum of a moving particle [the integrand in frequency spectrum (112)] essentially depends on its dielectric properties, and the position of the maximum is determined by the Lorentz factor γ, shifting toward higher frequencies with increasing γ.

5.3 Dynamics and emission of a large black-body particle

The problems discussed in Sections 5.1 and 5.2 are also relevant to the case of particles (bodies) of a large radius $R \gg \max[2\pi\hbar c/(k_B T_1), 2\pi\hbar c/(k_B T_2)]$, i.e., in the geometric optics approximation. The simplest but practically very important model of condensed bodies with a large radius that enables studying their thermal and radiation properties is the black-body model. However, interest in the relativistic dynamics of a black-body particle appeared only after the discovery of the cosmic microwave background (CMB) radiation by Penzias and Wilson in 1965. For example, papers [125–128] discussed the possibility of detection of the absolute motion of Earth relative to the CMB. For this, the expression for the tangent force F_x' [similar to formula (111) for a small particle] acting on a spherical particle with radius R in its proper frame (the frame Σ' in configuration 3) moving relative to the CMB center of mass with a velocity βc was found. The corresponding formula is [125]

$$F_x' = -\frac{4}{3}\,\beta\gamma^2(\pi R^2)\,\frac{8\pi^5}{15}\,\frac{(k_B T_2)^4}{(2\pi\hbar c)^3} = -\frac{4}{3}\,\frac{\beta\gamma^2}{c}\,aT_2^4\,, \quad (116)$$

where T_2 is the CMB temperature, $a = 4\pi R^2\sigma_B$, and $\sigma_B = \pi^2 k_B^4/(60\hbar^3 c^2)$ is the Stephan–Boltzmann constant. In addition, the formula for the energy density of equilibrium electromagnetic radiation in Σ', which is important for further discussion, was obtained in [125]:

$$\varepsilon' = \frac{4}{c}\,\sigma_B T_2^4\gamma^2\left(1+\frac{\beta^2}{3}\right). \quad (117)$$

We note that these results can be derived from the expression for the energy–momentum tensor of an electromagnetic field in the proper frame Σ of the radiation background [129]:

$$T_{\mu\nu} = (p+\varepsilon)\,u_\mu u_\nu - p g_{\mu\nu}\,, \quad (118)$$

where $p = \varepsilon/3$, $\varepsilon = 4\sigma_B T_2^4/c$, u_μ are the 4-velocity components, $g_{\mu\nu}$ is the metric tensor, and $\mu, \nu = 0, 1, 2, 3$. Lorentz transformations of $T_{\mu\nu}$ from Σ to Σ' allow expressing the quantities F_x' and ε' in terms of the $T_{\mu\nu}'$ components. Clearly, formula (116), as well as (108), does not depend on the particle temperature, i.e., the proper thermal emission of the particle does not lead to the appearance of a braking force.

The important fact that general formulas (6), (13), and (21)–(23) remain valid in this case was first noted in [111]. This allows us to analyze the dynamics and to find radiation characteristics of a black-body particle in the CMB frame Σ using (116) and (117).

Following [111], we write the expression for the power of proper thermal emission of a particle with a temperature T_1 according to the Stephan–Boltzmann law:

$$I_1' = \sigma_B T_1^4 4\pi R^2 = aT_1^4\,. \quad (119)$$

On the other hand, with (117), the power of absorbed background radiation in Σ' is

$$I_2' = \frac{c}{4}\,\varepsilon' 4\pi R^2 = aT_2^4\gamma^2\left(1+\frac{\beta^2}{3}\right). \quad (120)$$

Hence, the thermal heating (cooling) rate of the particle in Σ' is determined by the difference between (120) and (119):

$$\frac{dQ'}{dt'} = \dot{Q}' = I_2' - I_1' = aT_2^4\gamma^2\left(1+\frac{\beta^2}{3}\right) - aT_1^4\,. \quad (121)$$

Next, using formula (6), we find dQ/dt:

$$\frac{dQ}{dt} = aT_2^4\left(1+\frac{\beta^2}{3}\right) - \frac{1}{\gamma^2}\,aT_1^4\,. \quad (122)$$

The expression for the force F_x, similar to (109) for a dipole particle, is obtained after substituting (116) and (122) in (23):

$$F_x = -\frac{\beta}{c}\,a\left(T_1^4 + \frac{1}{3}\,T_2^4\right). \quad (123)$$

Finally, substituting (122) and (123) in (13), we arrive at a quite unexpected result:

$$I = I_1 - I_2 = a(T_1^4 - T_2^4)\,. \quad (124)$$

Formula (124) formally coincides with a similar expression for a particle at rest relative to the background, but is significantly different from formula (112) for the emission power of a small particle [see, in particular, (114) and (115)], in which contributions from I_1 and I_2 to I are highly dependent on the γ factor. Formulas (123) and (122) share similar features (partial or complete absence of the γ factor), unlike (109) and (110).

The apparent paradoxicality of (124) is somewhat relaxed if we recall that a 'large' particle can also reach the state of quasithermal equilibrium with the radiation background. The corresponding temperature can be found from (122) by setting $dQ/dt = 0$ [cf. (113)]:

$$T_s = T_2\gamma^{1/2}\left(1+\frac{\beta^2}{3}\right)^{1/4}. \quad (125)$$

Substituting T_s instead of T_1 in (124), we obtain

$$I = aT_2^4\left[\gamma^2\left(1+\frac{\beta^2}{3}\right) - 1\right]. \quad (126)$$

The characteristic time of establishing the quasithermal equilibrium τ_Q and the deceleration time τ_V are [111]

$$\tau_Q = \frac{C_s\rho R}{3\sigma_B T_2^3}\,, \qquad \tau_V = \frac{\rho R c^2}{8\sigma_B T_2^4}\,, \quad (127)$$

where ρ is the particle mass density. For example, for an ice H_2O particle with radius $R = 1$ cm and density $\rho = 0.9\ \mathrm{g\,cm^{-3}}$, for the background temperature $T_2 = 50$ K, we find $\tau_V \approx 10^{10}$ years from (127). On the other hand, $\tau_Q/\tau_V = 8C_s T_2/(3c^2) \approx 10^{-10} - 10^{-14}$ for the typical values $C_s = 10 - 10^3$ J kg^{-1} K^{-1} and $T_2 = 10 - 10^3$ K. Thus, as in the case of a small radius, the processes of establishing thermal and dynamic equilibrium can be treated independently: with a fixed velocity (in the first case) or a fixed temperature (in the

second case). Detailed time dependences of the temperature and velocity can be found from Eqns (24), (116), and (121). The above results can be easily extended to the case of a 'gray' particle with given absorption a_a $(0 < a_a < 1)$ and emission a_r $(0 < a_r < 1)$ coefficients.

5.4 Translational–rotational motion of a particle

The translational–rotational motion of a dipole particle in a vacuum was considered in [106, 109]. The tangential force, the heating rate, and the torque are calculated in the standard way using the general formulas (26)–(28). It is assumed that the proper (Cartesian) reference frame of the particle Σ'' moves with a velocity $\mathbf{V}$ along the x axis of the vacuum reference frame Σ and rotates with an angular velocity Ω relative to the comoving fame Σ', which also moves with the velocity V along the x axis of the Σ frame (this is different from the assumptions on reference frames in Sections 5.1 and 5.2). In view of the obvious azimuthal symmetry of all quantities relative to the vector $\mathbf{V}$ direction, we can conveniently choose the axes (x', y', z') of the frame Σ' such that the particle angular velocity vector $\Omega\mathbf{n}$ lies in the (x', z') plane (see Fig. 3). In such frames, FDRs (34)–(39) remain valid, and induced dipole moments of the particle can be calculated using formulas (B1)–(B6) with the electric and magnetic field vectors transformed from the frame Σ into Σ'. The FDRs for vacuum electric and magnetic fields are expressed as in (53)–(55). The final expressions for F_x, $\mathrm{d}Q/\mathrm{d}t$, M_x, and M_z have the form [106, 109]

$$F_x = -\frac{\hbar\gamma}{4\pi c^4}\int_{-\infty}^{+\infty}\mathrm{d}\omega\,\omega^4 \times\int_{-1}^{1}\mathrm{d}x\,x\left[\alpha''(\omega_\beta)f_1(x,\beta,\theta)\left(\coth\frac{\hbar\omega}{2k_\mathrm{B}T_2}-\coth\frac{\hbar\omega_\beta}{2k_\mathrm{B}T_1}\right) +\alpha''(\omega_\beta^+)f_2(x,\beta,\theta)\left(\coth\frac{\hbar\omega}{2k_\mathrm{B}T_2}-\coth\frac{\hbar\omega_\beta^+}{2k_\mathrm{B}T_1}\right)\right], \quad (128)$$

$$\frac{\mathrm{d}Q}{\mathrm{d}t} = \frac{\hbar\gamma}{4\pi c^3}\int_{-\infty}^{+\infty}\mathrm{d}\omega\,\omega^4\int_{-1}^{1}\mathrm{d}x\,(1+\beta x) \times\left[\alpha''(\omega_\beta)f_1(x,\beta,\theta)\left(\coth\frac{\hbar\omega}{2k_\mathrm{B}T_2}-\coth\frac{\hbar\omega_\beta}{2k_\mathrm{B}T_1}\right) +\alpha''(\omega_\beta^+)f_2(x,\beta,\theta)\left(\coth\frac{\hbar\omega}{2k_\mathrm{B}T_2}-\coth\frac{\hbar\omega_\beta^+}{2k_\mathrm{B}T_1}\right)\right], \quad (129)$$

$$M_x = -\frac{\hbar\gamma\cos\theta}{4\pi c^3}\int_{-\infty}^{+\infty}\mathrm{d}\omega\,\omega^3 \times\int_{-1}^{1}\mathrm{d}x\,\alpha''(\omega_\beta^+)\left[(1+x^2)(1+\beta^2)+4\beta x\right] \times\left(\coth\frac{\hbar\omega}{2k_\mathrm{B}T_2}-\coth\frac{\hbar\omega_\beta^+}{2k_\mathrm{B}T_1}\right), \quad (130)$$

$$M_z = -\frac{\hbar\sin\theta}{8\pi c^3}\int_{-\infty}^{+\infty}\mathrm{d}\omega\,\omega^3\int_{-1}^{1}\mathrm{d}x\,\alpha''(\omega_\beta^+)(3-x^2+2\beta x) \times\left(\coth\frac{\hbar\omega}{2k_\mathrm{B}T_2}-\coth\frac{\hbar\omega_\beta^+}{2k_\mathrm{B}T_1}\right), \quad (131)$$

where $\omega_\beta = \gamma\omega(1+\beta x)$, $\omega_\beta^+ = \gamma\omega(1+\beta x)+\Omega$, and auxiliary functions $f_i(x,\beta,\theta)$ $(i=1,2)$ are given as

$$f_1(x,\beta,\theta) = (1-\beta^2)(1-x^2)\cos^2\theta + \left[(1+\beta^2)(1+x^2)+4\beta x\right]\frac{\sin^2\theta}{2}, \quad (132)$$

$$f_2(x,\beta,\theta) = (1-\beta^2)(1-x^2)\sin^2\theta + \left[(1+\beta^2)(1+x^2)+4\beta x\right]\frac{1+\cos^2\theta}{2}. \quad (133)$$

In these formulas, $\alpha''(\omega) = \alpha_\mathrm{e}''(\omega)+\alpha_\mathrm{m}''(\omega)$, as in (112). The presence or absence of the precession torque M_y in this case requires an additional study, but, as we show in what follows, this does not affect the particle dynamics considered below.

Substituting (128) and (129) in (13) yields the general formula for the particle emission and absorption power balance [109]:

$$I = I_1(T_1)-I_2(T_2) = \frac{\hbar\gamma}{4\pi c^3}\int_{-\infty}^{+\infty}\mathrm{d}\omega\,\omega^4 \times\int_{-1}^{1}\mathrm{d}x\left[\alpha''(\omega_\beta)f_1(x,\beta,\theta)\left(\coth\frac{\hbar\omega_\beta}{2k_\mathrm{B}T_1}-\coth\frac{\hbar\omega}{2k_\mathrm{B}T_2}\right) +\alpha''(\omega_\beta^+)f_2(x,\beta,\theta)\left(\coth\frac{\hbar\omega_\beta^+}{2k_\mathrm{B}T_1}-\coth\frac{\hbar\omega}{2k_\mathrm{B}T_2}\right)\right], \quad (134)$$

where the terms $I_1(T_1)$ and $I_2(T_2)$ depending on the temperatures T_1 and T_2 respectively describe the power of emitted and absorbed electromagnetic radiation. For $\Omega = 0$, formula (134) reduces to (112), and for $V = 0$, to the results in [31, 32]. Insofar as the frequency Ω is sufficiently low compared to the frequencies $k_\mathrm{B}T_{1,2}/\hbar$ or to the resonance absorption frequencies of the particle, the rotational effects on the thermal radiation spectrum are insignificant, and the results in Section 5.2 can be used. The opposite case is considered in [130]; however, the qualitative character of thermal radiation persists in this case. In particular, as in the case of no rotation, the particle can reach a quasi-equilibrium state with some effective temperature, albeit dependent on both the γ factor and Ω.

A qualitatively different situation arises at $T_1 = T_2 = 0$, because a particle rotating in a vacuum can generate nonthermal radiation. The appearance of excessive electromagnetic radiation ('superradiation') from a rotating cylinder, scattering incident photons, was first noted by Zel'dovich [131]. In the context of this review, the problem of nonthermal radiation from spinning particles was discussed in [33, 132]. A more general problem of radiation from a spinning particle in relativistic translational motion was discussed in [106, 109, 130].

The general expression for the power (intensity) of nonthermal radiation emerging during the translational–rotational motion of a dipole particle with an arbitrary misalignment between the linear and angular velocity vectors follows from (134) in the limit $T_1 \to 0$, $T_2 \to 0$. The terms with the temperature T_2 (which are responsible for absorption) then vanish, and the resulting formula takes the form [109]

$$I^{(0)} \equiv I_1(0) = \frac{\hbar\gamma}{2\pi c^3}\int_{-1}^{1}\mathrm{d}x\,f_2(x,\beta,\theta) \times\int_0^{\Omega\gamma^{-1}(1+\beta x)^{-1}}\mathrm{d}\omega\,\omega^4\alpha''\big(\Omega-\gamma\omega(1+\beta x)\big). \quad (135)$$

After integrating (135) over x using (133), we obtain

$$I^{(0)} = \frac{4\hbar}{3\pi c^3}\int_0^{\Omega}\mathrm{d}\xi\,\xi^4\alpha''(\Omega-\xi). \quad (136)$$

Formula (136) coincides with the results obtained in [132] (ignoring the magnetic polarization), where the translational motion of the particle was not taken into account, however. But we note that as follows from (135) and (136), while the

integral radiation power does not depend on the γ factor, the angular spectral intensity distribution is essentially dependent on it and on the mutual orientation of the linear and angular velocity vectors.

Making the substitution $\theta \to \theta_0$ in (135) (to emphasize the difference from the photon emission angle θ relative to the velocity $\mathbf{V}$) and taking into account that $x \equiv -\cos\theta$, we have the angular spectral emission power per unit solid angle $\mathrm{d}\tilde{\Omega} = 2\pi \sin\theta \, \mathrm{d}\theta$:

$$\frac{\mathrm{d}^2 I}{\mathrm{d}\omega \, \mathrm{d}\tilde{\Omega}} = \frac{\gamma\hbar\omega^4}{4\pi^2 c^3} \, \Theta\big(\Omega - \gamma\omega(1-\beta\cos\theta)\big) \times \alpha''\big(\Omega - \gamma\omega(1-\beta\cos\theta)\big) \Big\{ (1-\beta^2)(1-\cos^2\theta)\sin^2\theta_0 + \big[(1+\beta^2)(1+\cos^2\theta) - 4\beta\cos\theta\big] \, \frac{1+\cos^2\theta_0}{2} \Big\}, \quad (137)$$

where $\Theta(x)$ is the Heaviside step function.

Equation (137) implies that the nonthermal radiation is generated in the frequency range

$$0 < \omega < \frac{\Omega\sqrt{1-\beta^2}}{1-\beta\cos\theta},$$

and the maximum frequency $\omega_{\max} = \Omega\sqrt{(1+\beta)/(1-\beta)}$ is emitted along the particle motion, $\theta = 0$. In the opposite direction, the radiation frequency is $\omega_{\min} = \Omega\sqrt{(1-\beta)/(1+\beta)}$. For $\beta \ll 1$, the angular spectral intensity does not depend on the linear velocity and takes the simplest form

$$\frac{\mathrm{d}^2 I}{\mathrm{d}\omega \, \mathrm{d}\tilde{\Omega}} = \frac{\hbar\omega^4}{4\pi^2 c^3} \, \Theta(\Omega-\omega)\alpha''(\Omega-\omega) \times \left[\sin^2\theta \sin^2\theta_0 + (1+\cos^2\theta) \, \frac{1+\cos^2\theta_0}{2} \right]. \quad (138)$$

Generally, as seen from (137) and (138), the spectral shape is determined by the particle dielectric properties.

The dynamics of translational and rotational motion in the case $T_1 \to 0$, $T_2 \to 0$ can easily be analyzed using Eqns (128)–(131). After making the corresponding limit transitions and integrating over x, we obtain

$$F_x^{(0)} = -\frac{4\hbar V}{3\pi c^5} \int_0^\Omega \mathrm{d}\xi \, \xi^4 \alpha''(\Omega-\xi), \quad (139)$$

$$\frac{\mathrm{d}Q}{\mathrm{d}t} = -\frac{4\hbar}{3\pi c^3 \gamma^2} \int_0^\Omega \mathrm{d}\xi \, \xi^4 \alpha''(\Omega-\xi), \quad (140)$$

$$M_x = -\frac{4\hbar\cos\theta}{3\pi c^3 \gamma} \int_0^\Omega \mathrm{d}\xi \, \xi^3 \alpha''(\Omega-\xi), \quad (141)$$

$$M_z = -\frac{4\hbar\sin\theta}{3\pi c^3} \int_0^\Omega \mathrm{d}\xi \, \xi^3 \alpha''(\Omega-\xi). \quad (142)$$

Substituting (139) and (140) in Eqn (23) yields $F_x' = 0$, and hence there is no dissipative force in the proper reference frame of the particle. Correspondingly, it follows from translational motion equation (24) that the particle velocity is constant: $\beta = \text{const}$. We also note that the important relation $F_x^{(0)} = -(\beta/c) I^{(0)}$ follows from the general formula (13) using Eqns (136), (139), and (140).

We next note that Eqns (99) and (100) of the rotational dynamics in this case hold in the comoving reference frame Σ' if the projections of the torques in the right-hand side of these equations are also expressed in Σ'. Using (141) and (142) and taking into account that $M_x' = \gamma M_x$ and $M_z' = M_z$ and that the projections M_n' and $M_\perp'$ are related to M_x' and M_z' as $M_n' = M_x'\cos\theta + M_z'\sin\theta$ and $M_\perp' = -M_x'\sin\theta + M_z'\cos\theta$, we find

$$M_n' = -\frac{4\hbar}{3\pi c^3} \int_0^\Omega \mathrm{d}\xi \, \xi^3 \big[\alpha_\mathrm{e}''(\Omega-\xi) + \alpha_\mathrm{m}''(\Omega-\xi)\big], \quad M_\perp' = 0. \quad (143)$$

The first equation in (143) substituted in (99) determines the dynamics of particle rotation deceleration, and the equation $M_\perp' = 0$ [in view of (100)] implies that $\theta = \text{const}$. Therefore, the angle θ between the linear and angular velocity vectors remains constant in time.

To analyze the particle heating kinetics, we use Eqn (16). Assuming that the particle is characterized by the heat capacity $C_0(T_1)$, we write the left-hand side of (16) in the form $\mathrm{d}Q''/\mathrm{d}t = \mathrm{d}(C_0 T_1)/\mathrm{d}t$ and substitute (140)–(142) in the right-hand side of this equation. As a result, we obtain

$$\frac{\mathrm{d}(C_0 T_1)}{\mathrm{d}t} = \frac{4\hbar}{3\pi c^3 \gamma} \int_0^\Omega \mathrm{d}\xi \, \xi^3 (\Omega-\xi)\alpha''(\Omega-\xi). \quad (144)$$

According to (144), the particle temperature must increase with time. A thermal component then emerges in the radiation spectrum, and the analysis of particle dynamics and radiation should be performed using general equations (128)–(131) and (134).

6. Relativistic fluctuation-electromagnetic interaction between a small particle and a plate

6.1 General results

As in the case of the nonrelativistic friction force arising in the motion of a small particle in the near field of a surface (see Fig. 1, configuration 2), there was no initial consensus among different authors as to the solution of the relativistic problem [48, 49, 66–70, 80]. The situation became more clear after papers [74, 81, 82, 86] and later [98, 99]. The authors of [99], in particular, using a covariant formulation of fluctuation electrodynamics, calculated the dissipative force F_x, compared it with our results [86], and showed their identity. It was shown in [74] that the contribution from the near-field modes to the relativistic expressions for tangent and normal forces can be obtained by the limit transition to a rarefied medium for the material of one of the plates from the corresponding expression for the friction force between two plates in configuration 1. The inverse transition is also possible [15, 87] (see Section 7).

The force projections F_x and F_z, as well as the rate $\mathrm{d}Q/\mathrm{d}t$, can be calculated using the general method presented in Sections 2 and 3. In detailed form, including contributions from the near and radiation modes of the electromagnetic field, the results are presented in [14, 15, 81, 86]. In a more compact form, the resulting expressions can be represented as [15, 87]

$$F_x = -\frac{\hbar\gamma}{2\pi^2} \int_0^\infty \mathrm{d}\omega \int_{-\infty}^{+\infty} \mathrm{d}k_x \int_{-\infty}^{+\infty} \mathrm{d}k_y \times \left[\alpha_\mathrm{e}''(\gamma\omega^+) \, \mathrm{Im}\left(\frac{\exp(-2q_0 z)}{q_0} \, R_\mathrm{e}(\omega, \mathbf{k}) \right) + (\mathrm{e} \leftrightarrow \mathrm{m}) \right] \times \left(\coth\frac{\hbar\omega}{2k_\mathrm{B}T_2} - \coth\frac{\gamma\hbar\omega^+}{2k_\mathrm{B}T_1} \right), \quad (145)$$

$$F_z = -\frac{\hbar\gamma}{2\pi^2}\int_0^\infty \mathrm{d}\omega \int_{-\infty}^{+\infty}\mathrm{d}k_x \int_{-\infty}^{+\infty}\mathrm{d}k_y \times \left\{\alpha_\mathrm{e}''(\gamma\omega^+)\,\mathrm{Re}\left[\exp\left(-2q_0 z\right)R_\mathrm{e}(\omega,\mathbf{k})\right]\coth\frac{\gamma\hbar\omega^+}{2k_\mathrm{B}T_1} + \alpha_\mathrm{e}'(\gamma\omega^+)\,\mathrm{Im}\left[\exp\left(-2q_0 z\right)R_\mathrm{e}(\omega,\mathbf{k})\right]\coth\frac{\hbar\omega}{2k_\mathrm{B}T_2} + (\mathrm{e}\leftrightarrow\mathrm{m})\right\}, \tag{146}$$

$$\frac{\mathrm{d}Q}{\mathrm{d}t} = \frac{\hbar\gamma}{2\pi^2}\int_0^\infty \mathrm{d}\omega \int_{-\infty}^{+\infty}\mathrm{d}k_x \int_{-\infty}^{+\infty}\mathrm{d}k_y\,\omega^+ \times \left[\alpha_\mathrm{e}''(\gamma\omega^+)\,\mathrm{Im}\left(\frac{\exp\left(-2q_0 z\right)}{q_0}\,R_\mathrm{e}(\omega,\mathbf{k})\right) + (\mathrm{e}\leftrightarrow\mathrm{m})\right] \times \left(\coth\frac{\hbar\omega}{2k_\mathrm{B}T_2} - \coth\frac{\gamma\hbar\omega^+}{2k_\mathrm{B}T_1}\right), \tag{147}$$

where $\omega^+ = \omega + k_x V$, and the term shown symbolically as $(\mathrm{e}\leftrightarrow\mathrm{m})$ is identical to the preceding one with the corresponding change in the polarizabilities and functions $R_\mathrm{e}(\omega,\mathbf{k})$. The auxiliary relations are

$$R_\mathrm{e}(\omega,\mathbf{k}) = \Delta_\mathrm{e}(\omega)\left[2(k^2-k_x^2\beta^2)\left(1-\frac{\omega^2}{k^2c^2}\right)+\left(\frac{\omega^+}{c}\right)^2\right] + \Delta_\mathrm{m}(\omega)\left[2k_y^2\beta^2\left(1-\frac{\omega^2}{k^2c^2}\right)+\left(\frac{\omega^+}{c}\right)^2\right], \tag{148}$$

$$R_\mathrm{m}(\omega,\mathbf{k}) = \Delta_\mathrm{m}(\omega)\left[2(k^2-k_x^2\beta^2)\left(1-\frac{\omega^2}{k^2c^2}\right)+\left(\frac{\omega^+}{c}\right)^2\right] + \Delta_\mathrm{e}(\omega)\left[2k_y^2\beta^2\left(1-\frac{\omega^2}{k^2c^2}\right)+\left(\frac{\omega^+}{c}\right)^2\right], \tag{149}$$

$$\Delta_\mathrm{e}(\omega) = \frac{q_0\varepsilon(\omega)-q}{q_0\varepsilon(\omega)+q}, \qquad \Delta_\mathrm{m}(\omega) = \frac{q_0\mu(\omega)-q}{q_0\mu(\omega)+q}, \qquad q = \left(k^2-\frac{\omega^2}{c^2}\,\varepsilon(\omega)\,\mu(\omega)\right)^{1/2}, \qquad q_0 = \left(k^2-\frac{\omega^2}{c^2}\right)^{1/2}, \tag{150}$$

$$k^2 = k_x^2 + k_y^2.$$

It is important to note that in deriving formulas (145)–(147), we assumed the plate to be in thermal equilibrium with the vacuum background (at the temperature T_2); however, in formula (145) for the tangent force and (147) for the heat exchange rate, the terms related to the particle interaction with the vacuum background are omitted. These terms are described by formulas (109) and (110). In the limit $c\to\infty$, as can be easily seen, formulas (145)–(147) reduce to (74)–(76).

6.2 Equilibrium and nonequilibrium Casimir–Polder forces for a particle at rest

For $V=0$ and $T_1 = T_2 = 0$, formula (146) describes the 'cold' Casimir–Polder force. After the standard rotation of the frequency integration contour to the imaginary axis, this force takes the form [14, 15, 133]

$$F_z = -\frac{\hbar}{\pi}\int_0^\infty \mathrm{d}\xi \int_0^\infty \mathrm{d}k\,k\exp\left(-2\sqrt{k^2+\frac{\xi^2}{c^2}}\,z\right) \times \left(R_\mathrm{e}(\mathrm{i}\xi,k)\alpha_\mathrm{e}(\mathrm{i}\xi) + R_\mathrm{m}(\mathrm{i}\xi,k)\alpha_\mathrm{m}(\mathrm{i}\xi)\right), \tag{151}$$

$$R_\mathrm{e}(\mathrm{i}\xi,k) = \left(2k^2+\frac{\xi^2}{c^2}\right)\Delta_\mathrm{e}(\mathrm{i}\xi) - \frac{\xi^2}{c^2}\,\Delta_\mathrm{m}(\mathrm{i}\xi), \tag{152}$$

$$R_\mathrm{m}(\mathrm{i}\xi,k) = \left(2k^2+\frac{\xi^2}{c^2}\right)\Delta_\mathrm{m}(\mathrm{i}\xi) - \frac{\xi^2}{c^2}\,\Delta_\mathrm{e}(\mathrm{i}\xi). \tag{153}$$

For an ideally conducting particle and plate, as $\xi\to 0$, we have $\varepsilon(\mathrm{i}\xi)\to\infty$, $\Delta_\mathrm{e}(\mathrm{i}\xi)\to 1$, $\Delta_\mathrm{m}(\mathrm{i}\xi)\to -1$, $\alpha_\mathrm{e}(\mathrm{i}\xi)\to R^3$, and $\alpha_\mathrm{m}(\mathrm{i}\xi)\to -R^3/2$, and Eqn (151) implies that

$$F_z = -\frac{9}{4\pi}\,\frac{\hbar c R^3}{z^5}. \tag{154}$$

The correct numerical coefficient in (154), which is consistent with the quantum electrodynamic calculation in [134], can be obtained only with the magnetic polarization taken into account. In the original paper by Casimir and Polder [4], the magnetic polarization of the particle was ignored, and the numerical coefficient was 1.5 times as small.

For $T_1 = T_2 = T$ and $V=0$, proceeding in the same way as in transforming formula (75), after passing to the integration over imaginary frequency, formula (146) can be rewritten in the form [14, 15]

$$F_z = -2k_\mathrm{B}T\sum_{n=0}^{\infty}{}'\,a_n\int_0^\infty \mathrm{d}k\,k\left[R_\mathrm{e}(\mathrm{i}\xi_n,k)\alpha_\mathrm{e}(\mathrm{i}\xi_n) + R_\mathrm{m}(\mathrm{i}\xi_n,k)\alpha_\mathrm{m}(\mathrm{i}\xi_n)\right]\exp\left(-2\sqrt{k^2+\frac{\xi_n^2}{c^2}}\,z\right), \tag{155}$$

where $a_n = 1-\delta_{0n}/2$ and $\xi_n = 2\pi k_\mathrm{B}Tn/\hbar$. In (155), it is interesting to separate the thermal contribution to the Casimir–Polder force for the ideally conducting particle and the surface. The corresponding expressions are [14, 15]

$$F_z(T) = -\frac{3}{8}\,k_\mathrm{B}T\,\frac{R^3}{z^4}\,\varphi(x), \qquad x = \frac{2\pi k_\mathrm{B}z}{\hbar c}, \tag{156}$$

$$\varphi(x) = -3x + 3x\coth^2 x + 3\coth x - 3x^2\coth x + 3x^2\coth^3 x - \frac{12}{x} + x^3 - 4x^3\coth^2 x + 3x^3\coth^4 x. \tag{157}$$

The 'cold' part of the force can be found from (154). The 'thermal' force (156) prevails over the cold force (154) for $x>8$ (this corresponds to distances $z>8$ μm at $T=300$ K). In the high-temperature limit or for large distances between the particle and the surface, when $x\gg 1$ and $\varphi(x)\to 3$, formula (156) gives

$$F_z(T) = -\frac{9}{8}\,k_\mathrm{B}T\,\frac{R^3}{z^4}. \tag{158}$$

With the magnetic polarizability of the particle ignored, the numerical coefficient in (158), as in (154), turns out to be 1.5 times smaller.

For a cold particle ($T_1=0$) and a heated plate in thermal equilibrium with the vacuum background ($T_2 = T_3 = T$), the resulting force F_z differs from (155) by the additional contribution [14, 15]

$$\Delta F_z = \frac{2\hbar}{\pi}\int_0^\infty \mathrm{d}\omega\,\Pi(\omega,T)\alpha_\mathrm{e}''(\omega) \times \mathrm{Re}\left\{\int_0^\infty \mathrm{d}k\,k\exp\left(-2q_0 z\right)R_\mathrm{e}(\omega,k)\right\} + \left\{\alpha_\mathrm{e}''\to\alpha_\mathrm{m}'', R_\mathrm{e}\to R_\mathrm{m}\right\}, \tag{159}$$

where $\Pi(\omega,T) = 1/\{\exp\left[\hbar\omega/(k_\mathrm{B}T)\right]-1\}$, and the last term in the right-hand side (symbolically represented by the expression in curly brackets) is identical to the main term with the corresponding changes. For an atom in the ground state, correction (159) is small compared to (155), but for particles with noticeable absorption at thermal frequencies, it

can be substantial (in addition, it has a repulsive character). We here have a thermally nonequilibrium system.

Another type of thermal nonequilibrium was considered in [97, 135–140], where the attraction force F_z between a cold neutral particle or an atom in the ground state ($T_1 = 0$) and a heated plate ($T_2 = T_S$) was calculated assuming the surrounding background with either a zero temperature ($T_3 = 0$) or a temperature $T_3 = T_E$ different from T_S. It is important to note that the contributions from the near field modes of the surface (with two-dimensional wave vectors $k > \omega/c$) to F_z are independent of the vacuum background temperature. The nonequilibrium force $F^{\,\mathrm{neq}}(T_S, T_E)$ can then be represented in the form [15] (see also [136])

$$F^{\,\mathrm{neq}}(T_S, T_E) = F^{\mathrm{eq}}(T_S) + F_{\mathrm{th}}^{\mathrm{rad}}(T_E) - F_{\mathrm{th}}^{\mathrm{rad}}(T_S)\,, \quad (160)$$

where $F^{\mathrm{eq}}(T_S)$ is the equilibrium force defined by formula (155) at $T = T_S$, and $F_{\mathrm{th}}^{\mathrm{rad}}(T_E)$ and $F_{\mathrm{th}}^{\mathrm{rad}}(T_S)$ are contributions from radiation modes to the thermal part of the equilibrium force F_z (at the respective temperatures T_E and T_S), determined by the difference between (155) and (151). The expression for $F_{\mathrm{th}}^{\mathrm{rad}}(T)$ is [140]

$$F_{\mathrm{th}}^{\mathrm{rad}}(T) = -\frac{2\hbar}{\pi}\int_0^\infty \mathrm{d}\omega\, \alpha_{\mathrm{e}}'(\omega)\Pi(\omega, T) \times \int_0^{\omega/c} \mathrm{d}k\, k\, \mathrm{Im}\left[R_{\mathrm{e}} \exp\left(-2q_0 z\right)\right] + \{\alpha_{\mathrm{e}}' \to \alpha_{\mathrm{m}}', R_{\mathrm{e}} \to R_{\mathrm{m}}\}. \quad (161)$$

Formulas (160) and (161) are equivalent to expressions for the nonequilibrium force given in [136–139].

We note that in the case of unequal surface and vacuum background temperatures, the radiation modes are emitted or absorbed by the plate (the Poynting vector on the plate surface is nonzero). Formula (160) disregards these effects. The corresponding 'wind' force is repulsive, does not depend on the distance to the plate, and increases as the plate temperature increases [15]. Calculations show that for ^{87}Rb neutral atoms over a diamond plate with the temperature $T_S = 300$ K and a zero vacuum background temperature $T_E = 0$, the wind force increases the attraction force toward the plate, Eqn (160), at distances larger than 8 mm [15].

6.3 Casimir–Polder force for a moving particle

In the absence of dynamic equilibrium, but under the condition $T_1 = T_2 = 0$, the Casimir–Polder force acting on a moving particle is found from (146) by taking the limit transition $T_1 \to 0$, $T_2 \to 0$:

$$\lim_{T_1 \to 0} \coth \frac{\hbar\gamma(\omega + k_x V)}{2k_{\mathrm{B}} T_1} = \mathrm{sign}\,(\omega + k_x V)\,, \qquad \lim_{T_2 \to 0} \coth \frac{\hbar\omega}{2k_{\mathrm{B}} T_2} = \mathrm{sign}\,\omega\,, \quad (162)$$

and, after substituting these relations in (146), we obtain [89]

$$F_z = F_z^{(0)} + F_z^{(1)}\,, \quad (163)$$

$$F_z^{(0)} = -\frac{\hbar\gamma}{2\pi^2}\int_{-\infty}^{+\infty} \mathrm{d}k_x \int_{-\infty}^{+\infty} \mathrm{d}k_y \times \mathrm{Im}\left\{\int_0^\infty \mathrm{d}\xi \exp\left(-2\sqrt{k^2 + \frac{\xi^2}{c^2}}\, z_0\right)\alpha\left(\gamma(\mathrm{i}\xi + k_x V)\right) \times \left[\mathrm{i}R_{\mathrm{e}}^{(1)}(\mathrm{i}\xi, k) - 2\beta k_x \frac{\xi}{c}\left(\Delta_{\mathrm{e}}(\mathrm{i}\xi) + \Delta_{\mathrm{m}}(\mathrm{i}\xi)\right)\right]\right\}, \quad (164)$$

$$F_z^{(1)} = \frac{2\hbar\gamma}{\pi^2}\int_0^\infty \mathrm{d}k_x \int_0^\infty \mathrm{d}k_y \int_0^{k_x V} \mathrm{d}\omega\, \alpha''\left(\gamma(\omega - k_x V)\right) \times \mathrm{Re}\left\{\exp\left(-2\sqrt{k^2 - \frac{\omega^2}{c^2}}\, z_0\right) \times \left[R_{\mathrm{e}}^{(1)}(\omega, k) - 2\beta k_x \frac{\omega}{c}\left(\Delta_{\mathrm{e}}(\omega) + \Delta_{\mathrm{m}}(\omega)\right)\right]\right\}, \quad (165)$$

$$R_{\mathrm{e}}^{(1)}(\mathrm{i}\xi, k) = \Delta_{\mathrm{e}}(\mathrm{i}\xi)\left(2k^2 + \frac{\xi^2}{c^2}\right) + \Delta_{\mathrm{m}}(\mathrm{i}\xi)\left[2\beta^2\left(k^2 + \frac{\xi^2}{c^2}\right) - \frac{\xi^2}{c^2}\right] - \beta^2\left(\Delta_{\mathrm{e}}(\mathrm{i}\xi) + \Delta_{\mathrm{m}}(\mathrm{i}\xi)\right)\left(k^2 + \frac{2\xi^2}{c^2}\right)\cos^2\theta\,, \quad (166)$$

$$R_{\mathrm{e}}^{(1)}(\omega, k) = \left(\frac{\omega^2}{c^2} + k^2\beta^2\cos^2\theta\right)\left(\Delta_{\mathrm{e}}(\omega) + \Delta_{\mathrm{m}}(\omega)\right) + 2\left(k^2 - \frac{\omega^2}{c^2}\right)\left[(1 - \beta^2\cos^2\theta)\Delta_{\mathrm{e}}(\omega) + \Delta_{\mathrm{m}}(\omega)\beta^2\sin^2\theta\right], \quad (167)$$

where $\cos\theta = k_x/k$, $\beta = V/c$, and $\gamma = (1 - \beta^2)^{-1/2}$.

In the nonrelativistic limit $c \to \infty$, Eqns (163)–(165) imply

$$F_z = -\frac{\hbar}{\pi^2}\int_{-\infty}^{+\infty} \mathrm{d}k_x \int_{-\infty}^{+\infty} \mathrm{d}k_y\, k^2 \exp\left(-2kz_0\right) \times \mathrm{Im}\left[\mathrm{i}\int_0^\infty \mathrm{d}\xi\, \Delta(\mathrm{i}\xi)\alpha(\mathrm{i}\xi + k_x V)\right] + \frac{4\hbar}{\pi^2}\int_0^\infty \mathrm{d}k_x \int_0^\infty \mathrm{d}k_y\, k^2 \exp\left(-2kz_0\right)\int_0^{k_x V} \mathrm{d}\omega\, \Delta'(\omega)\alpha''(\omega - k_x V). \quad (168)$$

Formula (81) [119] can be derived from (168) taking the relation $F_z = -\partial U(z, V)/\partial z$ between the force F_z and the potential energy of the particle–plate system into account. In the case of an ideally conducting plate ($\Delta_{\mathrm{e}}(\omega) \to 1$ and $\Delta_{\mathrm{m}}(\omega) \to -1$) and atomic polarizability (82), it follows from (164) and (165) that [89]

$$F_z^{(0)} \simeq \begin{cases} \dfrac{\hbar\omega_0\alpha(0)}{8\pi z_0^4}\displaystyle\int_0^\infty \mathrm{d}x\, \frac{x^4}{\sqrt{\lambda^2 + x^2}}\,\frac{\mathrm{d}^3 K_0(x)}{\mathrm{d}x^3}\left[1 - \frac{(x^2 + 2\lambda^2)\beta^2}{2(\lambda^2 + x^2)}\right], & \beta \ll 1\,, \\ \dfrac{\hbar c\alpha(0)}{16\pi z_0^5\gamma}\displaystyle\int_0^\lambda \mathrm{d}x\, x^4\,\frac{\mathrm{d}^3 K_0(x)}{\mathrm{d}x^3}\left(1 - \frac{x^2}{2\lambda_0^2}\right), & \gamma \gg 1\,, \end{cases} \quad (169)$$

$$F_z^{(1)} = \frac{\hbar\omega_0\alpha(0)}{8\pi z_0^4\gamma}\int_{\lambda/\beta}^\infty \mathrm{d}x\, \frac{x^4}{\sqrt{\lambda_0^2 + x^2}}\,\frac{\mathrm{d}^3 K_0(x)}{\mathrm{d}x^3}\,, \quad (170)$$

where $\lambda = 2\omega_0 z_0/(\gamma c) \equiv \lambda_0/\gamma$ and $K_0(x)$ is the Macdonald function. Several important asymptotic forms for the force F_z can be obtained from (169) and (170), depending on the parameters λ_0, β, and γ. In particular, for $\beta \ll 1$ and $z_0 \gg V/(2\omega_0)$, we find the following asymptotic form from (169) and (170) [89, 91]:

$$F_z = F_z^{(0)} + F_z^{(1)} \approx -\frac{3}{2\pi}\,\frac{\hbar c\alpha(0)}{z_0^5}\left(1 - \frac{\beta^2}{2}\right). \quad (171)$$

Therefore, the first relativistic correction to the static Casimir–Polder force has a repulsive character. In [89],

numerical calculations of the force F_z for a metal plate with the Drude dielectric permittivity were carried out.

6.4 Cherenkov friction and radiation from a relativistic particle

In configuration 2 at $T_1 = T_2 = 0$ and $\beta \to 1$, the fluctuation-electromagnetic interaction of the particle with a transparent medium with a refractive index n can be accompanied by electromagnetic emission for $\beta > 1/n$, which is analogous to the Vavilov–Cherenkov effect [34]. Here, the frequency of photons emitted inside the Cherenkov cone satisfies the anomalous Doppler effect condition $\omega' < 0$ (where ω' is the photon frequency in the particle rest frame). The corresponding process has been called 'Cherenkov friction' [34, 100, 110, 132]. It is well known [141, 142] that in the anomalous Doppler effect for a particle with internal degrees of freedom moving with a velocity $V > c/n$, the emission of photons is attended by its excitation. The necessary energy is drawn from the particle kinetic energy.

In the considered case of a transparent dielectric plate, the wave surface surrounding the particle can go inside the plate (Fig. 6a), and therefore all considerations made in deriving formula (13) for the emission power remain valid. The quantities F_x and $\mathrm{d}Q/\mathrm{d}t$ can be found from (145) and (147) by taking limit transition (162). After performing some algebra, we obtain [143]

$$F_x = \frac{2\hbar\gamma}{\pi^2}\int_0^\infty \mathrm{d}\omega\,\theta(n\beta-1)\int_{\omega/V}^{n\omega/c}\mathrm{d}k_x\,k_x \times\int_0^{\sqrt{n^2\omega^2/c^2-k_x^2}}\mathrm{d}k_y\sum_{i=\mathrm{e,m}}\alpha_i''(\gamma\omega^-)\,\mathrm{Im}\left[\frac{\exp(-2q_0z_0)}{q_0}R_i(\omega,-k_x)\right], \tag{172}$$

$$\dot{Q} = \frac{2\hbar\gamma}{\pi^2}\int_0^\infty \mathrm{d}\omega\,\theta(n\beta-1)\int_{\omega/V}^{n\omega/c}\mathrm{d}k_x\int_0^{\sqrt{n^2\omega^2/c^2-k_x^2}}\mathrm{d}k_y\,\omega^- \times\sum_{i=\mathrm{e,m}}\alpha_i''(\gamma\omega^-)\,\mathrm{Im}\left[\frac{\exp(-2q_0z_0)}{q_0}R_i(\omega,-k_x)\right], \tag{173}$$

where $R_i(\omega,-k_x)$ is identical to $R_{\mathrm{e,m}}(\omega,\mathbf{k})$ in (148) and (149) for $\mathbf{k}=(-k_x,k_y)$, and $\omega^- = \omega - k_xV$, and $\theta(x)$ is the unit Heaviside function. In addition, by taking into account that for a transparent dielectric $\varepsilon(\omega)=n^2$, $\mathrm{Im}\,\varepsilon(\omega)=0$, and $\mu(\omega)=1$, the functions $\Delta_\mathrm{e}(\omega)$ and $\Delta_\mathrm{m}(\omega)$ in (150) can be represented in the form

$$\Delta_\mathrm{e}(\omega) = \frac{n^2\sqrt{k^2-\omega^2/c^2}-\sqrt{k^2-n^2\omega^2/c^2}}{n^2\sqrt{k^2-\omega^2/c^2}+\sqrt{k^2-n^2\omega^2/c^2}}, \qquad \Delta_\mathrm{m}(\omega) = \frac{\sqrt{k^2-\omega^2/c^2}-\sqrt{k^2-n^2\omega^2/c^2}}{\sqrt{k^2-\omega^2/c^2}+\sqrt{k^2-n^2\omega^2/c^2}}. \tag{174}$$

Substituting (172) and (173) in (13) yields

$$I = -\frac{2\hbar\gamma}{\pi^2}\int_0^\infty \mathrm{d}\omega\,\theta(n\beta-1) \times\int_{\omega/V}^{n\omega/c}\mathrm{d}k_x\int_0^{\sqrt{n^2\omega^2/c^2-k_x^2}}\mathrm{d}k_y\,\omega\sum_{i=\mathrm{e,m}}\alpha_i''(\gamma\omega^-) \times\mathrm{Im}\left[\frac{\exp(-2q_0z_0)}{q_0}R_i(\omega,-k_x)\right]. \tag{175}$$

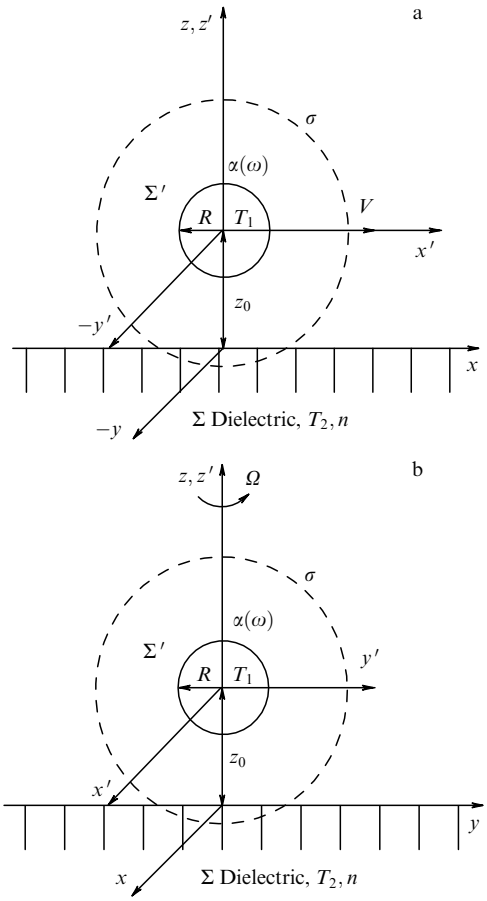

Figure 6. (a) Schematics of particle motion near a transparent dielectric under Cherenkov friction. (b) Schematics of the rotational motion and radiation of a particle near the transparent dielectric surface.

Formula (175) coincides with similar results in [100, 110], with the difference that the magnetic polarizability of the particle $\alpha_\mathrm{m}''(\omega)$ is also taken into account in (175).

The integration limits in (175) agree with the anomalous Doppler effect conditions in the particle rest frame Σ', because the photon frequency $\omega' = \gamma(\omega - k_xV)$ is negative in Σ'. Because of the analytic properties of $\alpha_{\mathrm{e,m}}''(\omega)$ and $\exp(-2q_0z_0)/q_0$ and the positive definiteness of $\Delta_{\mathrm{e,m}}(\omega)$ within the corresponding integration limits, Eqns (172)–(175) imply that $F_x < 0$, $\dot{Q} > 0$, and $I > 0$. Here, all three quantities are related by condition (13). This means that the Cherenkov friction leads to a partial conversion of the particle kinetic energy into radiation. The positive sign of $\dot{Q}$ is consistent with the concept of excitation of internal degrees of freedom in the anomalous Doppler effect. Here, the energy absorption rate by the particle in Σ' and $\mathrm{d}Q'/\mathrm{d}t'$ is obtained from formula (6). For a multi-atom particle or an atom, as above, $\mathrm{d}Q'/\mathrm{d}t'$ can be respectively associated with the heating rate and the inner atomic transition rate.

As stated in [34, 100, 132], a quantum vacuum instability occurs in the considered system, which is similar to the creation of electron–positron pairs in a strong electric field or to the Hawking radiation in a strong gravitational field. Zel'dovich's 'superradiation' from a rotating cylinder has the same nature [131]. We must note an important difference between formulas (175) and (136), however: the emission from a spinning particle does not have a lower angular velocity threshold, whereas radiation in the rectilinear motion does have a lower velocity threshold.

To conclude this section, we present a formula for the radiation force F'_x in the particle rest frame Σ', which is needed in solving dynamic equations (24). Substituting (172) and (173) in (23), we obtain [143] (see also [110])

$$F'_x = \frac{2\hbar\gamma^2}{\pi^2}\int_0^\infty \mathrm{d}\omega\,\theta(n\beta-1)\int_{\omega/V}^{n\omega/c}\mathrm{d}k_x\left(k_x-\frac{\beta\omega}{c}\right)\times\int_0^{\sqrt{n^2\omega^2/c^2-k_x^2}}\mathrm{d}k_y\sum_{i=\mathrm{e,m}}\alpha_i''(\gamma\omega^-)\times\mathrm{Im}\left[\frac{\exp\left(-2q_0z_0\right)}{q_0}\,R_i(\omega,-k_x)\right]. \tag{176}$$

Formula (176) implies that $F'_x<0$, i.e., the particle should be decelerating. In [100, 110], the radiation forces and radiation powers for model polarizabilities of atoms and dielectric particles were calculated numerically. We note, however, that the experimental detection of radiation in this situation is very difficult due to two factors: (1) the need to have an electrically neutral relativistic particle, and (2) the short fly-by time of the particle over an extended plate with an atomically smooth surface.

6.5 Radiation from a particle rotating near a transparent dielectric plate

As shown in Section 4.2, the angular velocity vector of a dipole particle rotating in the near field of a plate tends to become normal to its surface. Therefore, to facilitate the analysis, we consider just this configuration below. As in Section 6.4, we consider a dielectric plate. To calculate the emission power, we use Eqn (13) again with a zero translational velocity (Fig. 6b). In this case, the heating rate $\mathrm{d}Q/\mathrm{d}t$ cannot be calculated using formula (95), but the retardation effects should be taken into account. In agreement with the results in [144], we obtain

$$\frac{\mathrm{d}Q}{\mathrm{d}t}=\frac{\hbar}{4\pi^2}\int_{-\infty}^{+\infty}\mathrm{d}\omega\,\omega\left\{\int\mathrm{d}^2k\sum_{s=\mathrm{e,m}}\alpha_s''(\omega_+)\times\mathrm{Im}\left[\frac{\exp\left(-2q_0z_0\right)}{q_0}\,R_s(\omega,\mathbf{k})\right]\right\}\left(\coth\frac{\hbar\omega}{2k_\mathrm{B}T_2}-\coth\frac{\hbar\omega_+}{2k_\mathrm{B}T_1}\right)+\frac{\hbar}{4\pi^2}\int_{-\infty}^{+\infty}\mathrm{d}\omega\,\omega\left\{\int\mathrm{d}^2k\sum_{s=\mathrm{e,m}}\alpha_s''(\omega)\times\mathrm{Im}\left[\frac{\exp\left(-2q_0z_0\right)}{q_0}\,k^2\Delta_s(\omega)\right]\right\}\left(\coth\frac{\hbar\omega}{2k_\mathrm{B}T_2}-\coth\frac{\hbar\omega}{2k_\mathrm{B}T_1}\right), \tag{177}$$

$$R_\mathrm{e}(\omega,k)=\left(k^2-\frac{\omega^2}{c^2}\right)\Delta_\mathrm{e}+\frac{\omega^2}{c^2}\,\Delta_\mathrm{m}\,, \tag{178}$$

$$R_\mathrm{m}(\omega,k)=\left(k^2-\frac{\omega^2}{c^2}\right)\Delta_\mathrm{m}+\frac{\omega^2}{c^2}\,\Delta_\mathrm{e}\,,$$

$$\Delta_\mathrm{e}=\frac{n^2q_0-q}{n^2q_0+q}\,,\qquad \Delta_\mathrm{m}=\frac{q_0-q}{q_0+q}\,, \tag{179}$$

$$q_0=\sqrt{k^2-\frac{\omega^2}{c^2}},\qquad q=\sqrt{k^2-\frac{n^2\omega^2}{c^2}},\qquad \omega_+=\omega+\Omega\,.$$

It is easy to see that for $\Omega=0$, formula (177) coincides with (147) for $V=0$. In this particular case, Eqn (177) describes the thermally nonequilibrium situation of heat exchange between a particle at rest and the plate. On the other hand, in the nonrelativistic limit $c\to\infty$, Eqn (177) reduces to (95) (for $\theta=\pi/2$).

Of the greatest interest is nonthermal emission from a spinning particle. Making the limit transition $T_1=T_2=0$ in (177) using (162) and taking into account that $I=-\mathrm{d}Q/\mathrm{d}t$ due to (13), we obtain [112]

$$I=-\frac{\hbar}{\pi}\int_0^\Omega\mathrm{d}\omega\,\omega\int_0^{\omega n/c}\mathrm{d}k\,k\sum_{s=\mathrm{e,m}}\alpha_s''(\Omega-\omega)\times\mathrm{Im}\left[\frac{\exp\left(-2q_0z_0\right)}{q_0}\,R_s\right]. \tag{180}$$

The corresponding formula for the braking torque in this case is [112]

$$M_z=\frac{2\hbar}{\pi}\int_0^\Omega\mathrm{d}\omega\int_0^{\omega n/c}\mathrm{d}k\,k\sum_{s=\mathrm{e,m}}\alpha_s''(\Omega-\omega)\times\mathrm{Im}\left[\frac{\exp\left(-2q_0z_0\right)}{q_0}\,R_s\right]. \tag{181}$$

Formulas more convenient for analysis can be derived from these expressions by taking (178) and (179) into account:

$$I=-\frac{\hbar}{\pi c^3}\int_0^\Omega\mathrm{d}\omega\,\omega^4\sum_{s=\mathrm{e,m}}\alpha_s''(\Omega-\omega)\psi_s\left(n,\frac{\omega z_0}{c}\right), \tag{182}$$

$$M_z=\frac{2\hbar}{\pi c^3}\int_0^\Omega\mathrm{d}\omega\,\omega^3\sum_{s=\mathrm{e,m}}\alpha_s''(\Omega-\omega)\psi_s\left(n,\frac{\omega z_0}{c}\right), \tag{183}$$

$$\psi_\mathrm{e}(n,x)=\int_0^n\mathrm{d}t\,t\,\mathrm{Im}\left\{\frac{\exp\left(-2x\sqrt{t^2-1}\right)}{\sqrt{t^2-1}}\times\left[(t^2-1)\frac{n^2\sqrt{t^2-1}-\sqrt{t^2-n^2}}{n^2\sqrt{t^2-1}+\sqrt{t^2-n^2}}+\frac{\sqrt{t^2-1}-\sqrt{t^2-n^2}}{\sqrt{t^2-1}+\sqrt{t^2-n^2}}\right]\right\}, \tag{184}$$

$$\psi_\mathrm{m}(n,x)=\int_0^n\mathrm{d}t\,t\,\mathrm{Im}\left\{\frac{\exp\left(-2x\sqrt{t^2-1}\right)}{\sqrt{t^2-1}}\times\left[(t^2-1)\frac{\sqrt{t^2-1}-\sqrt{t^2-n^2}}{\sqrt{t^2-1}+\sqrt{t^2-n^2}}+\frac{n^2\sqrt{t^2-1}-\sqrt{t^2-n^2}}{n^2\sqrt{t^2-1}+\sqrt{t^2-n^2}}\right]\right\}. \tag{185}$$

Comparing formulas (136) and (142) for the radiation intensity from a particle spinning in a vacuum and the torque acting on it with formulas (182) and (183) reveals that the presence of the plate increases these quantities by numerical factors depending on the refractive index and distance. Calculations [112] show that the functions $\psi_{\mathrm{e,m}}(n,x)$ are negative and rapidly increase (by modulus) as n increases, which means that the transparent dielectric plate enhances the nonthermal emission. Here, a much stronger emission is expected from metal particles with high magnetic polarizability because $|\psi_\mathrm{m}(n,x)|\gg|\psi_\mathrm{e}(n,x)|$, $n\gg1$. The dependence on the distance is determined by the retardation factor $\Omega z_0n/c$ and turns out to be insignificant for $\Omega z_0n/c<1$.

Formulas (182) and (183) also imply that $-M_z\Omega>I$. The energy balance equation according to (15) (for $\gamma=1$) has the form $-M_z\Omega=I+\mathrm{d}Q''/\mathrm{d}t$, where $\mathrm{d}Q''/\mathrm{d}t$ is the particle heating rate, which suggests that part of the kinetic energy is expended for thermal excitation of the particle, as in the case of Cherenkov friction, and hence the state $T_1=0$ is unstable. The radiation spectrum, similarly to the particle radiation spectrum in a vacuum, is determined by dielectric characteristics of the particle and has no lower angular velocity (frequency) threshold. This creates more favorable condi-

tions for the experimental detection of nonthermal radiation from spinning particles (see Section 8.4).

7. Fluctuation-electromagnetic interaction in the plate–plate configuration

7.1 Modification of the rarefied medium limit for transitions between particle–plate and plate–plate configurations

The limit transition from the two-plate configuration to the small-particle–plate configuration (transition $1 \to 2$) in the static case was already found by Lifshitz [5]. Since then, this transition has been used in the original form to calculate FEI effects in configuration 2 in both equilibrium and nonequilibrium conditions [10, 11, 56, 72].

As shown in [87], based on the fact that all quantities characterizing the FEI in both configurations (F_x, F_z, and $\dot{Q}$) should be derived from the solution of one electrodynamic problem (in proper configurations), it can be asserted that any relation between them in one configuration also holds in other configurations. This enables formulas for configuration 1 to be uniquely obtained from the corresponding formulas for configuration 2, but only in the nonrelativistic approximation. Unfortunately, the use of the 'correspondence principle' in the relativistic case does not lead to unique results.

The rule for calculating the Casimir–Polder force $F_z^{(2)}(z)$ acting on a small particle (atom) located at a distance z from the plate is [23, 145, 146]

$$F_z^{(2)}(z) = -\frac{1}{n_1 S}\frac{\mathrm{d}F_z^{(1)}(l)}{\mathrm{d}l}\bigg|_{l=z}. \tag{186}$$

Here, indices 1 and 2 relate to the corresponding configurations, and $F_z^{(1)}(l)/S$ is the Casimir force in configuration 1 related to the area S of the vacuum interface between the plates separated by a gap of width l. The relation between the tangent forces $F_x^{(1,2)}$ and the heating rates $\mathrm{d}Q^{(1,2)}/\mathrm{d}t$ in configurations 1 and 2 are expressed in a form similar to (186):

$$\begin{aligned} F_x^{(2)}(z) &= -\frac{1}{n_1 S}\frac{\mathrm{d}F_x^{(1)}(l)}{\mathrm{d}l}\bigg|_{l=z}, \\ \frac{\mathrm{d}Q^{(2)}(z)}{\mathrm{d}t} &= -\frac{1}{n_1 S}\frac{\mathrm{d}\dot{Q}^{(1)}(l)}{\mathrm{d}l}\bigg|_{l=z}. \end{aligned} \tag{187}$$

Formulas (186) and (187) should be complemented by relations between the reflection amplitude $\Delta_{\mathrm{e,m}}$ and polarizabilities $\alpha_{\mathrm{e,m}}$ of the particle corresponding to a rarefied material of the plate [87],

$$\Delta_{1\mathrm{e}}(\omega) \to \frac{\pi n_1}{q_0^2}\left[\alpha_{\mathrm{e}}(\omega)\left(2k^2 - \frac{\omega^2}{c^2}\right) + \alpha_{\mathrm{m}}(\omega)\frac{\omega^2}{c^2}\right], \tag{188}$$

$$\Delta_{1\mathrm{m}}(\omega) \to \frac{\pi n_1}{q_0^2}\left[\alpha_{\mathrm{m}}(\omega)\left(2k^2 - \frac{\omega^2}{c^2}\right) + \alpha_{\mathrm{e}}(\omega)\frac{\omega^2}{c^2}\right]. \tag{189}$$

More simple limit relations $\Delta_{1\mathrm{e}}(\omega) \to 2\pi n_1 \alpha_{\mathrm{e}}(\omega)$, $\Delta_{1\mathrm{m}}(\omega) \to 2\pi n_1 \alpha_{\mathrm{m}}(\omega)$, as used in [10, 11, 56, 72], follow from (188) and (189) in the limit $c \to \infty$.

7.2 Nonrelativistic interaction between relatively moving plates

We begin with nonrelativistic formulas (74)–(76). Using (75), we first write an expression for the attraction force applied to the particle from the plate for $V = 0$ and $T_1 = T_2 = T$:

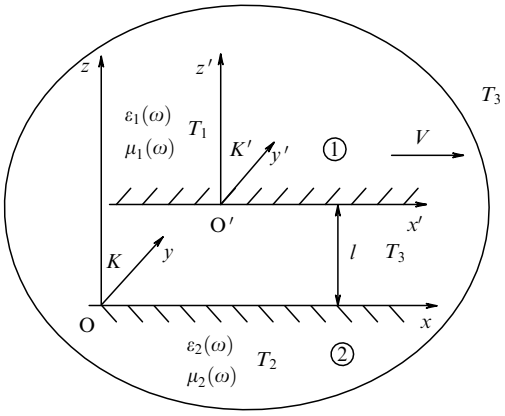

Figure 7. General nonequilibrium configuration 1 (Casimir–Lifshitz configuration) in the reference frame related to the plates. The temperature T_3 of the vacuum background between the plates and on their external sides can generally differ from the temperature T_2 of plate 2 at rest. In the nonrelativistic approximation, the FEI of the plates is independent of the temperature T_3 (i.e., of the background state).

$$\begin{aligned} F_z^{(1)}(z) = -\frac{\hbar}{\pi^2}\int_0^\infty \mathrm{d}\omega \int_{-\infty}^{+\infty}\mathrm{d}k_x \int_{-\infty}^{+\infty}\mathrm{d}k_y\, k^2 \exp(-2kz) \\ \times \left(\Delta''(\omega)\alpha_{\mathrm{e}}'(\omega)\coth\frac{\hbar\omega}{2k_{\mathrm{B}}T} + \Delta'(\omega)\alpha_{\mathrm{e}}''(\omega)\coth\frac{\hbar\omega}{2k_{\mathrm{B}}T}\right). \end{aligned} \tag{190}$$

A comparison of (190) and (75) reveals that the transition to nonequilibrium dynamic and thermal states of the interacting plates for configuration 1 (Fig. 7) is made using the transformations

$$\begin{aligned} &\Delta''(\omega)\coth\frac{\hbar\omega}{2k_{\mathrm{B}}T} \to \Delta''(\omega)\coth\frac{\hbar\omega}{2k_{\mathrm{B}}T_2}, \\ &\alpha_{\mathrm{e}}''(\omega)\coth\frac{\hbar\omega}{2k_{\mathrm{B}}T} \to \alpha_{\mathrm{e}}''(\omega^+)\coth\frac{\hbar\omega^+}{2k_{\mathrm{B}}T_1}, \\ &\alpha_{\mathrm{e}}'(\omega), \alpha_{\mathrm{e}}''(\omega) \to \alpha_{\mathrm{e}}'(\omega^+), \alpha_{\mathrm{e}}''(\omega^+). \end{aligned} \tag{191}$$

On the other hand, comparing (74) with (75) shows that the tangent force F_x is obtained from (75) using the transformations

$$\begin{aligned} &\mathrm{d}^2k k \to \mathrm{d}^2k k_x, \quad \Delta''(\omega) \to \Delta''(\omega), \quad \Delta'(\omega) \to \Delta''(\omega), \\ &\alpha_{\mathrm{e}}'(\omega^+) \to \alpha_{\mathrm{e}}''(\omega^+), \quad \alpha_{\mathrm{e}}''(\omega^+) \to -\alpha_{\mathrm{e}}''(\omega^+). \end{aligned} \tag{192}$$

Finally, it follows from (74) and (76) that $\mathrm{d}Q/\mathrm{d}t$ is obtained from F_x by the transformation

$$\mathrm{d}^2k k_x \to -\mathrm{d}^2k\omega^+. \tag{193}$$

Because Eqns (74)–(76) must follow from the analogous formulas in configuration 1 with account for linear relations (186) and (187) as $\varepsilon_1(\omega) - 1 = 4\pi n_1 \alpha_1(\omega) \to 0$, the quantities $F_x^{(1)}(l)$, $F_z^{(1)}(l)$, and $\dot{Q}^{(1)}(l)$ must be related similarly to expressions (191)–(193) after the change $\alpha_{\mathrm{e}}(\omega) \to \Delta_1(\omega)$.

We now use the exact expression for the retarded van der Waals force between two plates at $V = 0$ and $T_1 = T_2 = T$ in terms of a real frequency [145, 146], which can be conveni-

ently represented in the form [87]

$$F_z^{(1)}(l) = -\frac{\hbar S}{4\pi^3}\int_0^\infty \mathrm{d}\omega \int_{-\infty}^{+\infty} \mathrm{d}k_x \times \int_{-\infty}^{+\infty} \mathrm{d}k_y\, k\, \frac{\exp(-2kl)}{\left|1-\exp(-2kl)\Delta_1(\omega)\Delta_2(\omega)\right|^2} \times \left(\Delta_1''(\omega)\Delta_2'(\omega)\coth\frac{\hbar\omega}{2k_\mathrm{B}T} + \Delta_1'(\omega)\Delta_2''(\omega)\coth\frac{\hbar\omega}{2k_\mathrm{B}T}\right), \tag{194}$$

where $\Delta_{1,2}(\omega) = (\varepsilon_{1,2}(\omega)-1)/(\varepsilon_{1,2}(\omega)+1)$ and $\varepsilon_{1,2}(\omega)$ is the dielectric permittivity of plates 1 and 2. Making the transformations

$$\Delta_2''(\omega)\coth\frac{\hbar\omega}{2k_\mathrm{B}T} \to \Delta_2''(\omega)\coth\frac{\hbar\omega}{2k_\mathrm{B}T_2}\,,$$
$$\Delta_1''(\omega)\coth\frac{\hbar\omega}{2k_\mathrm{B}T} \to \Delta_1''(\omega^+)\coth\frac{\hbar\omega^+}{2k_\mathrm{B}T_1}\,, \tag{195}$$
$$\Delta_1'(\omega), \Delta_1''(\omega) \to \Delta_1'(\omega^+), \Delta_1''(\omega^+)$$

in (194), we arrive at the expression for the attraction force between the plates in nonequilibrium configuration 1:

$$F_z^{(1)}(l) = -\frac{\hbar S}{4\pi^3}\int_0^\infty \mathrm{d}\omega \int_{-\infty}^{+\infty} \mathrm{d}k_x \times \int_{-\infty}^{+\infty} \mathrm{d}k_y\, k\, \frac{\exp(-2kl)}{\left|1-\exp(-2kl)\Delta_1(\omega^+)\Delta_2(\omega)\right|^2} \times \left(\Delta_1''(\omega^+)\Delta_2'(\omega)\coth\frac{\hbar\omega^+}{2k_\mathrm{B}T_1} + \Delta_1'(\omega^+)\Delta_2''(\omega)\coth\frac{\hbar\omega}{2k_\mathrm{B}T_2}\right). \tag{196}$$

Similarly to the derivation of formulas (74) and (76), the following changes should be made in formula (196):

$$\mathrm{d}^2k k \to \mathrm{d}^2k k_x\,,\quad \Delta_2''(\omega) \to \Delta_2''(\omega)\,,\quad \Delta_2'(\omega) \to \Delta_2''(\omega)\,,$$
$$\Delta_1'(\omega^+) \to \Delta_1''(\omega^+)\,,\quad \Delta_1''(\omega^+) \to -\Delta_1''(\omega^+)\,. \tag{197}$$

As a result, we obtain

$$F_x^{(1)}(l) = -\frac{\hbar S}{4\pi^3}\int_0^\infty \mathrm{d}\omega \int_{-\infty}^{+\infty} \mathrm{d}k_x \times \int_{-\infty}^{+\infty} \mathrm{d}k_y\, k_x\, \frac{\exp(-2kl)}{\left|1-\exp(-2kl)\Delta_1(\omega^+)\Delta_2(\omega)\right|^2} \times \Delta_1''(\omega^+)\Delta_2''(\omega)\left(\coth\frac{\hbar\omega}{2k_\mathrm{B}T_2} - \coth\frac{\hbar\omega^+}{2k_\mathrm{B}T_1}\right). \tag{198}$$

Finally, making the change $\mathrm{d}^2k k_x \to -\mathrm{d}^2k\omega^+$ in (198), we find

$$\dot{Q}^{(1)}(l) = \frac{\hbar S}{4\pi^3}\int_0^\infty \mathrm{d}\omega \int_{-\infty}^{+\infty} \mathrm{d}k_x \times \int_{-\infty}^{+\infty} \mathrm{d}k_y\, \omega^+\, \frac{\exp(-2kl)}{\left|1-\exp(-2kl)\Delta_1(\omega^+)\Delta_2(\omega)\right|^2} \times \Delta_1''(\omega^+)\Delta_2''(\omega)\left(\coth\frac{\hbar\omega}{2k_\mathrm{B}T_2} - \coth\frac{\hbar\omega^+}{2k_\mathrm{B}T_1}\right). \tag{199}$$

Taking Eqns (186) and (187) into account, it is easy to see that formulas (74)–(76) follow directly from (196), (198), and (199). To take the magnetic properties of the plates into account, similar terms with the change $\Delta_{1,2}(\omega) = (\mu_{1,2}(\omega)-1)/(\mu_{1,2}(\omega)+1)$ should be added to the right-hand sides of these formulas [87]. It is straightforward to show that as $T_1 \to 0$ and $T_2 \to 0$, Eqn (198) yield a nonzero quantum friction force [cf. (78)]:

$$F_x^{(1)}(l) = \frac{\hbar S}{2\pi^3}\int_{-\infty}^{+\infty} \mathrm{d}k_y \int_0^\infty \mathrm{d}k_x\, k_x \times \int_0^{k_xV} \mathrm{d}\omega\, \frac{\exp(-2kl)}{\left|1-\exp(-2kl)\Delta_1(\omega^-)\Delta_2(\omega)\right|^2}\, \Delta_1''(\omega^-)\Delta_2''(\omega)\,, \tag{200}$$

where $\omega^- = \omega - k_xV$. Formula (200) coincides with the well-known result [60] (see formula (25) in [60]) up to the notation for plates 1 and 2 (also see the discussion in [82]). Using our method for calculating FEI effects, the 'shifted frequency' (ω^+ or ω^-) always relates to the moving body. In contrast, the plates in [60] were assumed to move with oppositely directed velocities $\pm V/2$.

To conclude, we note that the independence of the obtained results from the thermal state of the vacuum background surrounding the plates is one of the reasons for the correspondence between configurations 1 and 2 in the nonrelativistic case.

8. Discussion of experimental results

8.1 Equilibrium and nonequilibrium Casimir–Lifshitz forces

Presently, as in the time of Lebedev, experimental works related to quantitative measurements of FEI effects are scarce. It is sufficient to mention that the most compelling quantitative measurements of the Casimir–Lifshitz forces corresponding to theoretical predictions were carried out only in 1997 [147] (in the distance range from 0.6 to 6 μm) (see also [148]) and in 1998 [149] (in the distance range from 0.1 to 0.9 μm). These experiments were made possible thanks to significant improvement in locating the interacting bodies, which diminished the measurements errors to 1% in the micrometer and nanometer range.

Difficulties in measurements of the Casimir–Lifshitz force are due to its weakness and the significant influence of external factors. In particular, in vacuum measurements using atomic force microscopes (AFMs), electrostatic and interatomic forces (for nonmagnetic materials) can interfere with FEI forces. The lens–plate and sphere–plate configurations are thought to be the most favorable geometric configurations in such measurements. In the first case, a torsional pendulum suspension is used, as in the classical Cavendish experiment, with a microscopic spherical probe (the radius of the sphere is about 12.5 cm [147]), and in the second case, an AFM is used [145, 146, 149–153], with a metallized sphere about 100 μm in diameter attached to the AFM cantilever serving as the probe. The transition from configuration 1 to the sphere–plate geometry is performed using the locally flat Deryagin approximation [154]

$$F_z = 2\pi R U(h,T)\,, \tag{201}$$

where R is the sphere radius and $U(h, T)$ is the density of the regularized part of the free energy of the electromagnetic field localized in the gap, which depends on the distance z between the plates and the temperature T.

An up-to-date comparison of the experimental results with theory is presented in [12, 18, 155]. The comparison of the calculated and measured forces was done taking the effects of the dielectric functions of the material, the roughness of the surfaces, the temperature, and geometry factors into account.

In [152, 153], nonequilibrium thermal Casimir–Polder forces were first measured in an experiment with the Bose–Einstein condensate of ^{87}Rb atoms placed in a magnetic trap near a dielectric plate. The distance to the plate varied in the range 6–11 μm. The thermal part of the interaction force was determined from the shift of the oscillation frequency of the condensate center of mass caused by the externally induced force. Nonequilibrium thermal configurations with different combinations of the plate and ambient (vacuum background) temperatures from 310 to 605 K were investigated. It was shown in [153] that the results of measurements are in good agreement with a formula equivalent to (160).

Thermal Casimir forces were also measured in [156, 157] in the temperature range 77–300 K in the distance range 0.187–2 μm. A gold-covered glass sphere 50 μm in diameter attached to the ASM cantilever, which was in vacuum contact with an Au plate, served as the probe. Unexpectedly, no thermal contribution to the Casimir pressure was measured within the experimental errors. This fact was explained by the authors of [156] by a compensating effect from electrostatic forces due to charge spots on the sphere. The measurements of thermal contributions to the Casimir force at low temperatures are of special interest because of long-standing discussions about possible violations of the Nernst theorem and the form of dielectric functions of metals at low frequencies, which are used in calculations of the Casimir–Lifshitz force in configuration 1 (see, e.g., [17, 155, 157] and the references therein).

8.2 Radiation thermal exchange

Progress in measurements of the vacuum thermal exchange in the submillimeter and nanometer range is also related to the development of AFM and methods for positioning probes [158–165]. In this case, the major contribution to the heat exchange rate can be related to inhomogeneous (near-field) modes of the electromagnetic field. However, the presence of the near-field heat exchange remained undetected for a long time [166]. In vacuum conditions, it was first detected in [158] for the probe–surface distances in the range 1–100 nm. In this experiment, the heat output from a Pt–Ir needle of a scanning tunnel microscope with a curvature radius ≈ 60 nm was measured in the heat exchange with Au and GaN surfaces. A thermopair was mounted into the probe, whose sensor was in contact with the needlepoint.

The heat output is measured using the Seebeck effect, in which the generated thermo emf is $V_{\rm th} = S\Delta T$, where S is the Seebeck factor and ΔT is the temperature difference between the thermopair contacts. The cooling rate of the needlepoint $\mathrm{d}Q/\mathrm{d}t$ is determined by the temperature difference between the needle and the sample ΔT, as well as by the thermal resistance $R_{\rm th}$ of the contact: $\mathrm{d}Q/\mathrm{d}t = \Delta T/R_{\rm th}$. The above relations imply that $\mathrm{d}Q/\mathrm{d}t = V_{\rm th}/(SR_{\rm th})$. With the constants S and $R_{\rm th}$ found from the preliminary calibrations, measuring the voltage $V_{\rm th}$ for a known distance between the probe and the surface enables finding $\mathrm{d}Q/\mathrm{d}t$.

In the experiment in [158], the respective probe and surface temperatures were 300 K and 200 K. For both samples, the measured value $\mathrm{d}Q/\mathrm{d}t$ showed the initial plateau in the distance range 1–10 nm with a maximum cooling rate of 10^{-5} W, which further transformed into a power-law dependence $\mathrm{d}Q/\mathrm{d}t \sim z^{-3}$ at larger distances from the surface. The heat exchange rate can also be characterized by the thermal conductance

$$G = \frac{\mathrm{d}Q/\mathrm{d}t}{\Delta T}\,, \tag{202}$$

where $\Delta T = |T_1 - T_2|$, and T_1 and T_2 are the temperatures of contacting bodies. The measurements in [158] yielded $G = 5$ nW K^{-1} for a gap width of 30 nm in the (Pt–Ir)–Au contact. A later experiment [163] involved a 50 μm gold-covered glass sphere in contact with an Au surface, used as the AFM probe. For a gap width of 30 nm, the measurements yielded $G = 1.5$ nW K^{-1}. Taking into account that the conductance G increases with the probe radius (as R^n, $n = 0.5$–2, according to the estimates in [167]), it is clear that the results in [158] are significantly overestimated. This was noted in [163]. We note that the accuracy of the distance calibration between the probe and the surface [159–163] was significantly improved by taking the probe attraction to the surface by the Casimir–Lifshitz force into account.

The interpretation of the measurements in [158–163] was based on several assumptions, including the dipole approximation of fluctuation electrodynamics [168, 169] in configuration 2; the locally flat approximation

$$\frac{\mathrm{d}Q}{\mathrm{d}t} = -2\pi R\int_h^\infty S(z)\,\mathrm{d}z\,, \tag{203}$$

where $S(z)$ is the heat flux from the unit surface of the more heated plate (h is the gap width) calculated using the thermal exchange theory [170–172] in configuration 1, the transition to the small-particle limit for the material of one of the plates [11, 68], the dipole-additive approximation with the vacuum background taken into account based on formula (147) (for $V = 0$) [173, 174], and the dipole approximation for the heat exchange between two spherical particles [11, 159–161].

The results of the calculations allow the correct description of the characteristic values of $\mathrm{d}Q/\mathrm{d}t$, as well as of the dependences on the temperature, distance, and particle radius. It was noted that in the contact of a metal particle with a metal surface, the contribution to $\mathrm{d}Q/\mathrm{d}t$ due to the magnetic polarization of the particle dominates [173, 175]. It was stated theoretically and experimentally that the heat exchange rate in the dielectric contacts (SiO_2–SiO_2) is 10–50 times as high as in metal contacts. Experiments with cylindrically symmetric probes and in the case of heat exchange with planar surfaces are described in [162, 164, 176].

8.3 Dissipative forces of the fluctuation-electromagnetic interaction

Unlike conservative van der Waals and Casimir forces, which can undoubtedly be identified, measurements of dissipative FEI forces in the geometry of an oscillating probe above a plate (i.e., forces presumably caused by the component F_x of the FEI) are scarce [177–182], and the situation is far from clear. This is largely because the contact-free friction force, which is proportional to velocity, can be caused by the

cumulative action of different mechanisms [10, 11] (here, we do not discuss friction forces unrelated to FEIs arising in atomic-near contacts [183], when electron exchange and atomic interaction become significant).

The principal difficulty is that in a contact-free vacuum dynamic regime of AFMs with compensation of the contact potential difference, the contact interaction of the probe with the sample must be determined by the van der Waals force; therefore, it would be quite natural to expect that the vacuum friction forces should also have a similar nature in this case. But theoretical estimates showed that for a silicon–mica contact [178], the measured damping forces are two to three orders of magnitude higher than the calculated ones [83, 184], and for metal contacts [177, 179, 180], 5 to 11 orders of magnitude [10, 69, 184, 185].

Experiments lead to different dependences of the damping forces on the distance to the surface: from z^{-3} in [179] to $z^{-1.1}$ or $z^{-1.5}$ in [180], and also reveal a strong temperature influence and the contacting material effects [180–182].

We note that the damping of a probe oscillating perpendicular to the surface was investigated in [178, 179], and the damping during the parallel motion of a probe with a radius 30–50 times as large as in the first case (1 μm) was studied in [180]. The significantly different power-law dependence of the damping force found in [180] is apparently due to the electrostatic interaction of charge spots and not due to the van der Waals (dissipative) interaction, which has a z^{-3} dependence [179]. That the attraction force between the probe and the surface was not measured in this experiment complicates the interpretation of the results in [180].

In [179], in contrast, the attraction character of the (van der Waals) force is evident [184], but the problem is in the large difference between theoretical and experimentally found values of the damping forces. The strong temperature dependence of the damping forces does not correspond to the electrostatic friction [186, 187] and phonon friction [10, 11] mechanisms. For example, in [180], the damping forces at temperatures of 77 and 4.2 K were measured to be 1/6 and 1/24 those at 295 K. At the same time, the results of experiments in [181, 182] are in agreement with the electrostatic theory predictions [186, 187], but disagree with the FEI theory.

The damping force in AFMs (with the dependence $F_x \propto VTR/z^3$) close to the experimental results in [179, 180] can be obtained in accordance with formula (145) for a nonrelativistic velocity [86] if the particle and the surface have coincident absorption peaks at the frequency $\omega = 10^9$ Hz. Such frequencies are typical for rotational excitations of molecular complexes and phonon excitations. In addition, the inverse decay time of oscillators is of the same order in experiments with quartz microbalance [188–190].

To explain the experiments in [177–180], other mechanisms [10, 11] have also been proposed, but the present experimental accuracy does not allow a unique identification of the dissipative FEI forces (and quantum friction forces). New measurements of the damping forces of probes with different types of contacts at different temperatures and distances and for various geometric and mechanical characteristics of the probes are required.

8.4 Other experiments

Other experiments that could have previously related or can relate in the future to measurements of the FEI forces and radiation heat exchange are of interest. For example, the study of conservative van der Waals forces in an atomic beam with thermal velocities passing over metallic surfaces were carried out already 40 years ago [191–193]. In these experiments, however, the beam velocity was not sufficiently high to reveal dynamic corrections to the Casimir–Polder force [formulas (83) and (171)]. Later, several experiments were carried out to measure these forces with additional laser excitation of neutral atoms [194, 195] and the passing of a neutral bundle of sodium atoms in a microgap [196], albeit also with not too high velocities. Meanwhile, the correction term in formula (83) proportional to the velocity squared makes a significant contribution (about 1–10%) to the deviation angle of a beam over the plate only for atomic velocities of the order of $10^5 - 10^6$ m s^{-1} (at distances of 10 nm from the metal surface). At subrelativistic velocities ($\beta = 0.1 - 0.3$), dynamic correction (171) to the Casimir–Polder force can also be quite noticeable. In this connection, the experimental search for possible radiation in Cherenkov friction, in our opinion, is worth being started with measurements of conservative FEI forces (146).

The possibility of probing resonance dissipative FEI forces in passing neutral atomic–molecular beams through microgaps (microcapillars) or in reflection from surfaces was examined in [197, 198]. According to the estimates in [198], in the reflection of the beam of Cs^+ ions with an energy of 50–100 keV from a doped silicon surface, the SiC or GaAs part of the beam, which was neutralized after the reflection from the smooth surface, exhibits smaller energy losses compared with the charged component of the beam that can be measured (the difference can be as high as several dozen eV).

Dissipative FEI forces are likely to play an important role in damping quartz oscillators in quartz microbalance experiments [188, 189] and in measurements of friction forces in one- and two-dimensional structures (see [10, 11] and the references therein). Recently, the possibility of measuring the quantum friction force between the SiO_2 probe of an AFM and an SiO_2 surface covered with a graphene layer was discussed in [199]. The fluctuating electromagnetic field acting on the probe in this case is produced by a current of electrons in the graphene if their drift velocity is at least 10^5 m s^{-1}.

As for thermal FEI effects, experimental studies of coherent nonthermal radiation of optical diffraction grids [200] (see [8, 64] for more details) should be mentioned. The authors of [200], in particular, observed a significant (four orders of magnitude) increase in the intensity and spatial coherence of thermal radiation from a silicon carbide diffraction grid with a period of 11.4 μm at distances of 10–100 nm from it, i.e., in the near-field zone of the surface.

In the context of this review, it is interesting to discuss the possibility of measuring the braking torques and radiation of particles rotating near a surface. For example, the spin frequency of graphene nanoparticles (in an ion trap) was experimentally reached at $10^6 - 10^7$ Hz [201] and can be further increased to 10^9 Hz. This results in much more favorable conditions for measuring the FEI dissipative forces compared to conditions of linear motion in an AFM.

Indeed, assuming that a nanoparticle has the shape of a cylindrical tablet with radius R and thickness d and the gap width between them on the surface is h, it is straightforward to estimate the ratio of decay times of the linear and rotational motion using formulas (77) and (105). Their (integral) right-hand sides are identical, and we can pass to a cylindrical particle by the substitution $R^3 \to (3/4\pi)\pi R^2\, dz$ and subse-

quent integration over z from h to $h+d$. As a result, taking into account that the inertia moment of the cylinder is $MR^2/2$ (where M is the mass of the particle) and solving dynamic equations corresponding to (77) and (105), we obtain the ratio of decay times of linear motion τ_V to rotational motion τ_Ω: $\tau_V/\tau_\Omega = (R/h)^2 \gg 1$ (for $d \ll h$). Correspondingly, the equivalent dissipative forces slowing down the particle increase by the same ratio. The spectrum of nonthermal radiation from a spinning particle, according to formula (182), falls into the visible or ultra-high-frequency range. In addition, the produced emission can be significantly amplified in resonators [18]. In the spectrum from heated particles at $\hbar\Omega \ll k_B T$, the thermal component dominates, but nonthermal radiation related to rotation does not disappear and should be observed at low frequencies.

8.5 Astrophysical implications

We briefly discuss possible astrophysical applications of the results presented in Section 5 for thermal radiation of gas–dust clouds in regions of intense star formation in galaxies, as well as for other effects.

According to modern models, the typical size, mass, and temperature of gas–dust clouds are $L = 0.2$ pc, $M/M_\odot = 20$ (where $M_\odot$ is the solar mass), and $T = 30-50$ K, and the gas-to-dust mass ratio is $\kappa = 100$ [202]. It is important to note that κ can be much smaller at the initial stage of star formation. Dust particles have a typical size of 0.01–10 μm and apparently represent structures with silicate and metallic nuclear inclusions covered with an ice and gas frozen shell. We assume that the gas–dust cloud with such parameters is not irradiated by stellar light from inside, and the matter is in equilibrium with inner thermal radiation. The optical depth for the inner radiation is high, and photons escape outside the cloud only from the surface layers. Then the outgoing thermal radiation is described by the Stephan–Boltzmann law with the total power

$$W_{BB} = 4\pi L^2 \sigma_B T^4 = \frac{\pi^3}{15}\frac{k_B^4}{\hbar^3 c^2} L^2 T^4 . \tag{204}$$

The intensive star formation in the cloud is accompanied by accretion processes in gravitational condensation centers, where matter can acquire significant velocities. Under such conditions, the thermal balance between particles and radiation is violated, and the outgoing thermal radiation (per particle) acquires an additional contribution determined by the difference between (114) and (115). For nonrelativistic velocities $\beta \ll 1$, the total power from all particles of the cloud (where for simplicity, we disregard the excess contribution from the gas component) is expressed as

$$W_D = \frac{4\pi^3}{7}\frac{M}{\kappa\rho}\frac{\hbar}{c^3\sigma_0}\left(\frac{k_B T}{\hbar}\right)^6 \beta^2 , \tag{205}$$

where ρ is the mean density of one particle and T is the interior background radiation temperature. We note that formula (205) does not depend on the size of the particles: it is obtained under the assumption that the dielectric function of the particle material can be represented as $\varepsilon(\omega) = i4\pi\sigma_0/\omega$ (see Section 5.2). For cosmic dust grains, it can also have the relaxational form $\varepsilon(\omega) = a + b/(1 - i\omega/\omega_0)$, where a and b are numerical factors and ω_0 is the Debye relaxation frequency. In the last case, the imaginary part of the polarizability of spherical grains in the low-frequency range $\omega \ll \omega_0$ takes the form

$$\alpha''(\omega) = R^3 \operatorname{Im}\frac{\varepsilon(\omega)-1}{\varepsilon(\omega)+2} = R^3\,\frac{3b\omega/\omega_0}{(a+b+2)^2} \tag{206}$$

and, clearly, we can use formula (205) with the substitution $\sigma_0 \to (a+b+2)^2\omega_0/(4\pi b)$. Taking this into account, we have the W_D and W_{BB} power ratio

$$\frac{W_D}{W_{BB}} = \frac{180\pi}{7}\,\frac{b}{(a+b+2)^2}\,\frac{M}{\kappa L^2}\left(\frac{k_B T}{\hbar}\right)^2 \frac{\beta^2}{\omega_0 c} . \tag{207}$$

With the maximum value of the numerical coefficient in (207) equal to 10.1, for $a = 0$ and $b = 2$, and setting $\omega_0 = 10^9$ s^{-1}, $\beta = 1/30$, $T = 50$ K, $M = 4\times10^{34}$ g, $L = 0.2$ pc $= 6.16\times10^{17}$ cm, and $\rho = 0.5$ g cm^{-3}, from (207) we estimate $W_D/W_{BB} \approx 23$, with the radiation spectrum corresponding to (205) in the low-frequency part increasing as ω^4, not according to the Rayleigh–Jeans law. Such a spectral index of thermal radiation from dust clouds was reported in [203, 204] (see also [205]). Thus, radiation with these parameters can evidence the internal dynamics of protostellar condensations inside the cloud. The standard interpretation of such spectra is based on the combination of black-body radiation (204) from several sources with different temperatures.

The results presented in Sections 5.2 and 5.3 for small and larger particles should be taken into account in the analysis of the general balance between matter and radiation in cosmic conditions and during the transformation of the kinetic energy of matter into low-frequency background radiation in the Universe. Dust grains and larger bodies swept out into interstellar and intergalactic space can have large velocities. Relativistic effects in thermal radiation could possibly have an impact on the CMB anisotropy, and in later epochs, on powerful accretion and explosion processes in which matter outflows move with subrelativistic velocities.

9. Conclusion

Fluctuating electromagnetic fields of condensed bodies at rest cause the appearance of the van der Waals and Casimir–Lifshitz forces, as well as vacuum heat exchange. In dynamically and (or) thermally nonequilibrium systems, interesting new phenomena arise, such as the quantum or van der Waals friction of particles in translational motion or spinning particles, as well as a specific thermal and nonthermal radiation similar to Cherenkov radiation.

In the framework of a single review, it is impossible to discuss in detail the bulk of theoretical and experimental studies carried out in the last 10–20 years in this field. This is why we focused on the construction of the comprehensive picture of FEI based on the application of the theory of electromagnetic fluctuations to two nonequilibrium systems, in which relativistic theory turned out to be very useful: a moving particle in a vacuum and a moving particle over a plate.

The fundamental FEI characteristics related to a small polarizable particle include conservative and dissipative forces (torques), the rate of heating (cooling), and the power of thermal and nonthermal emission. There are general relations among them that follow from relativistic transformations of electrodynamic quantities characterizing FEI. Using all of these quantities enables the FEI effects to be fully described and the particle dynamics and kinetics of its

thermal state to be analyzed. Results related to particles spinning in a vacuum and near a surface, Cherenkov friction, thermal and nonthermal radiation of small particles, and thermal radiation of large particles are reviewed here for the first time.

The results presented bear a fundamental character and can be used to interpret modern and future experiments related to FEI measurements in systems of moving bodies (for example, in atomic traps and microelectromechanical systems). In cosmic conditions, the appearance of excessive low-frequency thermal and nonthermal radiation from gas and dust clouds with internal particle dynamics are expected from star-forming regions at the accretional growth of condensing centers. Spectral features of this radiation are determined by dielectric characteristics of dust grains.

Experimental results for conservative Casimir–Lifshitz forces and the thermal exchange rate are generally consistent with the existing theory, but the problems of experimental discovery of dissipative FEI forces and dynamic corrections to conservative FEI forces and the heat exchange rate remain unresolved.

Appendix A

In general, the retarded Green's function $D_{lk}(\omega, \mathbf{r}, \mathbf{r}')$ for a photon in a homogeneous medium satisfies the equation [115]

$$\left(\mathrm{rot}_{im}\,\mathrm{rot}_{ml} - \frac{\omega^2}{c^2}\,\varepsilon(\omega)\,\mu(\omega)\delta_{il}\right) D_{lk}(\omega, \mathbf{r}, \mathbf{r}') = -4\pi\hbar\mu(\omega)\delta_{ik}\delta(\mathbf{r}-\mathbf{r}')\,. \tag{A1}$$

For configuration 2, due to translation invariance with respect to coordinates x, y in the plate plane, it is most natural to use the two-dimensional Fourier decomposition of the Green's function:

$$D_{lk}(\omega, \mathbf{r}, \mathbf{r}') = \int \frac{\mathrm{d}^2k}{(2\pi)^2}\, D_{ik}(\omega, \mathbf{k}, z, z') \times \exp\left[\mathrm{i}k_x(x-x') + \mathrm{i}k_y(y-y')\right]. \tag{A2}$$

Substituting (A2) in (A1), we obtain an equation for $D_{ik}(\omega, \mathbf{k}, z, z')$, whose solution with the corresponding boundary conditions on the surface $z = 0$ separating the vacuum and the medium leads to formulas (45)–(50).

In the case of configuration 3, there is translation invariance with respect to all three spatial coordinates (x, y, z); therefore, the solution of Eqn (A1) can be sought in the form of the Fourier integral over a three-dimensional wave vector:

$$D_{ik}(\omega, \mathbf{r}, \mathbf{r}') = \int \frac{\mathrm{d}^3k}{(2\pi)^3}\, D_{ik}(\omega, \mathbf{k}) \times \exp\left[\mathrm{i}k_x(x-x') + \mathrm{i}k_y(y-y') + \mathrm{i}k_z(z-z')\right]. \tag{A3}$$

Substituting (A3) in (A1) and taking into account that $\varepsilon(\omega) = 1 + \mathrm{i}\delta\,\mathrm{sign}\,\omega$, $\delta \to +0$, and $\mu(\omega) = 1$ in the vacuum [115], we obtain formula (52) for the retarded Green's function in the (ω, k_x, k_y, k_z) representation. We also note that the differentiation operators with respect to spatial variables in the right-hand sides of formulas (43), (44), (54), and (55) ($\mathrm{rot}_{il} = e_{inl}\,\partial/\partial x_n$ and $\mathrm{rot}'_{jm} = e_{jnm}\,\partial/\partial x'_n$) are straightforwardly expressed in terms of $k_x, k_y, k = (k_x^2 + k_y^2)^{1/2}$ in the case of configuration 2, and in terms of k_x, k_y, k_z in the case of configuration 3.

Appendix B

To find the induced dipole moments of a particle using (92) and (93), the following obvious relations should be used

$$\int_0^\infty \mathrm{d}\tau\,\alpha(\tau)E_{\mathrm{m}}^{\mathrm{sp}}(t-\tau) = \int \frac{\mathrm{d}\omega\,\mathrm{d}^2k}{(2\pi)^3}\,\alpha(\omega)E_{\mathrm{m}}^{\mathrm{sp}}(\omega, \mathbf{k})\exp(-\mathrm{i}\omega t)\,, \tag{B1}$$

$$\int_0^\infty \mathrm{d}\tau\,\alpha(\tau)\cos(\Omega t)E_{\mathrm{m}}^{\mathrm{sp}}(t-\tau) = \int \frac{\mathrm{d}\omega\,\mathrm{d}^2k}{(2\pi)^3}\,\frac{\alpha(\omega_+)+\alpha(\omega_-)}{2}\,E_{\mathrm{m}}^{\mathrm{sp}}(\omega, \mathbf{k})\exp(-\mathrm{i}\omega t)\,, \tag{B2}$$

$$\int_0^\infty \mathrm{d}\tau\,\alpha(\tau)\sin(\Omega t)E_{\mathrm{m}}^{\mathrm{sp}}(t-\tau) = \int \frac{\mathrm{d}\omega\,\mathrm{d}^2k}{(2\pi)^3}\,\frac{\alpha(\omega_+)-\alpha(\omega_-)}{2\mathrm{i}}\,E_{\mathrm{m}}^{\mathrm{sp}}(\omega, \mathbf{k})\exp(-\mathrm{i}\omega t)\,, \tag{B3}$$

where $\omega_\pm = \omega \pm \Omega$. Substituting (B1)–(B3) in (92) and noting that $\mathbf{n} = (\cos\theta, 0, \sin\theta)$, we obtain

$$d_x^{\mathrm{ind}}(t) = \int \frac{\mathrm{d}\omega\,\mathrm{d}^2k}{(2\pi)^3}\exp(-\mathrm{i}\omega t) \times \left[\alpha(\omega)\left(\cos^2\theta\,E_x^{\mathrm{sp}}(\omega, \mathbf{k}) + \sin\theta\cos\theta\,E_z^{\mathrm{sp}}(\omega, \mathbf{k})\right) + \frac{\alpha(\omega_+)+\alpha(\omega_-)}{2}\left(\sin^2\theta\,E_x^{\mathrm{sp}}(\omega, \mathbf{k}) - \sin\theta\cos\theta\,E_z^{\mathrm{sp}}(\omega, \mathbf{k})\right) - \frac{\alpha(\omega_+)-\alpha(\omega_-)}{2\mathrm{i}}\sin\theta\,E_y^{\mathrm{sp}}(\omega, \mathbf{k})\right], \tag{B4}$$

$$d_y^{\mathrm{ind}}(t) = \int \frac{\mathrm{d}\omega\,\mathrm{d}^2k}{(2\pi)^3}\exp(-\mathrm{i}\omega t)\left[\frac{\alpha(\omega_+)+\alpha(\omega_-)}{2}\,E_y^{\mathrm{sp}}(\omega, \mathbf{k}) + \frac{\alpha(\omega_+)-\alpha(\omega_-)}{2\mathrm{i}}\left(\sin\theta\,E_x^{\mathrm{sp}}(\omega, \mathbf{k}) - \cos\theta\,E_z^{\mathrm{sp}}(\omega, \mathbf{k})\right)\right], \tag{B5}$$

$$d_z^{\mathrm{ind}}(t) = \int \frac{\mathrm{d}\omega\,\mathrm{d}^2k}{(2\pi)^3}\exp(-\mathrm{i}\omega t) \times \left[\alpha(\omega)\left(\sin\theta\cos\theta\,E_x^{\mathrm{sp}}(\omega, \mathbf{k}) + \sin^2\theta\,E_z^{\mathrm{sp}}(\omega, \mathbf{k})\right) + \frac{\alpha(\omega_+)+\alpha(\omega_-)}{2}\left(-\sin\theta\cos\theta\,E_x^{\mathrm{sp}}(\omega, \mathbf{k}) + \cos^2\theta\,E_z^{\mathrm{sp}}(\omega, \mathbf{k})\right) + \frac{\alpha(\omega_+)-\alpha(\omega_-)}{2\mathrm{i}}\cos\theta\,E_y^{\mathrm{sp}}(\omega, \mathbf{k})\right]. \tag{B6}$$

Similar relations for magnetic dipole moments can be derived from (B1)–(B6) with the substitution $\alpha_{\mathrm{e}}(\omega) \to \alpha_{\mathrm{m}}(\omega)$ and using the projections of the Fourier transformations of the electric fields on the Fourier transformations of the magnetic field.

References

1. Lebedev P N *Sobranie Sochinenii* (Collected Works) (Moscow: Mosk. Fiz. Obshch. im. P.N. Lebedeva, 1913); Lebedew P *Wied. Ann.* **52** 621 (1894)
2. Einstein A, Hopf L *Ann. Physics* **33** 1105 (1910)
3. Casimir H B G *Proc. Kgl. Ned. Akad. Wet.* **51** 793 (1948)

4. Casimir H B G, Polder D *Phys. Rev.* **73** 360 (1948)
5. Lifshitz E M *Sov. Phys. JETP* **2** 73 (1956); *Zh. Eksp. Teor. Fiz.* **29** 94 (1955)
6. Kardar M, Golestanian R *Rev. Mod. Phys.* **71** 1233 (1999)
7. Milton K A *The Casimir Effect: Physical Manifestations of Zero-Point Energy* (Singapore: World Scientific, 2001)
8. Joulain K et al. *Surf. Sci. Rep.* **57** 59 (2005)
9. Buhmann S Y, Welsch D-G *Prog. Quantum Electron.* **31** (2) 51 (2007); quant-ph/0608118
10. Volokitin A I, Persson B N J *Rev. Mod. Phys.* **79** 1291 (2007)
11. Volokitin A I, Persson B N J *Phys. Usp.* **50** 879 (2007); *Usp. Fiz. Nauk* **177** 921 (2007)
12. Bordag M et al. *Advances in the Casimir Effect* (International Series of Monographs on Physics, Vol. 145) (Oxford: Clarendon Press, 2015)
13. Vinogradov E A, Dorofeyev I A *Phys. Usp.* **52** 425 (2009); *Usp. Fiz. Nauk* **179** 449 (2009)
14. Dedkov G V, Kyasov A A *Phys. Solid State* **51** 1 (2009); *Fiz. Tverd. Tela* **51** 3 (2009)
15. Dedkov G V, Kyasov A A *Nanostrukt. Matem. Fiz. Modelirovanie* **1** (2) 5 (2009)
16. Dorofeyev I A, Vinogradov E A *Phys. Rep.* **504** 75 (2011)
17. Milton K A *Am. J. Phys.* **79** 697 (2011)
18. Dalvit D A R, Neto P A M, Mazzitelli F D *Lecture Notes Phys.* **834** 419 (2011); arXiv:1006.4790
19. Buhmann S Y *Dispersion Forces II. Many-Body Effects, Excited Atoms, Finite Temperature and Quantum Friction* (Springer Tracts in Modern Physics, Vol. 248) (Heidelberg: Springer, 2012)
20. Simpson W, Leonhardt U (Eds) *Force of the Quantum Vacuum: An Introduction to Casimir Physics* (Singapore: World Scientific, 2015)
21. Rytov S M *Teoriya Elektricheskikh Fluktuatsii i Teplovogo Izlucheniya* (Theory of Electric Fluctuations and Thermal Radiation) (Moscow: Izd. AN SSSR, 1953)
22. Levin M L, Rytov S M *Teoriya Ravnovesnykh Elektromagnitnykh Fluktuatsii v Elektrodinamike* (Theory of Equilibrium Electromagnetic Fluctuations in Electrodynamics) (Moscow: Nauka, 1967)
23. Dzyaloshinskii I E, Lifshitz E M, Pitaevskii L P *Sov. Phys. Usp.* **4** 153 (1961); *Usp. Fiz. Nauk* **73** 381 (1961)
24. Barash Yu S, Ginzburg V L *Sov. Phys. Usp.* **18** 305 (1975); *Usp. Fiz. Nauk* **116** 5 (1975)
25. Barash Yu S, Ginzburg V L *Sov. Phys. Usp.* **27** 467 (1984); *Usp. Fiz. Nauk* **143** 345 (1984)
26. Barash Yu S *Sily Van-der-Vaal'sa* (Van der Waals Forces) (Moscow: Nauka, 1988)
27. Mahanty J, Ninham B W *Dispersion Forces* (London: Academic Press, 1976)
28. Parsegian V A *Van der Waals Forces: A Handbook for Biologists, Chemists, Engineers, and Physicists* (New York: Cambridge Univ. Press, 2006)
29. Barton G *Ann. Physics* **245** 361 (1996)
30. Pendry J B *J. Mod. Opt.* **45** 2389 (1998)
31. Manjavacas A, García de Abajo F J *Phys. Rev. A* **82** 063827 (2010)
32. Manjavacas A, García de Abajo F J *Phys. Rev. Lett.* **105** 113601 (2010)
33. Maghrebi M F, Jaffe R L, Kardar M *Phys. Rev. Lett.* **108** 230403 (2012)
34. Maghrebi M F, Golestanian R, Kardar M *Phys. Rev. A* **88** 042509 (2013)
35. Peebles P J E *Principles of Physical Cosmology* (Princeton, NJ: Princeton Univ. Press, 1993)
36. Weinberg S *Rev. Mod. Phys.* **61** 1 (1989)
37. Poppe T, Blum J, Henning T *Adv. Space Res.* **23** 1197 (1999)
38. Decca R S et al. *Phys. Rev. D* **68** 116003 (2003)
39. Chan H B et al. *Science* **291** 1941 (2001)
40. Chan H B et al. *Phys. Rev. Lett.* **87** 211801 (2001)
41. Buks E, Roukes M L *Europhys. Lett.* **54** 220 (2001)
42. Buks E, Roukes M L *Phys. Rev. B* **63** 033402 (2001)
43. Munday J N, Capasso F, Parsegian V A *Nature* **457** 07610 (2009)
44. Boström M et al. *Eur. Phys. J.* **385** 377 (2012)
45. Teodorovich E V *Proc. R. Soc. London A* **362** 71 (1978)
46. Mahanty J *J. Phys. B* **13** 4391 (1980)
47. Schaich W L, Harris J *J. Phys. F* **11** 65 (1981)
48. Levitov L S *Europhys. Lett.* **8** 499 (1989)
49. Polevoi V G *Sov. Phys. JETP* **71** 1119 (1990); *Zh. Eksp. Teor. Fiz.* **98** 1990 (1990)
50. Høye J S, Brevik I *Physica A* **181** 413 (1992)
51. Høye J S, Brevik I *Physica A* **196** 241 (1993)
52. Høye J S, Brevik I *Europhys. Lett.* **91** 60003 (2010)
53. Høye J S, Brevik I *Eur. Phys. J. D* **64** 1 (2011)
54. Høye J S, Brevik I *Int. J. Mod. Phys. A* **27** 1260011 (2012)
55. Høye J S, Brevik I *Eur. Phys. J. D* **68** 61 (2014)
56. Høye J S, Brevik I, Milton K A *J. Phys. A* **48** 365004 (2015)
57. Høye J S, Brevik I *J. Phys. Condens. Matter* **27** 214008 (2015)
58. Milton K A, Høye J S, Brevik I *Symmetry* **8** 29 (2016)
59. Tomassone M S, Widom A *Phys. Rev. B* **56** 4938 (1997)
60. Pendry J B *J. Phys. Condens. Matter* **9** 10301 (1997)
61. Pendry J B *J. Phys. Condens. Matter* **11** 6621 (1999)
62. Pendry J B *New J. Phys.* **11** 033028 (2010)
63. Pendry J B *New J. Phys.* **12** 068002 (2010)
64. Philbin T G, Leonhardt U *New J. Phys.* **11** 033035 (2009)
65. Leonhardt U *New J. Phys.* **12** 068001 (2010)
66. Volokitin A I, Persson B N J *Phys. Low-Dim. Struct.* **7/8** 17 (1998)
67. Volokitin A I, Persson B N J *J. Phys. Condens. Matter* **11** 345 (1999)
68. Volokitin A I, Persson B N J *Phys. Rev. B* **63** 205404 (2001)
69. Volokitin A I, Persson B N J *Phys. Rev. B* **65** 115419 (2002)
70. Volokitin A I, Persson B N J *Phys. Rev. B* **68** 155420 (2003)
71. Volokitin A I, Persson B N J *Phys. Rev. B* **74** 205413 (2006)
72. Volokitin A I, Persson B N J *Phys. Rev. B* **78** 155437 (2008)
73. Volokitin A I, Persson B N J *New J. Phys.* **13** 068001 (2011)
74. Volokitin A I, Persson B N J *New J. Phys.* **16** 18001 (2014)
75. Mkrtchian V E *Phys. Lett. A* **207** 299 (1995)
76. Mkrtchian V E et al. *Phys. Rev. Lett.* **91** 220801 (2003)
77. Mkrtchian V E *Armen. J. Phys.* **1** 229 (2009)
78. Mkrtchian V E, Henkel C *Ann. Physik* **526** 87 (2014)
79. Mkrtchian V E, Henkel C *Armen. J. Phys.* **7** 106 (2014)
80. Dedkov G V, Kyasov A A *Phys. Lett. A* **259** 38 (1999)
81. Kyasov A A, Dedkov G V *Nucl. Instrum. Meth. Phys. Res. B* **195** 247 (2002)
82. Dedkov G V, Kyasov A A *Phys. Solid State* **45** 1815 (2003); *Fiz. Tverd. Tela* **45** 1809 (2003)
83. Dedkov G V, Kyasov A A *Phys. Low.-Dim. Struct.* **1/2** 1 (2003)
84. Dedkov G V, Kyasov A A *Tech. Phys. Lett.* **29** (1) 16 (2003); *Pis'ma Zh. Tekh. Fiz.* **29** (1) 36 (2003)
85. Dedkov G V, Kyasov A A *Phys. Lett. A* **339** 212 (2005)
86. Dedkov G V, Kyasov A A *J. Phys. Condens. Matter* **20** 354006 (2008)
87. Dedkov G V, Kyasov A A *Surf. Sci.* **604** 562 (2010); arXiv: 1408.6995
88. Dedkov G V, Kyasov A A *Nucl. Instrum. Meth. Phys. Res. B* **268** 599 (2010)
89. Dedkov G V, Kyasov A A *Surf. Sci.* **606** 46 (2012)
90. Dedkov G V, Kyasov A A *Europhys. Lett.* **99** 64002 (2012)
91. Dedkov G V, Kyasov A A *J. Comput. Theor. Nanosci.* **10** 1 (2013)
92. Barton G *New J. Phys.* **12** 113044 (2010)
93. Barton G *New J. Phys.* **12** 113045 (2010)
94. Barton G *New J. Phys.* **13** 043023 (2011)
95. Barton G *J. Phys. Condens. Matter* **23** 335004 (2011)
96. Barton G *Int. J. Mod. Phys. A* **27** 1260002 (2012)
97. Henkel C et al. *J. Opt. A Pure Appl. Opt.* **4** S109 (2002)
98. Intravaia F, Henkel C, Antezza M *Lecture Notes Phys.* **834** 345 (2011)
99. Pieplow G, Henkel C *New J. Phys.* **14** 023027 (2013)
100. Pieplow G, Henkel C *J. Phys. Condens. Matter* **27** 214001 (2015)
101. Intravaia F, Behunin R O, Dalvit D A R *Phys. Rev. A* **89** 050101(R) (2014)
102. Intravaia F et al. *J. Phys. Condens. Matter* **27** 214008 (2015)
103. Krüger M et al. *Phys. Rev. B* **86** 115423 (2012)
104. Maghrebi M F, Golestanian R, Kardar M *Phys. Rev. D* **87** 025016 (2013)
105. Dedkov G V, Kyasov A A *Phys. Scripta* **89** 105501 (2014)
106. Kyasov A A, Dedkov G V *Armen. J. Phys.* **2** (3) 176 (2014)
107. Dedkov G V, Kyasov A A *Int. J. Mod. Phys.* **32** 1550237 (2015)
108. Volokitin A I *Phys. Rev. A* **91** 032505 (2015)
109. Dedkov G V, Kyasov A A *Tech. Phys. Lett.* **42** 8 (2016); *Pis'ma Zh. Tekh. Fiz.* **42** (1) 17 (2016);

110. Volokitin A I, Persson B N J *JETP Lett*. **103** 228 (2016); *Pis'ma Zh. Eksp. Teor. Fiz*. **103** 251 (2016)
111. Kyasov A A, Dedkov G V *Phys. J*. **2** (3) 176 (2016)
112. Dedkov G V, Kyasov A A, arXiv:1601.02353
113. Goldstein H, Poole C, Safko J *Classical Mechanics* (Cambridge, Mass.: Addison-Wesley Press, 1950); Translated into Russian: *Klassicheskaya Mekhanika* (Moscow – Izhevsk: RKhD, 2012)
114. Landau L D, Lifshitz E M *Statistical Physics* Vol. 1 (Oxford: Pegramon Press, 1980); Translated from Russian: *Statisticheskaya Fizika* Pt. 1 (Moscow: Fizmatlit, 2002)
115. Lifshitz E M, Pitaevskii L P *Statistical Physics* Vol. 2 (Oxford: Pegramon Press, 1980); Translated from Russian: *Statisticheskaya Fizika* Pt. 2 (Moscow: Fizmatlit, 2001)
116. Landau L D, Lifshitz E M *Electrodynamics of Continuous Media* (Oxford: Pegramon Press, 1984); Translated from Russian: *Elektrodinamika Sploshnykh Sred* (Moscow: Fizmatlit, 2001)
117. Ferrell T L, Ritchie R H *Phys. Rev. A* **21** 1305 (1980)
118. Annett J F, Echenique P M *Phys. Rev. B* **34** 6853 (1986)
119. Dedkov G V, Kyasov A A *Surf. Sci*. **605** 1077 (2011)
120. Dedkov G V, Kyasov A A *Tech. Phys*. **59** 616 (2014); *Zh. Tekh. Fiz*. **84** (4) 148 (2014)
121. Zhao R et al. *Phys Rev. Lett*. **109** 123604 (2012)
122. Dedkov G V, Kyasov A A *Tech. Phys*. **62** 1266 (2017); *Zh. Tekh. Fiz*. **87** 1255 (2017); Kyasov A A, Dedkov G V, arXiv:1605.06036
123. Lach G, de Kieviet M, Jentschura U D *Cent. Eur. J. Phys*. **10** 763 (2012)
124. Lach G, DeKieviet M, Jentschura U D *Phys. Rev. Lett*. **108** 043005 (2012)
125. Henry G R et al. *Phys. Rev*. **176** 1451 (1968)
126. Bracewell R N, Conklin E K *Nature* **219** 343 (1968)
127. Heer C V, Kohl R H *Phys. Rev*. **174** 1611 (1968)
128. Peebles P J E, Wilkinson D T *Phys. Rev*. **174** 2168 (1968)
129. Landau L D, Lifshitz E M *The Classical Theory of Fields* (Oxford: Butterworth-Heinemann, 2000); Translated from Russian: *Teoriya Polya* (Moscow: Fizmatlit, 2003)
130. Dedkov G V, Kyasov A A, arXiv:1504.01588
131. Zel'dovich Ya B *JETP Lett*. **14** 180 (1971); *Pis'ma Zh. Eksp. Teor. Fiz*. **14** 270 (1971)
132. Maghrebi M F, Jaffe R L, Kardar M *Phys. Rev. A* **90** 012515 (2014)
133. Dedkov G V, Kyasov A A *Europhys. Lett*. **78** 44005 (2007)
134. Datta T, Ford L H *Phys. Lett. A* **83** 314 (1981)
135. Dorofeyev I A *J. Phys. A* **31** 4369 (1998)
136. Antezza M, Pitaevskii L P, Stringari S *Phys. Rev. Lett*. **95** 113202 (2005)
137. Antezza M et al. *Phys. Rev. Lett*. **97** 223203 (2006)
138. Antezza M et al. *J. Phys. A* **39** 6117 (2006)
139. Buhmann S Y, Scheel S *Phys. Rev. Lett*. **100** 253201 (2008)
140. Dedkov G V, Kyasov A A *Tech. Phys. Lett*. **34** 950 (2008); *Pis'ma Zh. Tekh. Fiz*. **34** (22) 1 (2008)
141. Frank I M, Ginzburg V L *J. Phys. USSR* **9** 353 (1945)
142. Ginzburg V L *Phys. Usp*. **39** 973 (1996); *Usp. Fiz. Nauk* **166** 1033 (1996)
143. Dedkov G V, Kyasov A A *Tech. Phys. Lett*. **43** 763 (2017); *Pis'ma Zh. Tekh. Fiz*. **43** (16) 70 (2017); arXiv:1602.03432
144. Kyasov A A, Dedkov G V, arXiv:1303.7421
145. Chen F et al. *Phys. Rev. Lett*. **88** 101801 (2002)
146. Chen F et al. *Phys. Rev. A* **72** 020101(R) (2005)
147. Lamoreaux S K *Phys. Rev. Lett*. **78** 5 (1997)
148. Lamoreaux S K *Rep. Prog. Phys*. **68** 201 (2005)
149. Mohideen U, Roy A *Phys. Rev. Lett*. **81** 4549 (1998)
150. Harris B W, Chen F, Mohideen U *Phys. Rev. A* **62** 052109 (2000)
151. Chen F, Mohideen U *J. Phys. A* **39** 6223 (2006)
152. Harber D M et al. *Phys. Rev. A* **72** 033610 (2005)
153. Obrecht J M et al. *Phys. Rev. Lett*. **98** 063201 (2007)
154. Derjaguin B V, Abrikosova I I, Lifshitz E M *Q. Rev. Chem. Soc*. **10** 295 (1956)
155. Klimchitskaya G L, Mostepanenko V M *Proc. Peter The Great St. Petersburg Polytechnic Univ*. (1) 41 (2015); arXiv: 1507.02393
156. Castillo-Garza R et al. *Phys. Rev. B* **88** 075402 (2013)
157. Klimchitskaya G L, Mohideen U, Mostepanenko V M *Rev. Mod. Phys*. **81** 1827 (2009)
158. Kittel A et al. *Phys. Rev. Lett*. **95** 224301 (2005)
159. Narayanaswamy A, Shen S, Chen G *Phys. Rev. B* **78** 115303 (2008)
160. Shen S, Narayanaswamy A, Chen G *Nano Lett*. **9** 2909 (2009)
161. Shen S et al. *Appl. Phys. A* **96** 357 (2009)
162. Ottens R S et al. *Phys. Rev. Lett*. **107** 014301 (2011)
163. Shen S et al. *Appl. Phys. Lett*. **100** 233114 (2012)
164. Park K, Zhang Z *Front. Heat Mass Transfer* **4** 013001 (2013)
165. Gu N, Sasihithlu K, Narayanaswamy, in *Renewable Energy and the Environment, OSA Technical Digest* (Washington, DC: Optical Society of America, 2011) CD
166. Xu J B et al. *J. Appl. Phys*. **76** 7209 (1994)
167. Tschikin M et al. *Eur. Phys. J. Appl. Phys*. **50** 10603 (2010)
168. Mulet J P et al. *Appl. Phys. Lett*. **78** 2931 (2001)
169. Dorofeyev I A *J. Phys. D* **31** 600 (1998)
170. Polder D, Van Hove M *Phys. Rev. B* **4** 3303 (1971)
171. Levin M L, Polevoi V G, Rytov S M *Sov. Phys. JETP* **52** 1053 (1980); *Zh. Eksp. Teor. Fiz*. **79** 2087 (1980)
172. Loomis J J, Maris H J *Phys. Rev. B* **50** 18517 (1994)
173. Dedkov G V, Kyasov A A *Tech. Phys. Lett*. **33** 594 (2007); *Pis'ma Zh. Tekh. Fiz*. **35** (7) 305 (2007)
174. Dedkov G V, Kyasov A A *Surf. Sci*. **605** 429 (2011)
175. Chapuis P-O et al. *Appl. Phys. Lett*. **92** 210906 (2008)
176. Lim M, Lee S S, Lee B J *Phys. Rev. B* **91** 195136 (2015)
177. Dorofeyev I A et al. *Phys. Rev. Lett*. **83** 2402 (1999)
178. Gotsmann B et al. *Phys. Rev. B* **60** 11051 (1999)
179. Gotsmann B, Fuchs H *Phys. Rev. Lett*. **86** 2597 (2001)
180. Stipe B C et al. *Phys. Rev. Lett*. **87** 096801 (2001)
181. Kuehn S, Loring R F, Marohn J A *Phys. Rev. Lett*. **96** 156103 (2006)
182. Kisiel M et al. *Nature Mater*. **10** 119 (2011)
183. Giessibl F G *Rev. Mod. Phys*. **75** 949 (2003)
184. Dedkov G V *Phys. Solid State* **48** 747 (2006); *Fiz. Tverd. Tela* **48** 700 (2006)
185. Persson B N J, Volokitin A I *Phys. Rev. Lett*. **84** 3504 (2000)
186. Volokitin A I, Persson B N J, Ueba H *Phys. Rev. B* **73** 165423 (2006)
187. Volokitin A I, Persson B N J, Ueba H *JETP* **104** 96 (2007); *Zh. Eksp. Teor. Fiz*. **131** 107 (2007)
188. Krim J, Widom A *Phys. Rev. B* **38** 12184 (1988)
189. Tomassone M S et al. *Phys. Rev. Lett*. **79** 4798 (1997)
190. Bruschi L, Mistura G *Phys. Rev. B* **63** 235411 (2001)
191. Shih A, Parsegian V A *Phys. Rev. A* **12** 835 (1975)
192. Mehl M J, Schaich W L *Phys. Rev. A* **16** 921 (1977)
193. Arnold W, Hunklinger S, Dransfeld K *Phys. Rev. B* **19** 6049 (1979)
194. Failache H et al. *Phys. Rev. Lett*. **83** 5467 (1999)
195. Fichet M et al. *Europhys. Lett*. **77** 54001 (2007)
196. Sukenik C I et al. *Phys. Rev. Lett*. **70** 560 (1993)
197. Dedkov G V, Kyasov A A *Nucl. Instrum. Meth. Phys. Res. B* **183** 241 (2001)
198. Dedkov G V, Kyasov A A *Nucl. Instrum. Meth. Phys. Res. B* **237** 507 (2005)
199. Volokitin A I *JETP Lett*. **104** 504 (2016); *Pis'ma Zh. Eksp. Teor. Fiz*. **104** 534 (2016)
200. Greffet J-J et al. *Nature* **416** 61 (2002)
201. Kane B E *Phys. Rev. B* **82** 115441 (2010)
202. Wibe D S, Thesis for Doct. Phys.-Math. Sci. (St. Petersburg: The Central Astronomical Observatory of the RAS at Pulkovo, 2003)
203. Draine B T *Annu. Rev. Astron. Astrophys*. **41** 241 (2003)
204. Krügel E *An Introduction to the Physics of Interstellar Dust* (New York: Taylor and Francis, 2008)
205. Izotov Y I et al. *Astron. Astrophys*. **570** A97 (2014)